6-1-2010

Fabrication and properties of Carbon nanotube (CNT)-reinforced aluminium composites

Ahmed Sayed Salim Mohamed

The American University in Cairo

School of Sciences & Engineering

Fabrication and Properties of Carbon Nanotube (CNT) – Reinforced Aluminium Composites

By

Ahmed Sayed Salim Mohamed

B.Sc. in Mechanical Engineering

A thesis submitted in partial fulfillment of the requirements for the degree of

Master of Science in Engineering

With specialization in

Materials Science and Manufacturing

Under the supervision of

Dr. Amal Esawi

Associate Professor of Materials & Manufacturing

Mechanical Engineering Department, American University in Cairo

Dr. Khaled Morsi

Professor

Mechanical Engineering Department, San Diego State University, USA

Spring 2010

The American University in Cairo

School of Sciences and Engineering

Fabrication and Properties of Carbon Nanotube (CNT) – Reinforced Aluminium Composites

A Thesis Submitted by

Ahmed Sayed Salim Mohamed

May 31st, 2010

In partial fulfillment of the requirements for the degree of

Masters of Science in Engineering

With specialization in

Materials Science and Manufacturing

Has been approved by

Dr. Amal Esawi (Advisor)

Associate Professor, Department of Mechanical Engineering,

The American University in Cairo

Dr. Khaled Morsi (advisor)

Professor, Mechanical Engineering Department,

San Diego State University, California, USA

Dr. Kamal Bedewy

Professor, Mechanical Engineering Department,

Cairo University

Dr. Hanadi Salem

Professor, Mechanical Engineering Department,

The American University in Cairo

Program Director	**Date**	**Dean**	**Date**

ABSTRACT

Nanostructured materials have attracted many researchers due to their outstanding mechanical and physical properties. One example is Carbon Nanotube (CNT) reinforced composites. Although most researchers have focused on using CNTs to reinforce polymeric and ceramic matrices, CNT-reinforced metallic composites are quickly emerging as attractive materials combining light weight with superior strength and stiffness. Potential applications include automotive and aerospace industries.

In this research work, powder metallurgy techniques were employed to produce a nano composite with unique mechanical properties. 99.7% purity Aluminium (Al) powder was used along with two different types of multiwall carbon nanotubes (MWCNTs) having different aspect ratios to produce Al-CNT composites. In the first phase of the work, Al-CNT composite powders were produced by mechanical milling at low milling speed (200 rpm) for 3 and 6 hours using one type of CNT (140nm diameter) whereas in the second phase pure Al and up to 5 wt% of two types of CNT (40nm and 140nm diameters) were milled at the highest available speed (400 rpm) for 30 minutes.

The composite powders were processed into bulk material by compaction, and hot extrusion using a cylindrical compaction and extrusion die with extrusion ratio 4:1. Scanning electron microscopy (SEM), transmission electron microscopy (TEM), and X-Ray diffraction (XRD) were used to evaluate CNT dispersion, powder morphology, CNT damage, phase analysis and crystal size determination. Tensile testing, microhardness and nanoindentation were used to characterize the mechanical properties.

For the powders milled at 200 rpm for 6 hrs, the samples demonstrated high notch sensitivity and consistently fractured outside the gauge length during tensile testing. This necessitated annealing at 500 °C for 10 h prior to testing to enhance ductility. Reduction in milling time from 6 to 3 hrs was also investigated in order to reduce the work hardening of the aluminium matrix and to accentuate the reinforcing effect of the CNT. The composite samples that were milled for 3 hrs and annealed at 500 °C resulted in the best enhancement in tensile strength (21%) compared with pure Al with the same process history. Also, it was proven by XRD that a nanostructure is present in all samples; that structure was retained after annealing at high temperatures. The tensile testing fracture surfaces showed uniform dispersion and alignment of the CNTs in the Al matrix.

Regarding the powders milled at 400 rpm for 30 min using two types of CNT, it was found that the aspect ratio of CNT had an effect on dispersion, carbide formation, and CNT damage. As a result, the mechanical properties of the composite were significantly affected. Despite the theoretically expected advantage of reinforcements with higher aspect ratios, it was found that the difficulty in dispersing higher aspect ratio CNTs generally led to a decrease, rather than an increase, in tensile properties and hardness. Concerning the effect of CNT content, enhancements of 96% in tensile strength, 33% in Young's modulus, and 119% in hardness were observed for the sample containing 2 wt% of the large diameter CNT.

It is thus concluded that high energy ball milling and powder metallurgy techniques are attractive manufacturing techniques for the fabrication of CNT-reinforced aluminium with enhanced mechanical properties. However, careful selection of the type and amount of CNT, the milling conditions and the processing parameters should be exercised.

ACKNOWLEDGEMENTS

I would like to express my deep appreciation to all who offered help in fulfilling this research and rendering it to such a level. First and foremost, I would like to sincerely thank my supervisor Dr. Amal Esawi for her valuable contributions to this research. Her support, guidance, effort, and encouragement were fundamental and her experience and knowledge in this field were of great importance. I would also like to acknowledge the support of Dr. Khaled Morsi at San Diego State University and his help in conducting XRD analysis as well as his valuable remarks and comments.

The Yousef Jameel Science and Technology Research Center (YJ-STRC) has provided me with financial support and state-of-the-art equipment to conduct this work. I am profoundly thankful to the entire center's staff for offering me generous support throughout my research. I would also like to sincerely thank Dr. Fadel Assabghy the center's former director and Dr. Sherif Sedky the center's new director for their continous encouragement and support.

Also, I would also like to acknowledge the financial support of the US-Egypt Joint Science and Technology Fund (grant number MAN11-011-007).

Honestly, if I wanted to express my gratitude towards my family, books could have been written. They are my everlasting source of love and inspiration, and if I were to say something today to my mother, I would say that "your love, motivation and guidance have always been and will always be in front of me".

I would like to thank my colleagues who dedicated much of their time and effort in providing me with help and support. I would sincerely thank my colleague and dear friend Eng.

Ahmed Abdel Gawad for his valuable collaboration and contribution in nano-indentation testing and analysis. Also, I would like to thank Eng. Mostafa El Borady, and Eng. Ahmed Nagi for the fruitful training they gave me on the SEM. In addition, I would like to thank Eng. Mohamed Taher for his help in the second phase of this work. Finally I profoundly thank Eng. Abdel Hamid Mostafa and Eng. Mohy El Din Safwat for their continuous help and support in many aspects of my work.

Special thanks to Eng. Hanady Hussein, Mr. Zakaria Yehia, Eng. Khaled Eraki, and all metallurgy laboratory and workshop technicians (Hussein, Saeed, Sobhy, Magdy, and Hamdy) for their support.

DEDICATION

I sincerely dedicate this work to my grandfather's soul…

TABLE OF CONTENTS

LIST OF FIGURES

LIST OF TABLES

CHAPTER 1

INTRODUCTION

1.1 Metal Matrix Composites (MMCs)

Metal matrix composites (MMCs) are composite materials in which the basic constituent (the matrix) contribute at least 50% by volume is a metal, and the reinforcements whether one element or more could be a metal, ceramic or an organic compound [1]. The materials used as a matrix in these composites are usually Al, magnesium, copper, titanium, Al-lithium, and super alloys [2]. According to Bustamanate *et. al.,* Al-based (MMC) are widely spreading and required by many industries due to their relatively low density, high specific stiffness, and wear resistance. MMC's can be fabricated by dispersing reinforcing materials that have unique physical properties such as oxides, carbides or nitrides in the Al matrix. The composite carries the applied load by transferring it from the matrix to the reinforcement. The produced composite will have combined properties of its constituting elements, and this is the main reason behind the development and success of MMC manufacturing since the type and amount of the constituents of the composite could easily be altered to obtain the desired properties of the new product [3].

There are different techniques for the manufacturing of (MMCs); classified as follows: (1) the solid state method where the constituents are processed in their solid form which is considered a PM technique. (2) The liquid state method where one or some of the constituents are processed in a liquid form such as stir casting, spray casting and electroplating. (3) The vapor deposition technique [1].

MMCs have some advantages over other types of matrix composites. For example, MMs outclass polymer matrices in having higher elastic modulus, resisting elevated temperatures, no moisture absorption, and their higher toughness and ductility [2]. Uniformly dispersing the reinforcing material in addition to using the appropriate consolidation process helps greatly in eliminating the segregation problem. Moreover, the properties of a specific MMC could easily be altered by changing the contents of the composite according to the application or even by changing the processing technique which open the way for materials scientists to excel in inventing new materials with superior properties in all aspects [4].

Powder metallurgy is considered one of the promising techniques for manufacturing MMC's, and a lot of research is currently taking place in that field. There are some constraints and parameters which guide the PM process and greatly affect the characteristics of the resulting product that will be discussed later.

1.2 Aluminium (Al)

Al is a soft silver colored ductile malleable metal that is abundant in the earth's crust. It is impossible to keep it in its pure form without chemical reactions; when exposed to air it directly forms an oxide layer on the surface which will act as a protective shield from further oxidation. It has a relatively low density compared to other metals which makes it one of the best choices for manufacturing components used in light weight applications. Using Al in its pure form is not applicable due to many factors of which the most important is the relatively low strength. That's why different Al based alloys and composites have been developed to enhance these factors while keeping most of the desired properties of the base metal (Al) present in the formed alloy or

composite. Various types of Al composites have been used extensively over the past decades in aerospace and automotive industries. [5]

1.3 Carbon Nanotubes (CNTs)

CNTs were first discovered in 1991 by the scientist Sumio Iijima. He was working in the research and development laboratory of the NEC Company in Tsukuba, Japan. First, he discovered a strange structure of carbon tubes concentric inside each other which are now known as Multi-Wall Carbon Nanotubes (MWCNT) shown in Figure 1.1 [5].

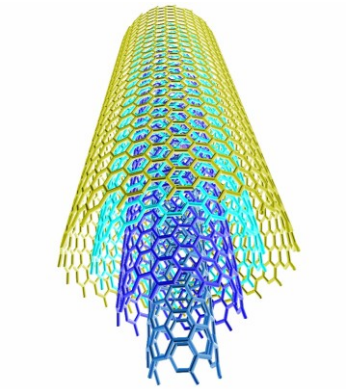

Figure 1. 1 A schematic illustration of a MWCNT. [5]

Two years later he discovered another form of CNT, the Single Wall Carbon Nanotubes (SWCNT). The SWCNT is a one-dimensional fullerene with the tubular structure of an atom. The MWCNT's have a lower aspect ratio compared to the SWCNT. The two forms of CNT have different electrical and mechanical characteristics. CNT are like rolled graphene sheets, and in the case of MWCNT many sheets are rolled over each other. The nanotubes have electrical conductivity that is equal to that of copper, and thermal conductivity that is equal to that of a diamond, and they also have excellent mechanical properties [6]. There are three main structures

for a CNT depending on their chirality: zigzag, armchair and chiral shape. What controls the final shape is related to the graphite sheet as shown in Figure 1.2.

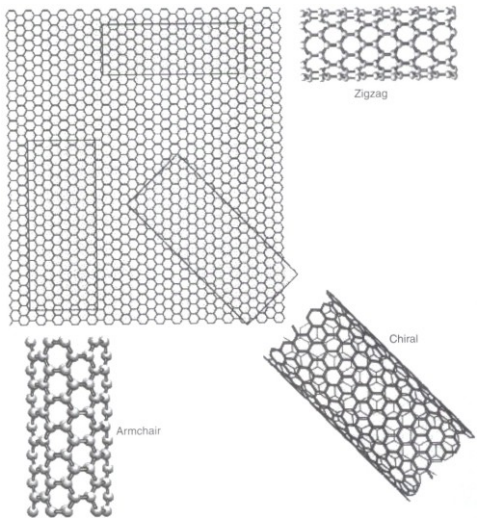

Figure 1. 2 Types of CNT structures. [7]

The mechanical properties especially the remarkable elasticity due to the high aspect ratio attracted the eyes of many researchers around the globe to try to benefit from that great discovery. There are different techniques available now for the production of nanotubes. The method and production characteristics directly affect the properties of the CNT produced.

1.3.1 Carbon Nanotubes Synthesis Techniques

There are three main techniques for manufacturing CNTs. First, the arc discharge method; this method can produce both MWCNTs and SWCNTs. In case of the MWCNTs, a direct current operates between two graphite electrodes installed in a water cooled chamber under helium gas. In case of the SWCNT, a mixture of graphite and a metal is vaporized on a composite anode. This is made by drilling a hole in the graphite anode and filling it with the graphite and metal. Many pure metals can be used such as Fe, Co and Ni. Second, the laser ablation of a carbon metal target; this method can only manufacture SWCNT using a laser pulse

to evaporate carbon metal on a composite target. Third, is the chemical vapor deposition technique; a quartz tube is installed inside a furnace. Then, a substrate is placed inside the tube. A flow of CO, methane, or ethane gas is introduced inside the tube along with an inert gas till the temperature of the furnace reaches the required limit, after which the inert gas flow is stopped. At the end of the process the inert gas is introduced again till the temperature reaches 300ºC, then the CNT can be exposed to air [7].

The high price of CNTs can be justified by their superior mechanical and electrical properties. In addition the development of synthesis techniques for CNTs has resulted in substantial reduction in the cost of production of CNTs. According to Esawi and Farag, the cheapest price is $13,000 per kg for SWCNT (purity 60%), $15,000 per kg for ARC-MWCNT (purity 30-40%), and $400 per kg for CVD-MWCNT. [8] Table 1.1 compares the different synthesis techniques for the two types of CNT.

Table 1. 1 A comparison between synthesis methods for SWNT and MWNT while presenting the pros and cons of each synthesis method [5]

Method	Arc discharge method	Chemical vapour deposition	Laser ablation (vaporization)
Who	Ebbesen and Ajayan, NEC, Japan 1992 [15]	Endo, Shinshu University, Nagano, Japan [53]	Smalley, Rice, 1995[14]
Typical yield	30 to 90%	20 to 100 %	Up to 70%
SWNT	Short tubes with diameters of 0.6 - 1.4 nm	Long tubes with diameters ranging from 0.6-4 nm	Long bundles of tubes (5-20 microns), with individual diameter from 1-2 nm.
MWNT	Short tubes with inner diameter of 1-3 nm and outer diameter of approximately 10 nm	Long tubes with diameter ranging from 10-240 nm	Not very much interest in this technique, as it is too expensive, but MWNT synthesis is possible.
Pro	Can easily produce SWNT, MWNTs. SWNTs have few structural defects; MWNTs without catalyst, not too expensive, open air synthesis possible	Easiest to scale up to industrial production; long length, simple process, SWNT diameter controllable, quite pure	Primarily SWNTs, with good diameter control and few defects. The reaction product is quite pure.
Con	Tubes tend to be short with random sizes and directions; often needs a lot of purification	NTs are usually MWNTs and often riddled with defects	Costly technique, because it requires expensive lasers and high power requirement, but is improving

1.4 Carbon Nanotubes Metal-Matrix Composites (CNT-MMCs)

As it was mentioned earlier, CNTs have extremely high mechanical and electrical properties in addition to their ultra low density, which makes them very attractive and appropriate for use as a reinforcement in composite materials. Using CNT in MMC manufacturing is very promising because this could be the way for producing lightweight, ultra high strength, and stiff products made out of Metal Matrix-Nanotubes. Morelli [9] emphasizes that there are two major problems that face scientists and researchers in manufacturing CNT reinforced composites which are: achieving a homogeneous and uniform dispersion of CNT in the matrix, and forming a strong bond at the CNT-metal interface. Lots of papers dealing with these problems have been published and some researchers were able to come up with techniques that deal with the dispersion problem, but there is no study up till now that shows a method for enhancing the bond between CNT and their matrix.

1.5 Powder Metallurgy (PM)

Powder Metallurgy deals with converting powder materials into bulk materials. The reason behind the usage and the spreading of the PM technique in many applications starting from house-hold tools and automotive industry till we reach aerospace industry lies in the ability to process a variety of materials having different physical properties [10]; Figure 1.3 represents products processed by PM.

Figure 1. 3 Products processed by PM techniques [11]

The properties of the final product processed by PM greatly depends on the accuracy of the processing technique which is common in all PM produced parts and on the secondary operations employed to the product depending on the application. The basic PM production stages are as follows: (1) powder production and preparation, (2) powder blending, (3) powder compaction, and (4) sintering of the compact. These steps are then followed by secondary operations like extrusion, forging, rolling, etc., depending on the application and structure of the final product, and some of these operations are just employed to enhance the finishing or readjust the final dimensions [11]. Figure 1.4 represents a detailed schematic of the processes and operations for manufacturing parts by PM [2].

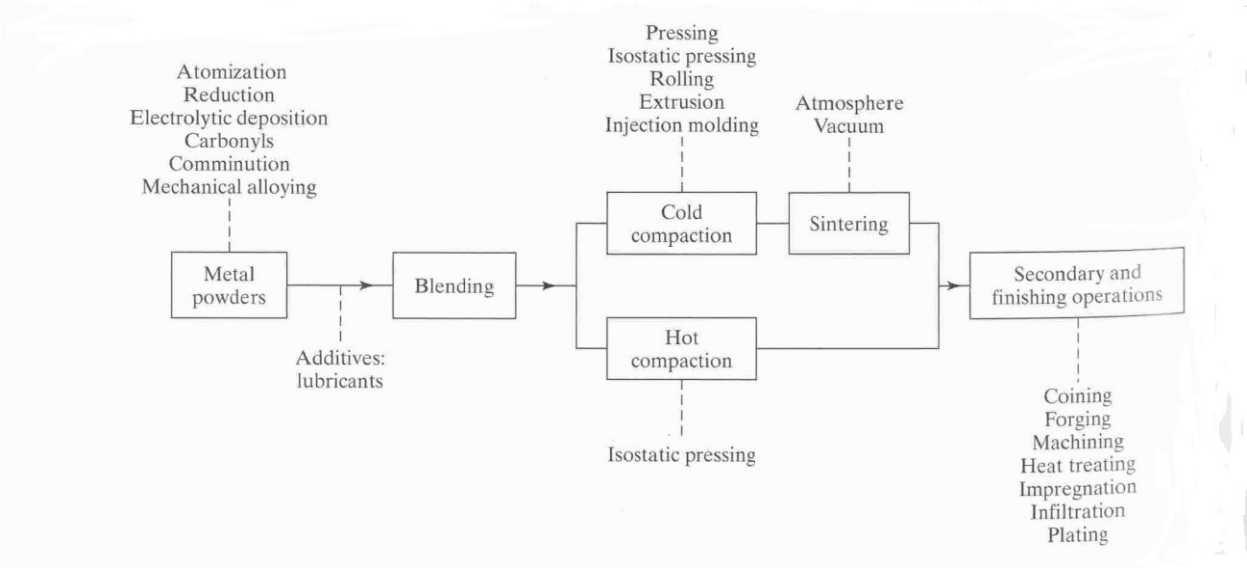

Figure 1. 4 A flow diagram of the different PM processes [2]

1.5.1 Fabrication of metal powders

There are different methods used for the production of metal powders, and the selection of the technique depends on the application and the quality of the final product. Almost all metal powders can be manufactured, and there are new techniques and enhancements that arise from time to time on the manufacturing processes to make them more economic and increase the quality of the manufactured powders. Powder production could be achieved by different techniques like oxide reduction by carbon or hydrogen, thermal decomposition of a compound, electrolysis, or precipitation of the metal. Powder characterization is performed to determine the morphology of the powder as well as the physical properties such as specific surface area, and compressibility. The powder is then separated into fractions by particle size. In addition, reduction is done to minimize the oxygen content to avoid the formation of oxides [10]. From the above mentioned techniques, atomization is considered to be a very common powder manufacturing technique, and it was the technique used for manufacturing the pure Al powder used throughout this work.

1.5.2 Powder Blending

This stage is done for several reasons such as: achieving uniform particle size, and refining the particle size. Blending could also be done for mixing more than one powder type to form a composite. Usage of a lubricant is a must to avoid agglomeration that may arise as a result of particles cold welding together [10].

1.5.3 Powder Compaction

This stage is done to fuse powder particles together in order to get a green compact. It is considered a very crucial step in the process. This stage could be done using different methods such as: cold and hot uni-directional compaction, cold and hot isotactic pressing, or rolling. [10] The focus will be on the type of compaction that is used throughout this work, which is cold uni-directional pressing. Compaction results in the particles becoming rearranged by plastic deformation because of the applied force resulting in a remarkable volumetric reduction. The particles rearrange during the compaction process and the force applied on the particles helps in filling the voids by deforming these particles plastically. The application of excessive and unneeded pressures may result in particle-interlocking, which may form stress concentrations at these points [13].

Unidirectional pressing is a traditional and one of the well known compaction techniques. After compaction the produced part is called a green compact or a preform that is ejected from the die in one piece. Densities of 90% and a bit higher are obtained after compaction. In this work the die cavity is circular and the transmission of pressure takes place from the punching plunger to the powder particles. The pressure is transmitted from the plunger axially and laterally from the die walls as a reaction to the applied vertical pressure. A good height to diameter ratio

has to be maintained to make sure that the applied pressure reached the lower sections of the compact because the pressure decreases along the section of the compact as shown in Figure 1.5. The variation of pressure is due to the inter-particle friction and the friction between the die walls and the powder particles. Lubrication is a very crucial parameter in compaction, in Figure 1.5 the difference that lubrication can do is clearly shown [14, 15].

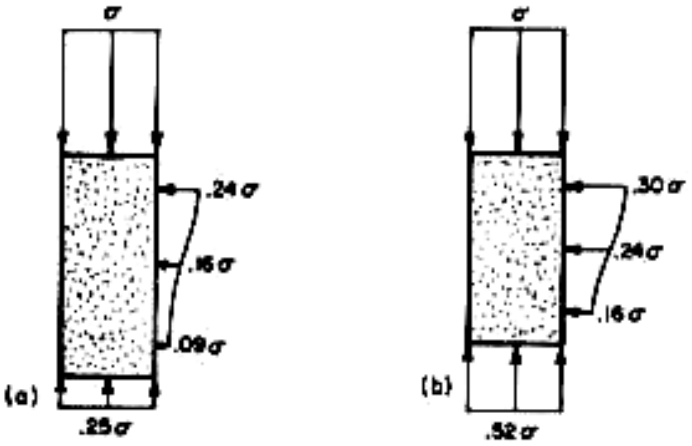

Figure 1. 5 Schematic representation of pressure variations in a unidirectional pressing die (a) without and (b) with lubricant [16]

1.5.4 Sintering

Sintering is the final operation in obtaining a bulk solid material from metal powders. Heat has to be applied to the compact achieved from the previous stage to temperatures reaching about 0.7-0.9 the melting temperature, some sources say 0.70-0.75 of the melting temperature [2, 17]. Before sintering, the compact is brittle, and its strength which is known as green strength is low. There are many variables that controls the type and the strength of the bonding between particles, and hence, that of the sintered product. These variables are; plastic flow, the mechanism of diffusion, evaporation of volatile materials in the compact, recrystallization, grain growth, and pore shrinkage [2].

The main variables in the sintering process are temperature, time, and the furnace atmosphere. There are two main sintering mechanisms; the solid-state bonding, and liquid-phase sintering. In the solid-state bonding, two adjacent particles are bonded together by diffusion mechanism as shown in Figure 1.6(a). This mechanism results in an increased strength, density, ductility, and the thermal and electrical conductivities of the compact. In liquid-phase sintering, alloying takes place at the interface of the two particles shown in Figure 1.6(b); since one of the particles may have lower melting point than the other, it melts and surrounds the particle that hasn't melted. This method helps in obtaining stronger and denser parts. A very well known problem that may occur in this type of sintering is segregation, which occurs due to the effect of gravity causing higher concentration of the heavier metal at the bottom. In general, the supplied heat in all sintering processes helps in joining adjacent particles by lowering the energy of the system and reducing the surface area of the particles. The sintering process could be concluded in three fundamental steps [2]:

- Initial contact formation between particles
- Neck growth, which occur at the boundaries between the particles
- Coalescence of the particles together

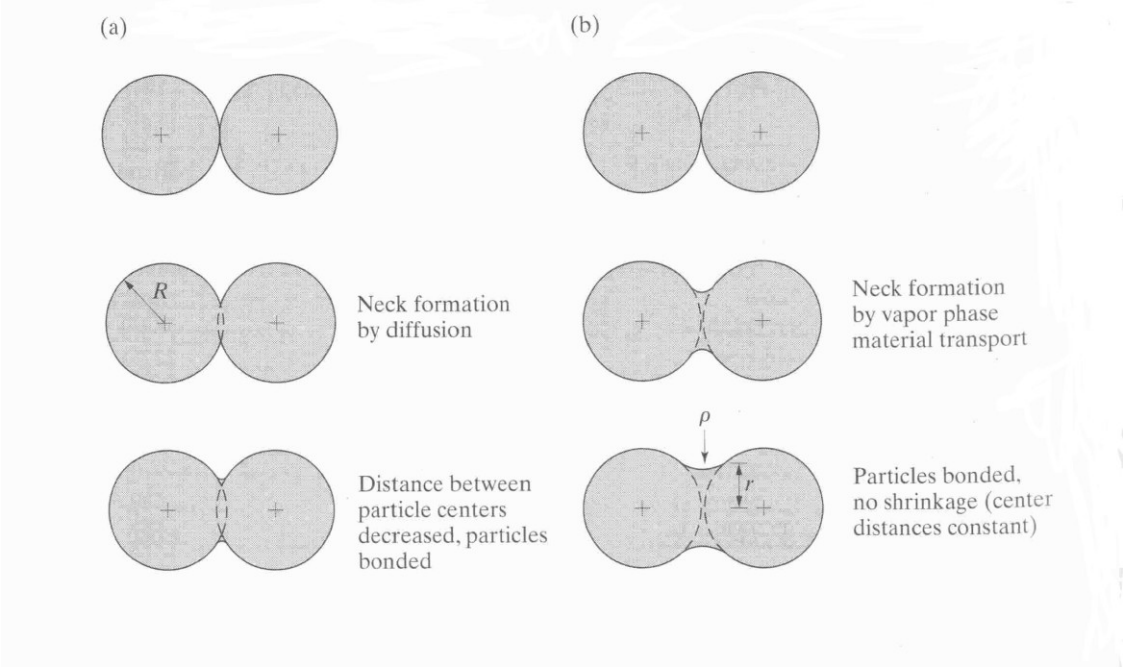

Figure 1. 6 sintering by solid-state bonding (b) sintering by liquid-phase bonding. [2]

Compaction and sintering could be done in one step, and this is done by hot compaction where a lower pressure is needed in compaction because heat compromises pressure in bringing the particles close together by reducing the pressure needed for plastic deformation. Another sintering method that is still in the experimental stage is spark sintering. In this process the metal powder is placed in a graphite mold and heated by means of an electric current, and compacted in one step. The rapid discharge helps in eliminating contaminants and oxide coatings in case of Al from the surface of the particles which helps in enhancing the bonding between particles [2, 17].

1.5.5 Forming of the sintered powders

There is a wide variety of processes for forming the sintered product into the desired final shape with the desired final properties according to the application. Some of these processes are: extrusion, rolling, and forging. The importance of these processes is not only in forming the

sintered product into the desired shape but it also lies in improving the mechanical and structural properties of the bulk material via enhancing the density of the final product by eliminating voids and maybe any immaturity in the sintering process.

1.5.5.1 Extrusion

Extrusion, which is the process used in this work, is simply defined as forcing a billeted material with a certain cross section to gradually flow through an orifice with a smaller diameter at a constant velocity. The process is used to transform powder or bulk metal processed by different means into the desired final product such as tubes, rods, and many other types of sections depending on the extruder die. Figure 1.7(a,b,c, and d) shows the different types of extrusion techniques [2].

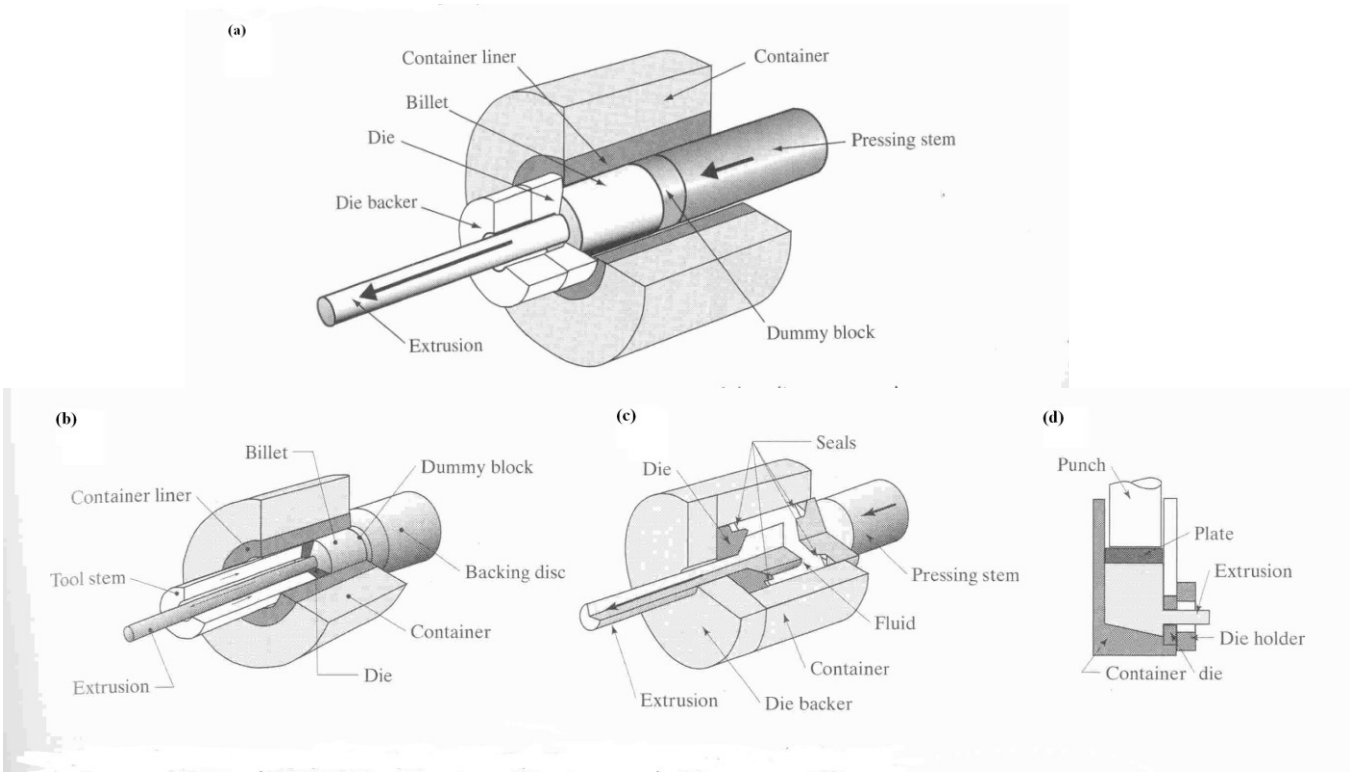

Figure 1. 7 (a) the direct extrusion process, (b) indirect extrusion process, (c) hydrostatic extrusion process, (d) lateral extrusion process [2]

This process became famous and widely used as a forming process because it helps in eliminating voids, refines the microstructure, and minimizes segregation. The reduction ratio in cross section before and after extrusion is determined according to the required overall material properties after extrusion. The ratio is determined according to equation 1.1 for cylindrical dies [4], and it controls the amount of strain induced in the material, and as the ratio increase better material properties are obtained and better grain refinement is guaranteed [10].

Since Al is known for its ductility and the flexibility of its slip systems, it can allow for high extrusion ratios if compared to other metals. The extrusion process is employed in the preparation of various Al MMCs by PM. The reason behind this is accredited to the process ability to maintain a uniform distribution and partial alignment of the reinforcement in the matrix which is important in order to obtain the desired isotropic properties of the composite, and this was reported by many researchers using this technique [2, 4].

$$\text{Extrusion ratio} = \frac{A_f}{A_i} = \frac{d_f^2}{d_i^2} \qquad \text{……..……..(1.1)}$$

Extrusion can be carried out at elevated temperatures, and this is done for a number of reasons; for materials that do not have enough ductility at room temperature, reduce the extrusion forces, or to control the properties of the extrudate such as: recrystallization, grain size, etc. The determination of the temperature at which the operation takes place is always dependent on the recrystallization temperature of the material because this helps in obtaining a denser final product with better mechanical properties [2, 4].

Hot extrusion has some special requirements due to its high operating temperatures. For example, die wear can cause problems, and the cooling of the billet due to the different temperature gradients between the billet and the die can be a problem resulting in highly non uniform deformations as shown in Figure 1.8(b), and (c).

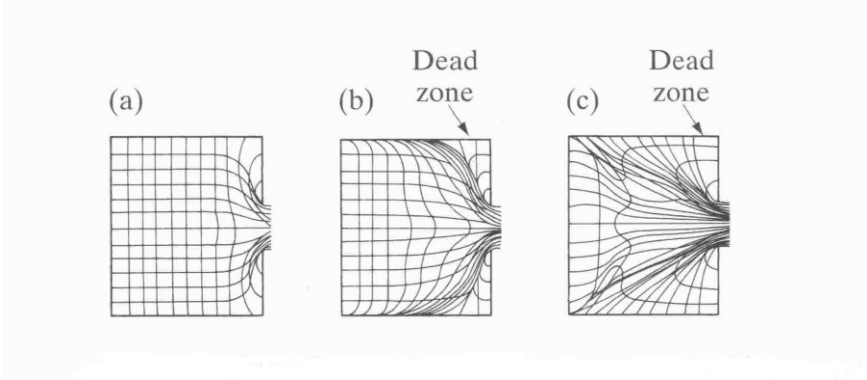

Figure 1. 8 (a) low friction flow pattern, (b) high friction at billet chamber interface, (c) high friction or cooling of the billet's outer regions [2].

These problems can be easily solved by preheating the extrusion die. Another problem is the abrasive oxide film that develops at the interface between the billet and the die, this occurs mainly because the billet is hot and can only be avoided if the heating took place in an inert atmosphere. This oxide film could affect the flow pattern of the material, and result in an unacceptable output concerning the surface finish. In order to avoid this oxide shell from being extruded the backing disk pushing the billet during extrusion is made smaller than the container with an allowable tolerance, leaving that layer to stick on the walls of the die which can be removed later [2].

In some cases hot extrusion replaced sintering and other kinds of heat treatments because it could combine more than one PM process step in one. Examples of powder metallurgical

extrusions done using hot extrusion are Powder direct extrusion, extrusion of pre-compacted powder either sintered or not, and extrusion of canned powder [4].

1.5.6 Advantages and disadvantages of PM [2, 17]

PM is considered superior to many traditional manufacturing processes. It has many advantages in various research and industrial aspects. On the other hand, like any technique PM has its problems and drawbacks that researchers are working hard on minimizing. Here are some of these pros and cons in points:

Pros:

1. PM can be used in the processing of nanosized powder materials into bulk and final desired shapes.
2. PM is considered to be very effective in terms of the final product quality and price.
3. PM is very useful in the processing of high performance materials like MMCs, superalloys, and tool steel in to final products taking into consideration the feasibility aspects of the product.
4. PM helps in utilizing the raw materials by eliminating some of the finishing manufacturing processes because it produces net shape products.

Cons:

1. The PM processing die is considered to be relatively expensive because it is designed to withstand and tolerate friction, and high pressures induced during the process.

2. The PM processing technique has some constraints concerning the design which in turn imposes some limitations on the production of certain components.
3. The PM process is considered to be extremely hazardous because the fine powders used might be very harmful on human health, the thing that requires the applications of strict safety precautions during the powder processing.

1.5.7 Using PM in Producing MMCs

The usage MMCs is increasing day after the other and is considered a breakthrough in materials science due to the fact that these materials are known for their high strength, stiffness, toughness, and wear resistance. MMCs are produced by the PM technique by dispersing a reinforcing material with a concentration below 50% inside the metal matrix, and the resultant will be a composite material with combined properties from both constituents. The good connotation of PM is that it eliminated one of the traditional ingot metallurgy most tiring processing problems that is segregation which has a negative effect on the mechanical properties of MMCs. The key behind segregation lies in material properties related issues like: density, particle size, and the flow characteristics between the constituents. By controlling the particle size and morphology of materials produced by PM it has become possible to improve the bonding between the MMC constituents [1].

1.6 Mechanical Alloying via Ball Milling

Mechanical alloying is defined as "powders of two or more pure metals mixed in a ball mill. Under the impact of the hard balls, the powders repeatedly fracture and weld together forming alloy powders" [1]. This technique is considered to be economical and unique in the fact that all reactions occur in the solid state in different media (gas, vacuum, or liquid.) That kind of

alloying is different from traditionally casted alloys in the sense that no melting took place in the process, which leaves us with option of using immiscible materials in the process and experiencing new kinds of materials bonding outside the boundaries of phase diagrams. There are different aims behind using a ball mill, it could be used for: particle size reduction (grinding), strain hardening, mixing, and mechanical alloying. The procedure is as follows, the powder or powders to be milled are put in jars (steel, agate, etc.) with or without the presence of grinding balls (steel, titanium carbide, agate, etc.) to create a grinding medium according to the application. In case of powdered composites this method was used successfully to disperse a variety of reinforcements in different matrices [18, 20].

1.6.1 Ball Milling parameters [20, 21]

1.6.1.1Types of Ball Mills

Ball mills can be classified into two main types: high and low energy ball mills. The high energy mills are considered to be new in the field of milling, and with their appearance new terminologies and techniques like mechanical alloying started to be spoken of. There are many types of high energy mills available such as: attrition ball mill, planetary ball mill, vibratory ball mill, and spex mill. The most popular and spreading type is the *planetary ball mill*, and its significance comes from its ability to mechanically alloy different powders and form composites. A detailed description of its theory and operation will be discussed later. Another type is the attrition ball mill where milling occurs by the stirring action of a rotating container called agitator, which is connected to a rotating shaft through the impellers. The speed of this type varies but it can only reach a high speed of 500 rpm and its capacity is 3.8×10^{-3} m^3. The vibratory ball mill is considered a very specialized kind of mill that is specifically used when preparing amorphous alloys, and in this case the milling is done in three directions.

1.6.1.2 Milling container

Container sizes depend on the mill type and size. It could be in different shapes but at the end it's a closed container filled with powders and balls for grinding. Container materials vary according to the application but the most common types are made out of: steels, agate and maybe titanium.

1.6.1.3 Milling media

Milling media means the grinding balls or rods. They are added to the powder mixture in ratios depending on their type, size, shape, and the powder mixture itself. Of course the ball to powder ratio whether by weight or volume is very important to be chosen wisely when dealing with the conditions of milling. There is a wide variety in the type of the balls used, it could be made out of: stainless steel, chromium steel, tempered steel, or titanium. In addition, a material like agate could be used because it has special properties concerning heat dissipation so it could be useful if the heating of powders is undesirable.

1.6.1.4 Milling speed

Milling speed is a very important factor that has to be chosen wisely along with other milling parameters. The variation of milling speed results in the variation of the energy generated inside the jars. This is because of the increased number of collisions and collision forces between the milling media and the powders. Increased energies might be beneficial in the sense of enhancing diffusion or providing the atmosphere for exothermic reactions to occur. On the other hand, the high energy could be non beneficial because it results in the presence of high energy which might result in grain coarsening. In addition, if the milling speed exceeds the limits, the

balls might stick to the walls of the jars resulting in decreasing the milling efficiency. A good compromise must be made when choosing the speed putting in mind all these effects.

1.6.1.5 Milling time

Milling of powders passes through stages starting with fine powder; then, due to ball milling they are turned into flakes which are cold-welded together forming spherical particles. The resulting spheres grow in size due to the effect of cold welding. Yet, the growth of the spherical particles is ceased by the effect of strain-hardening. As the milling media gets more brittle, the formed spheres are reduced back in size till, eventually, reaching a steady state where the particles becomes uniform. If the milling time extends for long durations contamination increases, and undesirable phases or compounds start to appear.

1.6.1.6 Process control agents PCAs

Also called surfactants or lubricants, they are used as a lubricant to decrease the effect of cold welding in ductile materials. The amount used usually varies between 1 to 5 wt. percent of the powder charge but the exact amount used is subject to change based on the material and other milling parameters. The most commonly used PCAs are: ethanol, stearic acid, benzene, and wax.

1.6.2 The formation of nanocomposites by mechanical milling

During the process the powders collide with the grinding balls creating high pulverization energy which is responsible for introducing lattice defects that cause the powder particles to deform plastically. The temperature resulting from the energy created is estimated to be varying between 100 and 200° C depending on the speed of the mill, vial size, number of balls, and their weight. As the process continues, the powder particles fracture and the reinforcement particles are cold welded to the matrix particles and this occur at the atomic scale. Further milling leads to

the enlargement of the forming particles with reinforcement as an intermediate phase appearing inside or at the surface of these particles. After several hours of ball milling, the particles are expected to fracture again into submicron matrix particles with fine dispersion of the reinforcement phase. Those stages could occur repeatedly if the process continues and this was proven by scanning electron microscope which could easily track the particle morphology at different milling times. Figure 1.9 shows the composite formation stages just described in 5 steps during milling [22].

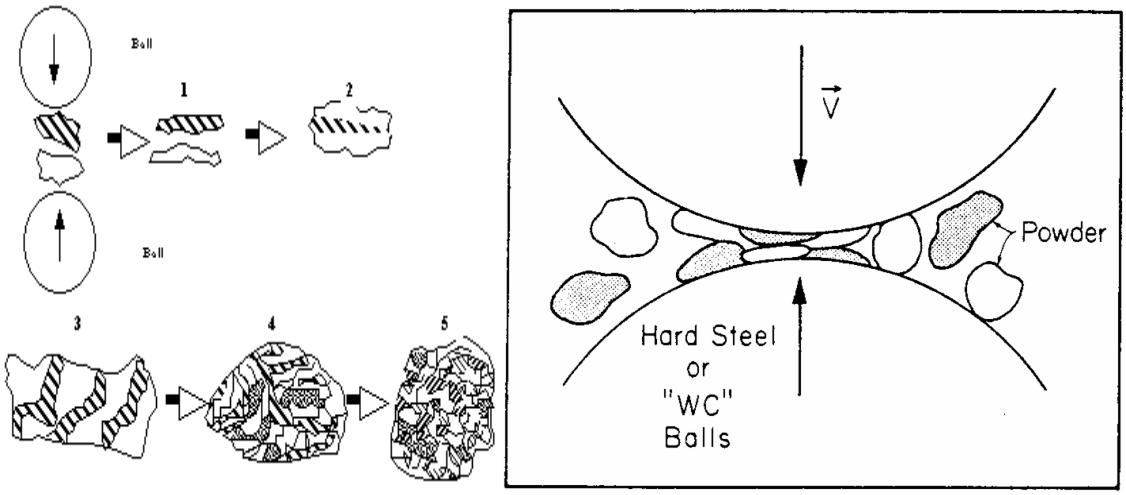

Figure 1. 9 General behavior of the powder particles during mechanical milling process [22]

At some point the rate of fracturing could be higher than that of welding which causes particle refinement on a large scale. Consequently, the internal structure decreases in size and could reach the nano dimensions in a matter of hours as it appears in Figure 1.10. Controlling the balance between cold welding and fracturing is not easily done and is considered a main issue in the milling process. This balance is obtained after increased milling time depending on the powder materials and their concentration in addition to other milling parameters, and that balance is usually reflected by the particle size uniformity [18].

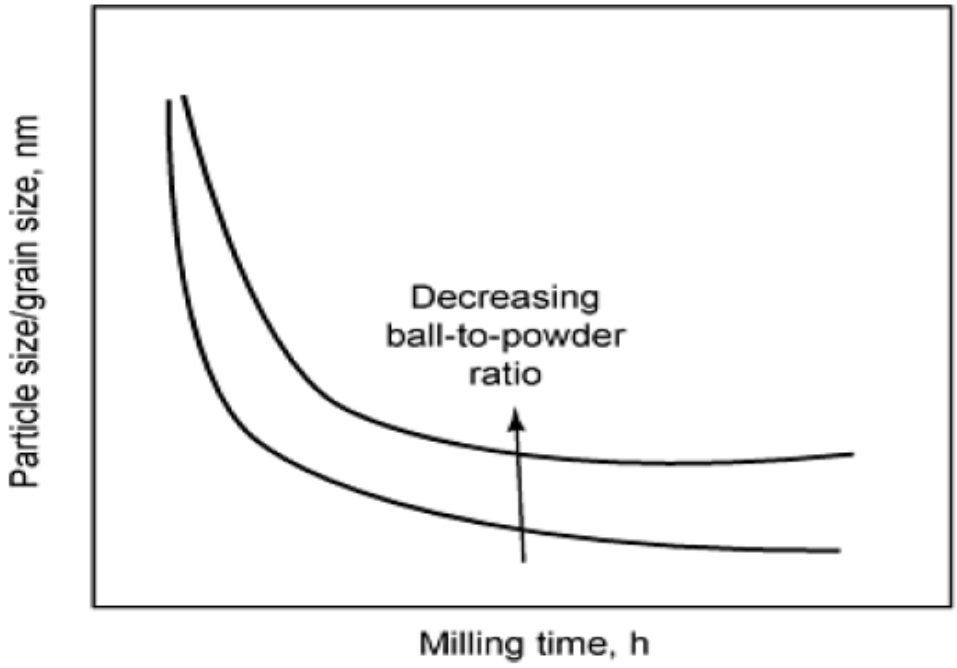

Figure 1. 10 The refinement of particle size with increasing milling time [18]

1.6.3 Dynamics of a planetary ball mill [18, 20, 23]

The size reduction and mixing effect produced by the planetary ball milling is due to the dynamics of the motion of the jars and the balls. As the sun wheel rotates, the jars rotate in the opposite direction with a certain speed ratio. The movement inside the jars is affected by 2 forces:

Friction effect:

The centrifugal force created by the rotation of the jar around the axis of rotation of the sun wheel and the *Coriolis* forces resulting from increasing the rotational speed of the jar.

Impact effect:

As the jars rotate the balls inside rotate in the same direction sticking with the walls of the jars until the effect of the impact forces resulting from *Coriolis* forces appear causing the balls to be pushed away from the container walls. This behavior was found to be helpful in:

1. Creating high pulverization energy resulting from the combination of the centrifugal force and impact forces, which result in size reduction down to 1μm.
2. Effective mixing because the balls do not stick to the jar wall.

Figure 1.11(a) represents the interaction between the powder particles and the balls in the milling media in the presence of different forces emerging from the jar rotation. Figure 1.11(b) represents the impacts of the balls with powder particles.

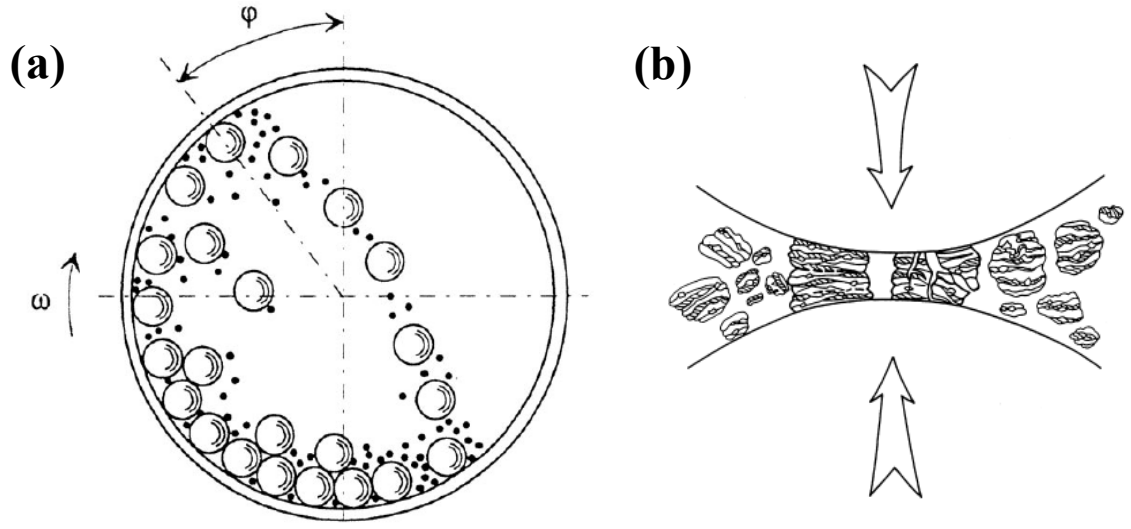

Figure 1. 11 (a) a schematic representation of a ball mill vial showing the impact of milling media on powder particles, (b) Ball-powder-ball impact [22]

CHAPTER 2

OBJECTIVE

The aim of this work is to fabricate carbon nanotube-aluminium composites with well dispersed CNTs and to investigate their mechanical properties. In addition, the effects of CNT content as well as CNT aspect ratio on the mechanical properties are investigated. Ball milling conditions that lead to uniform dispersion of the CNTs, minimum matrix strain hardening and minimum CNT damage are also investigated.

CHAPTER 3

LITERATURE REVIEW

3.1 Fabrication and characterization of Aluminium-CNT composites using different techniques

The literature on Al-CNT composites is limited to a few number of published papers. There have been a lot of trials to produce Al-CNT composites using different types and sizes of CNT synthesized using the different techniques that were discussed earlier in the introduction chapter. Processing Al from its powder form using PM technique is one of the famous methods used to produce a bulk material Al-CNT composite due to the low vaporization temperature of CNT. Three mixing or deposition techniques have been used for Al-CNT composites; first, the matrix metal can be deposited on the CNT directly forming the composite. Second, the CNTs also can be mixed with the metallic powder, for example by ball milling, turbula mixing, or sonication, and then the resulting mixture powder is processed into bulk material using PM techniques. Third, the mixture powder could be deposited on a substrate and after the deposition is complete the substrate is removed (the plasma spray forming process). The second processing technique happens to be the most widely researched and is the one used in this study.

3.1.1 Processing of Al-CNT canned powder via compaction and hot extrusion

The first breakthrough was published by Kuzumaki *et. al.,* He was using CNTs which were synthesized using arc discharge. The purity of CNT used was reported to be about 60% by volume which, compared to CNT produced nowadays, is considered low. He mixed 5 and 10% volume of CNT with pure Al and stirred the mix in ethanol for half an hour in order to disperse

CNT. The mix was then dried and packed in an Al case. The case was preheated and compressed in a steel die, then hot extrusion was performed at 773 K. Several characterization techniques were performed, but the significant results came from the tensile strength and elongation percentage tests versus annealing time. Figures 3.1, 3.2 show that 5 and 10 % vol. CNT prohibits the deterioration in the tensile strength as the annealing time increases, also it prevents the percentage elongation from increasing as annealing time increases [25].

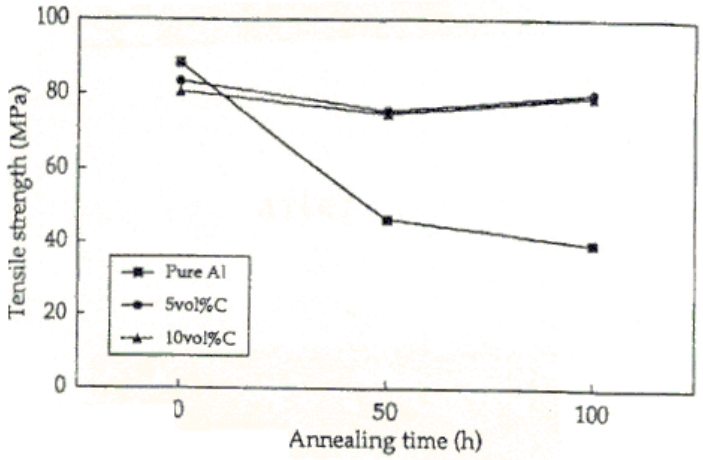

Figure 3. 1 Tensile strength vs. annealing time at 873 k. [25]

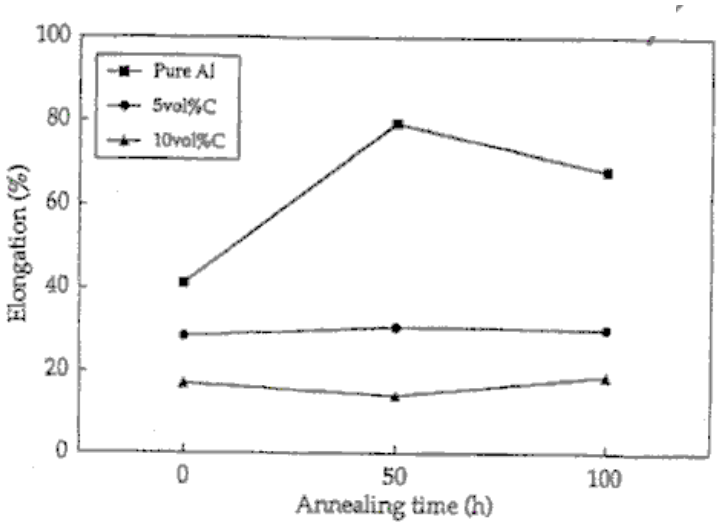

Figure 3. 2 Elongation vs. annealing time at 873 k. [25]

Five years later a paper published by Zhong *et. al.,* discussed the effect of mixing SWCNTs with 50 nm Al powder. The processing of the powder was done nearly the same way as Kuzumaki *et. al.,* [25] did, except that the sintered compact was not extruded. The coefficient of thermal expansion was measured in a 15% vol. CNT and was found to be 65% less than the unreinforced Al. Also, a noticeable increase in hardness was recorded for the composite compared to the unreinforced sample [26].

3.1.2 First ball milling attempt in the presence of a wetting agent

The year 2005 witnessed the first attempt to mix Al-CNT powders using ball milling. It was done by George *et. al.,* He used MWCNT synthesized by the arc evaporation method, and ball milled it with Al powder for 5 min after sonication in alcohol for 20 min. The reason for the short milling time came from the author's belief that long milling times will damage the CNT. K_2ZrF_6 was added to the composite samples. The mixture was compacted in a cylindrical die under the load of 120 KN. The billet was then sintered at 580ºC for 45 minutes under nitrogen atmosphere then extruded at 560ºC. The results obtained from the Raman spectroscopy and TEM images (Figures 3.3, 3.4) shows that the CNT was not damaged by the process, and that there were no chemical reactions what so ever and that there were no carbides formed at the interface [27].

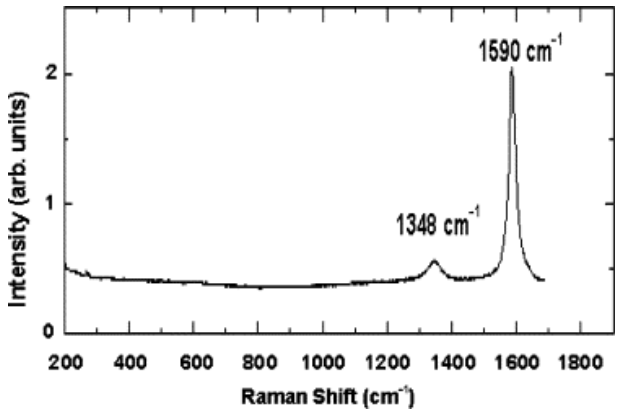

Figure 3. 3 Raman Spectroscopy of MWCNT [27]

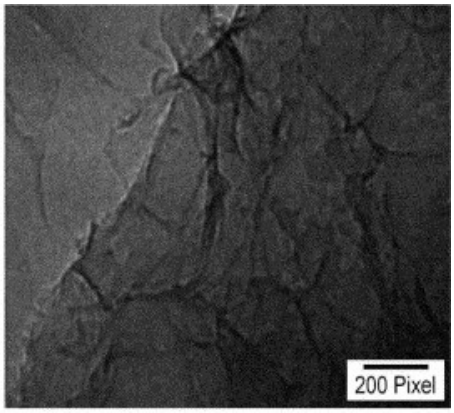

Figure 3. 4 TEM image of MWCNT/Al composite [27]

Another important conclusion from George's *et. al.,* work was the positive effect of adding K_2ZrF_6 as a wetting agent. The ultimate tensile strength was noticeably increased especially when K_2ZrF_6 was added to the SWCNT composite. The author claims that the increase in UTS came from the effect of K_2ZrF_6 which from the author's point of view partially wetted the surface of the CNT. In addition, young's modulus increased with increasing the CNT content but wasn't affected by the existence of a wetting agent. These results comply with the values calculated by the shear lag method with a small error. Yield strength increased with the addition

of wetting agent and with increasing the CNT content as well, which emphasizes the applicability of the shear lag model concerning the interaction between CNT and matrix [27].

3.1.3 Interfacial Al-CNT reactions

In the following year Ci *et. al.,* published a paper investigating the interfacial region of the Al-CNT composite. He used conventional MWCNT which were aligned vertically (as shown in Figure 3.5) to produce composite films which were fabricated by sputtering pure Al on the surface of the aligned CNT. He used hot pressing and sintering to process the composite, and then annealed them at temperatures ranging between 400-950 degrees Celsius to investigate the interfacial behavior. [28]

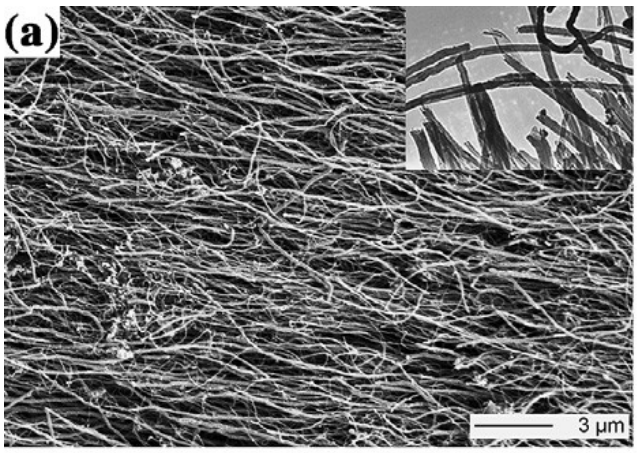

Figure 3. 5 SEM image of surface structure of the CNT film [28]

From the XRD results (shown in Figure 3.6) it was found that there were several new peaks for the samples processed at lower temperatures. TEM studies revealed that Al-C reactions occurred at locations containing amorphous carbon, at defect sites and at open ends of CNT; this is pointed out in Figure 3.7 [28].

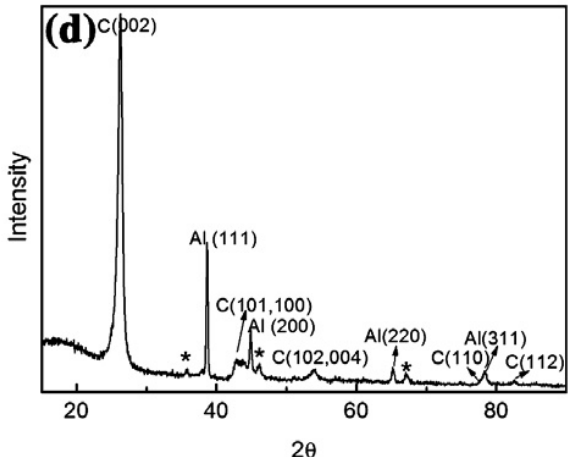

Figure 3. 6 The possible carbide phase [28]

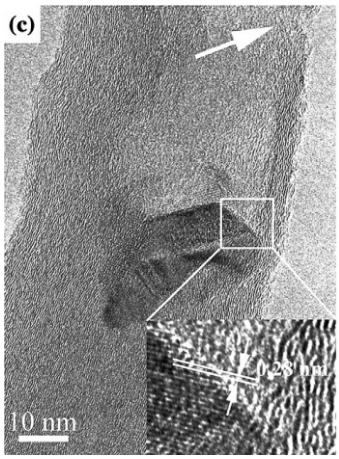

Figure 3. 7 HRTEM image showing reaction between Al and CNT at 650 degrees Celsius [28]

SEM investigations of samples annealed at temperatures higher than the melting point of Al showed a change in the morphology of the composite film. Al beads were formed on the surface of the films due to the poor wettability between Al and CNT. There were irregular shaped particles formed at the end of the CNT which were forming a bond with them as well as the Al beads. These particles were nano-sized. The author claim that these whiskers are carbides which may enhance the mechanical properties due to the improvement in interfacial properties.

Since the carbide particles are nano-sized and finely dispersed in the matrix, they could strengthen the Al composite by precipitation hardening. The author emphasized that the problem with using temperatures higher than the melting temperatures of Al lies in the severe reactions which may affect the mechanical properties of CNT. It was concluded based on the above results that powder metallurgy involving temperatures lower than the melting point of Al might be the best technique of choice to manufacture Al-CNT composites. Also, it could be inferred that using amorphous MWCNT with carbon deposited on the outer layer might be the best choice when preparing such composites because the defects and carbon will encourage a reaction to take place at the interfacial region [28].

At high temperatures, a reaction may occur in CNT reinforced Al between the Al and the carbon to form Al_3C_4 on the interface taking the shape of needles which reduce the composite strength. Xu *et. al.,* reported the presence of some Al carbides in an Al-CNT composite manufactured by hot pressing. Also, Zhang *et. al.,* and other researchers observed the formation of Al carbides when the Al-CNT composite was subjected to 800ºC for one hour [3, 25, 26, 29, 30].

These findings were further proved by Deng *et. al.,* who used sonication and ball milling but with a different matrix; 2024 Al alloy powder with particle size of about 50 μm. A 95% pure MWCNT was used. The CNT went through several purification steps to enhance its dispersion and purify it more. It was treated using concentrated Nitric acid for 10 hours at 120ºC then washed by distilled water several times to completely remove acid. The Al alloy powder and the CNT were sonicated for 30 minutes using a mechanical stirrer to help achieving a good dispersion. The mixture was dried in vacuum at 120ºC and ball milled for 10 minutes. Several

mixtures were made with CNT% ranging from 0-2%. The mixture was then cold pressed at 300 MPa, and the billet was extruded at 460ºC. The author claims that the cold pressing was preferred in order to avoid any reaction between the CNT and the Al which he proved to exist if high temperature was used during the manufacturing process of samples. A 5 wt% CNT was prepared using the same technique and heated to 800ºC during manufacturing. was examined by the TEM imaging shown in Figure 3.8 revealed that there were no CNTs at all in the sample; just needles of Al_4C_3 with almost the same dimensions of the original CNT which suggest that the CNT reacted with the Al and formed Al_4C_3 in the alloy; mostly at the grain boundaries but some of them were found inside the grains as well [31].

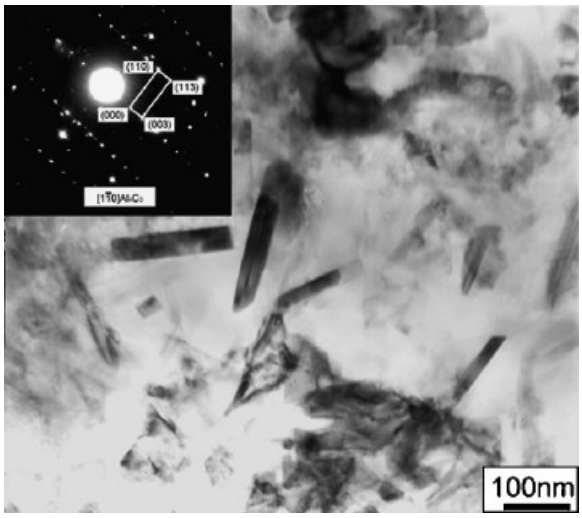

Figure 3. 8 TEM images of Al4C3 phases [31]

Figure 3.9 shows the difference between the raw and purified CNT. The black areas in the raw CNT represent Lanthanum and Nickel which were removed through the purification process [31].

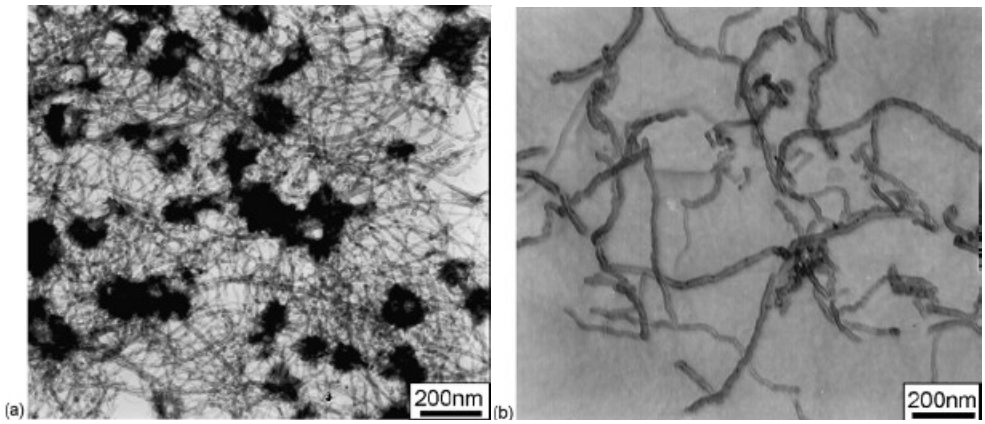

Figure 3. 9 TEM images of CNTs (a) raw CNTs; (b) purified CNTs [31]

The author argued that the nitric acid treatment is expected to introduce the functional groups OH and >C=O to the CNT surface which will reduce the Van der Waals forces to facilitate binding with the metal and reduce agglomeration [31].

Based on what Edtmaier *et. al.,* mentioned in reference to work done by different researchers, melting the metal in some cases did not wet the surface. Also, metals with low surface tension ranging between 100-200 mN m^{-1} could wet the surface of CNT. These properties are only found in specific elements in the periodic table such as S, Cs, Rb and Se. These elements were capable of wetting the surface of CNT [32]. These findings made researchers shift their concentration to another method to achieve a strong Al-CNT bonding. Researchers are trying to modify the surface of CNT by oxidation in order to obtain nucleation of metal compounds on the CNT surface. Decorations such as Hydroxyl (OH), and Carboxylic (COOH) groups are of the most common groups that are added on the surface of CNT to nucleate the metal onto the surface. Ang *et. al.,* argued that chemical methods used for deposition will cause an uneven distribution of metal on the surface due to the low density of the decorations. In addition, the nanotube surface does not catalyze the metal [33].

3.1.4 Using Nano Sized Al Powder as a Starting Material

Zhong *et. al.,* examined the effect of Al nano-powder on the dispersion and the properties of the final composite. [26] The Al powder used was made by the active H_2 plasma evaporation method. [34] The particle size was about 50nm as identified by the X-ray diffraction (XRD), with a spherical shape and a thin layer of Al_2O_3. The CNT used was manufactured by a semi-continuous hydrogen arc discharge method [35]. 5% SWCNTs were stirred for 30 minutes with Al powder in the presence of ethanol then dried in an ultrasonic stirrer. The mixture was compressed into a disk with a diameter of 9 mm and thickness 1.2 mm under 1.5 GPa of pressure at room temperature. The sintering process took place at a temperature ranging from 260-480ºC for 30 minutes under 1 GPa of pressure. This caused the Al nano particles to grow slightly. Figure 3.10 shows an Al particle which grew to a size of 800 nm. Figure 3.11 shows a SWCNT which proves that they were not damaged by the high pressure applied during compaction and sintering [26].

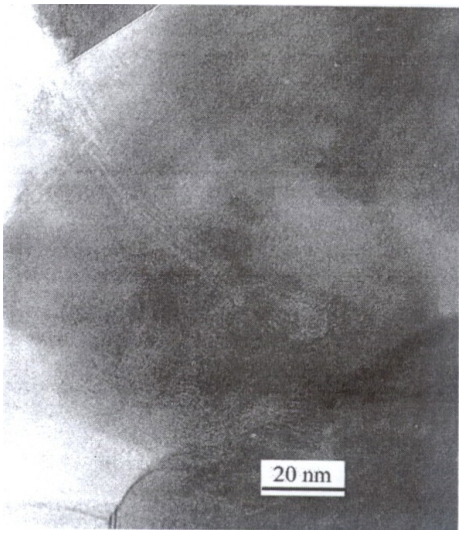

Figure 3. 10 TEM image for a nano Aluminium particle grown abnormally [26]

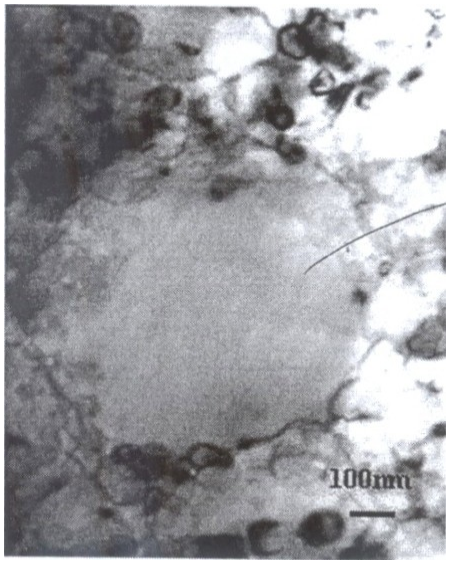

Figure 3. 11 A bundle of SWCNT found intact in the matrix [26]

The hardness of the pure nano Al and the SWCNT reinforced Al samples were measured at different consolidation temperatures, Figure 3.12. The hardness of the pure nano Al increased from room temperature till 320ºC reaching 1.69 GPa then declined, while the composite had a maximum hardness of 2.89 GPa at 480ºC then declined rapidly. The author claims that the hardness increase is mostly due to the bonding that took place between the Al particles during sintering, while the decline is due to the grain growth. The reinforced Al experienced hardness 178% greater than that of the pure nano Al and about 20 times higher than the as cast pure Al. [26]

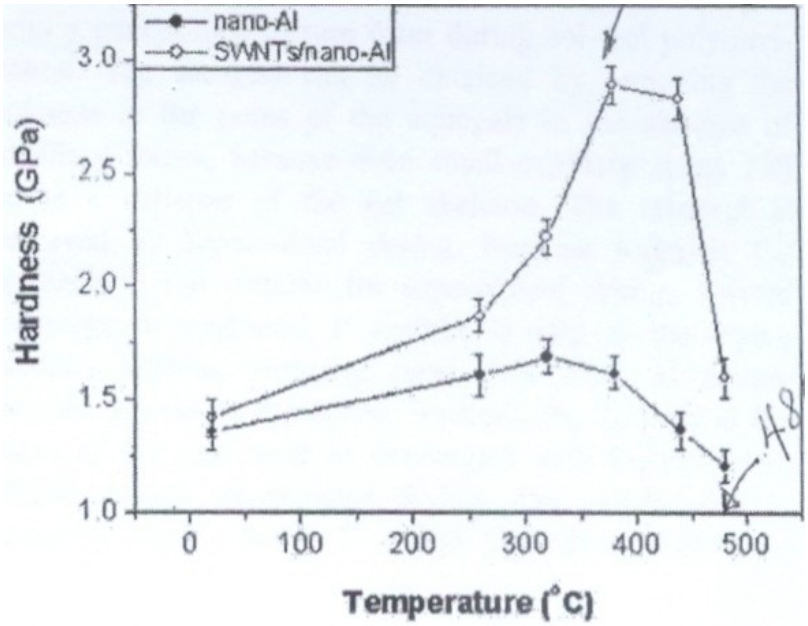

Figure 3. 12 The change in hardness with the consolidation temperature for pure and composite maaterial [26]

3.1.5 Dispersion of CNT in Al powders

A paper published by Esawi and Morsi, investigated the morphological changes occurring when ball milling Al powder with 2wt% CNT and focused on the effect of milling on the dispersion of the CNTs. A comparison was made when Al-CNT powders were mixed using dry mixing techniques and when using high energy ball milling. Images taken by FESEM showed that CNT agglomerates still existed after 8 hours of dry mixing (Figure 3.13) whereas after only 0.5 hours showed that CNT were dispersed on the surface of the Al particles (Figure 3.14). After 48 hours of milling, individual CNTs were still observed at high magnifications embedded inside the large Al particles, as shown in Figure 3.15. The large particles obtained from milling the 2% wt CNT for prolonged times shown in Figure 3.16 were a result of the high ductility of Al which promotes the cold welding of Al flakes. The most useful conclusion from this experiment is that it proved the CNT could survive the severe conditions of ball milling for

long times by being embedded inside the soft Al matrix. Additional experiments by Esawi and Morsi with 5wt% MWCNT, showed that Al particle size is influenced by the CNT content of the composite [36, 37].

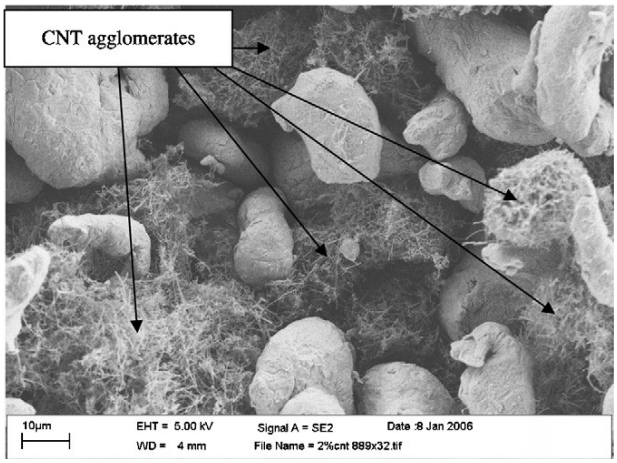

Figure 3. 13 Clusters of CNT after dry mixing [36]

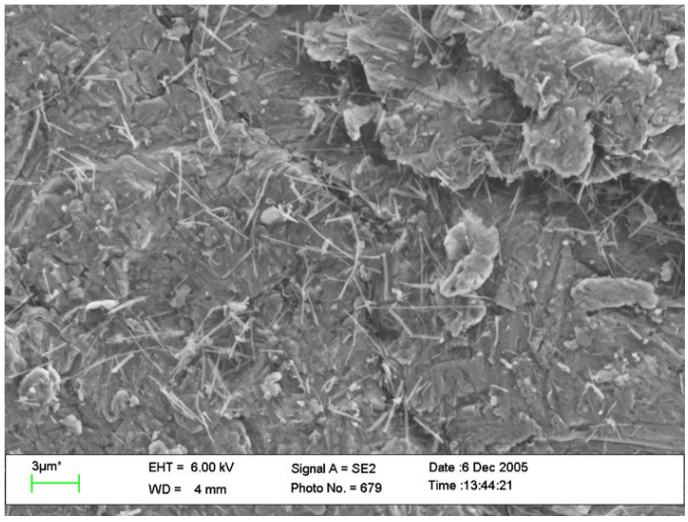

Figure 3. 14 Dispersed CNT after 0.5 hours of ball milling [36]

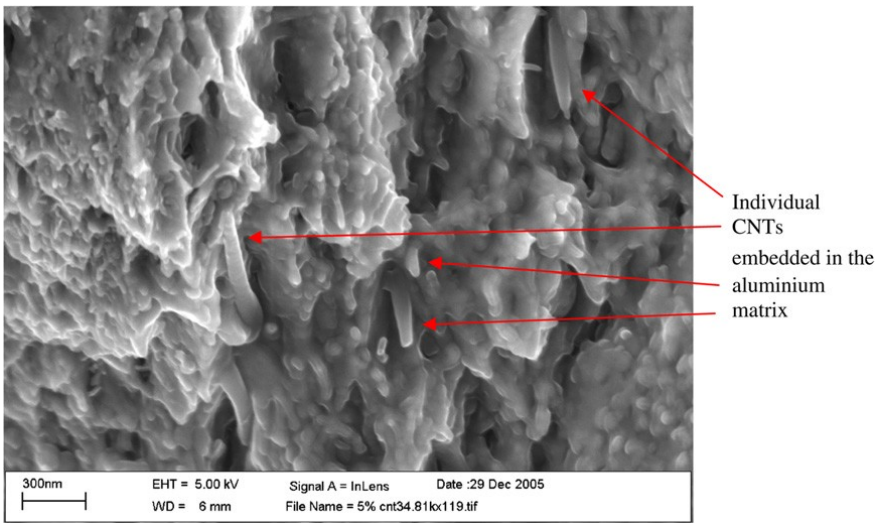

Figure 3. 15 2wt% individual CNTs after 48 hrs milling [36]

The results from this experiment oppose the results of Ang *et. al.,* [33] who processed Cu-CNT by ball milling and came to the conclusion that high energy ball milling resulted in nanotube degradation to amorphous carbon, a problem which has also been reported by Edtmaier *et. al.,* [32] who mechanically alloyed Al-CNT mixtures.

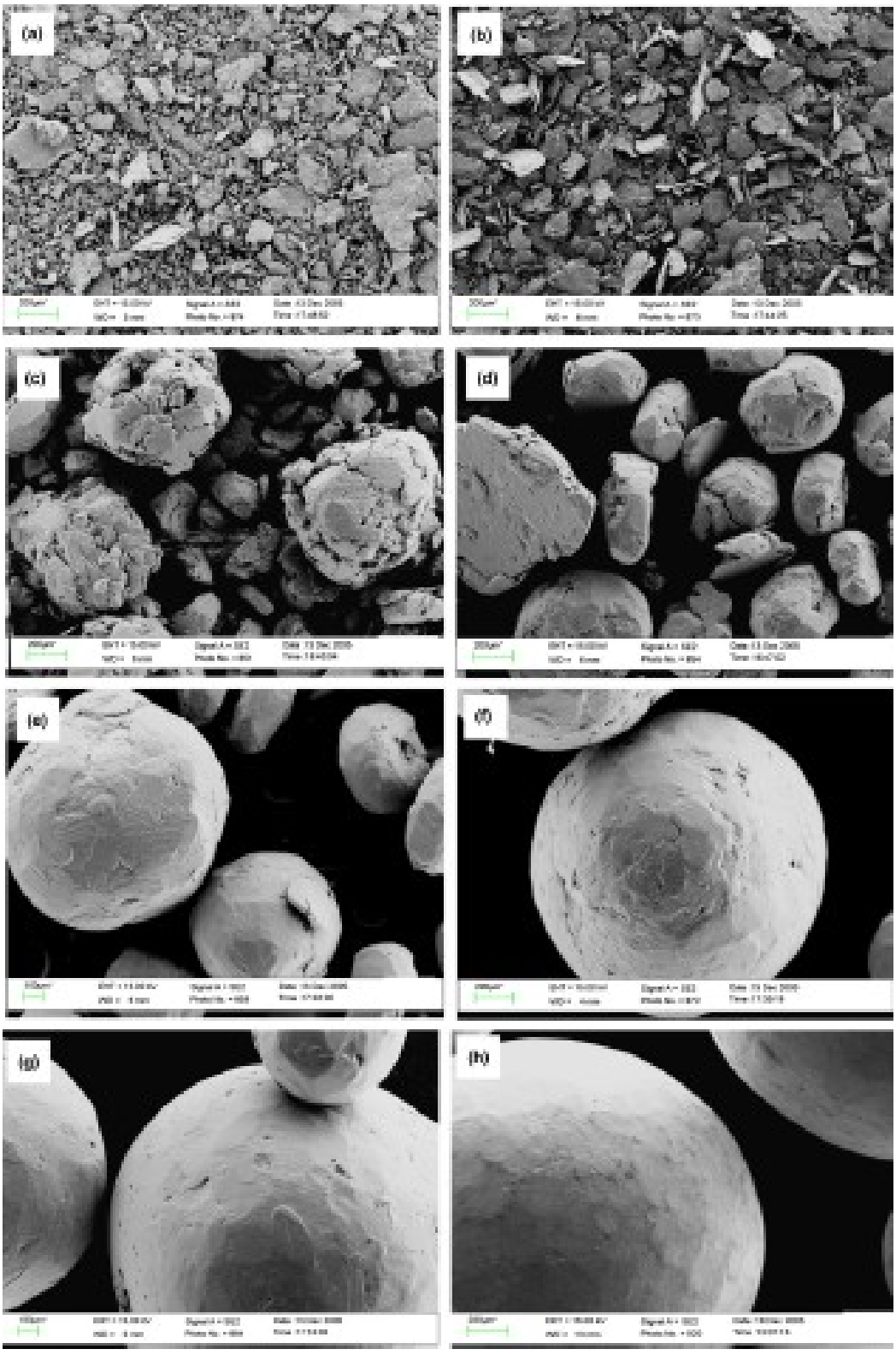

Figure 3. 16 SEM micrographs of mechanically alloyed 2 wt% CNT/Al powder after (a) 0.5 h, (b) 1 h, (c) 3 h, (d) 6 h, (e) 12 h, (f) 18 h, (g) 36 h and (h) 48 h [36]

A paper published by Poirier *et. al.,* was also pretty much concerned with the analysis of the Al-CNT composite processed by high energy ball milling. 10 vol. % MWCNT with a diameter of 60-80 nm was added to pure Al and the mix was milled with tungsten carbide balls and stearic acid as a control agent in a spex mill at 1200 rpm for 5 hours. In addition, CNT alone was milled for 5 hours with the same milling conditions for comparison purposes. Comparing the two specimens after milling it was concluded from SEM images and x-rays that the amount of damage done to CNT if milled alone is very small compared to the amount of damage done to it if milled in the presence of a matrix even if it was a ductile metal like Al [38].

Also, the author showed that there is a big jump in hardness values from 168 to 329 VHN if the milled sample was heat treated at 635 degrees Celsius. He argues that this jump could be due to the formation of aluminium carbide that emerged from the reaction of Al with the free carbon atoms from the amorphized nanotubes [38].

3.1.6 Examining The Effect of Milling Time on Al-CNT Composites

In a recent study the authors Choi *et. al.,* focused their efforts on emphasizing the effect of CNTs and the variation of grain size on the mechanical properties of Al-CNT composites. Pure Al, and 4 vol.% Al-CNT samples were milled for 6 and 12 hours in a ball mill with BPR of 15:1. The resulting samples were then sealed in a copper can under vacuum, compacted, sintered at 470 ˚C, and then hot extruded with an extrusion ratio of 15:1. The author claims that the grain size calculated from TEM images for pure Al powder was found to be 200nm after 6 hrs of milling which was reduced to 70nm after 12 hrs of milling, and that the grain size of the composite powder was identical to that of the pure Al at the same milling times. After extrusion the grain size was found to be almost unchanged for both the pure and composite samples.

Compression testing was conducted for pure and composite samples; the results are shown in table 3.1. The author didn't comment on the compression results but it is clear from these results that there is a remarkable effect when CNT is added in case of the 6 hrs milled sample. As for the 12 hrs milled samples, the very small grain size and the heavily strain hardened material made the strengthening effect of CNTs unremarkable [39].

Table 3. 1 Compression test results for pure and composite samples [39]

	6 hrs milling (200nm)	12 hrs milling (72nm)
UTS for Pure Al Samples	238	383
UTS for Al-CNT samples	380	405

The author claims in his conclusion that the CNTs were aligned in the extrusion direction without any clustering, and that the sintering and extrusion temperatures are comparatively low (470 ° C) which in his opinion prevented the formation of Aluminium carbide reported in other studies [27, 40].

3.1.7 Producing Al-CNT composite via Intense Plastic Straining (IPS)

In addition to ball milling and hot extrusion described earlier there are other techniques used to produce Al/CNT composites such as: high pressure torsion, plasma spraying, and spark plasma sintering and extrusion. Tokunaga *et. al.,* argues that all these methods used to produce Al-CNT composites in addition to some other methods that require heating the mixture in order to produce a densely packed homogenous compact are vulnerable to undergo reactions between the Al, and CNT forming carbides. He continues that these carbides are brittle and that it will cause the composite to crack if it is deformed. They came up with a method that they called high

pressure torsion which according to the authors helps in the formation of a carbide free composite because the whole process is done at room temperature. The materials used in this process are: Al 99.99 pure with a particle size of 75µm, and SWCNT with tube diameter of 1-2 nm. They prepared a mixture of 5 wt. % CNT in Al to be processed and the mixture was sonicated for 5 min. The process description is illustrated in Figure 3.17 [41].

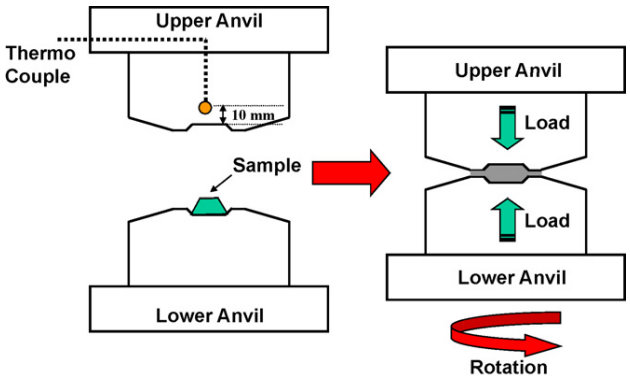

Figure 3. 17 Illustration showing the setup for HPT test. [41]

The sample is introduced between the two anvils and is pressed at 30 tons, then the lower anvil starts to rotate at a speed of 1 rpm for 30 min. In addition to the Al-CNT powder, samples of Al powder and Al bulk were prepared using the same technique. Different testing and analysis methods were applied to characterize the samples. Vickers micro hardness shows that the strain hardening that was induced from the process was not homogeneous on the cross section of the sample which is logical and expected, and this is very clear in Figure 3.18 from the Al-CNT sample. Also, it is clear that the powder samples in general have a higher vicker's hardness value than the bulk sample. The author explained this to be due to the presence of alumina layers on the particles of the powder, and this was confirmed using electron energy loss spectroscopy [41].

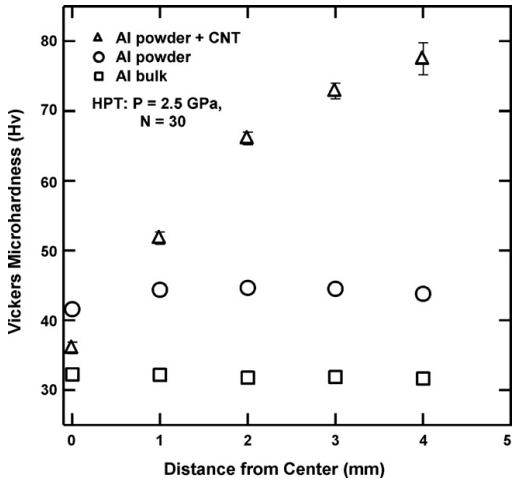

Figure 3. 18 VHN vs. distance from the center for pure and composite Al-CNT samples [41].

In addition, it is obvious that the hardness of the Al-CNT increases tremendously as we go away from the center of the sample whereas there is almost no increase in hardness for the Al powder sample. The author explains that this to be due to the dislocation activity within grains as well as the interaction between the dislocation and the grain boundary, and he argues that this didn't happen in the pure Al powder because it has already reached the steady state. The author claims that the HPT technique resulted in breaking and deforming the CNT as we go away from the center. This will result in decreasing the distance between CNT's present in the matrix which in turn increases the accumulation sites for dislocations in the matrix and that is the main reason behind the increasing hardness trend as we go far from the center of the sample. He proved and strengthened this theory using raman spectroscopy shown in Figure 3.19 where the D-band became pronounced which proves that the CNT's have been deformed [41].

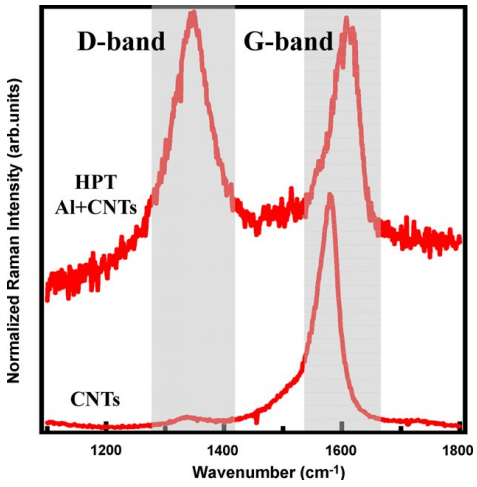

Figure 3. 19 Raman Spectroscopy D-bands and G-bands comparing original CNTs and HPT Al-CNT [41]

3.1.8 Effect of CNTs size and structure on the composite

Lin Wang *et. al.,* made an argument that the shape and size of the CNT used in the composite would have a great influence on the particle size after milling. They used small diameter MWCNT's (20 nm diameter) with a curly structure and milled them with pure Al powder after sonication using the same milling conditions and CNT wt% as used by Esawi and Morsi [36] for comparison purposes. The resulting particle size of both the Al-CNT, and the pure Al were different from the results reported by Esawi and Morsi. Figure 3.20 (a) shows that the particle size of pure Al increased from 29.3 microns to 106.0 microns after 72 hours of milling, and Figure 3.20 (b) shows that the particle size of Al-CNT didn't increase or decrease after 72 hours of milling. The particle size values reported by Esawi and Morsi were 1-2 mm diameter particles after 48hrs of milling in case of the 2wt% Al-CNT composite. The author explained this difference in results to be due to the difference in size and structure of the MWCNT used in both experiments [42].

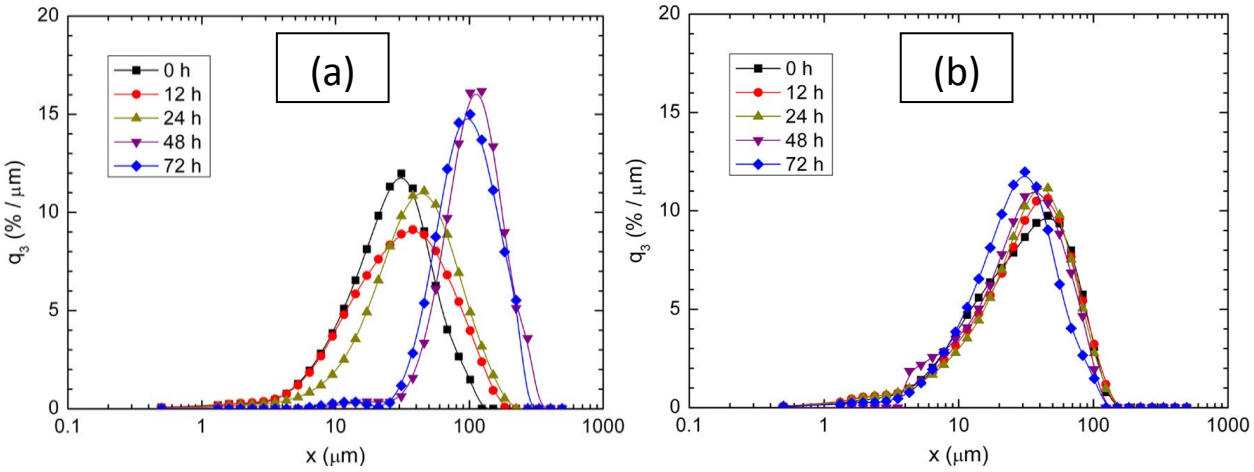

Figure 3. 20 (a) Pure Al powder distribution, (b) Al-CNT mixture powders [42]

Lin Wang *et. al.,* argued that using smaller diameter CNT increases the total surface area of the CNT in contact with Al, which imply the reduced contact area between the Al particles themselves during ball milling, which would hinder the cold welding of Al particles together. Furthermore, they explained based on mechanics of materials concepts that the bending stiffness and critical buckling load were small in their case compared to Esawi and Morsi due to the smaller diameter CNT's they used, which would encourage the CNT's to be deformed, and entrapped laterally just beneath the surface of the Al particles which they showed using SEM images in Figure 3.21 [42].

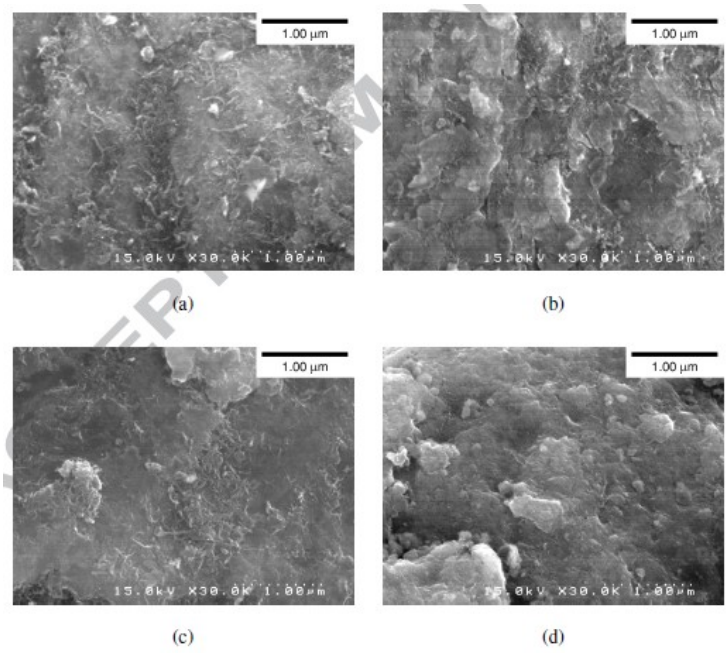

Figure 3. 21 The development in particle morphology after (12,24,48,72hrs) [42]

The author compared this structure to an SEM image presented by Esawi and Morsi that shows the CNTs to be driven vertically from the Al matrix in order to prove his point concerning the particle size and surface morphology [42].

3.1.9 Combination of hot extrusion, spark plasma sintering, and extrusion to produce Al-CNT Composites

Research done in the past 3 years started introducing a new processing technique for the consolidation of Al-CNT composite powder which is spark plasma sintering and extrusion. Morsi *et. al.,* discuss the detailed characterization of SPEX milled Al-CNT powders (well dispersed CNTs in an Al matrix at 2.5 and 5 wt% loading), their heat treatment and consolidation using spark plasma sintering. They used CNTs with average diameter of 30nm, and 45 µm 99.7% pure Al powder. The author reported that spex milling have resulted in powders with varying size and morphology. The author claims that the crystal size of the 2.5 wt.% CNT /Al composite powder after 90 minutes milling was 88 nm as compared to 52 nm for the 5.0 wt.% CNT (after 120 min milling), showing a grain refining effect

with addition of CNTs. In addition, annealing experiments were conducted on the 5wt% CNT-Al powder at temperatures ranging from 300^{o}C to 500^{o}C. XRD scans revealed that aluminium carbide is present at temperatures of 500^{o}C, and there also appears to be a trace at 400^{o}C. The author showed by deep etched plasma sintered microstructures that CNTs are still present as indicated in Figure 3.22. They also reported that the Vickers hardness was found to increase from 91 to 107 HV with the increase in CNT content from 2.5 wt% to 5 wt% [43]. Other publications by the same authors investigated the consolidation of the same Al-CNT composites using a novel process: spark plasma extrusion (SPE) process. "Compared with SPS, SPE has the added advantages of allowing the production of powder-based materials of extended geometries and bulk deformation under the influence of electric current which may yield materials with unique properties." [44] The authors successfully spark plasma extruded Milled Al (1hr) and Al-CNT (1.5 hr) powders. In addition, the Al-CNT composite displayed higher hardness (~33%) and compressive strength (~10%) than the pure Al counterpart under the investigated processing parameters, which is claimed to be due to the strengthening effects of CNTs and reduced Al crystal size compared to milled Al [44, 45].

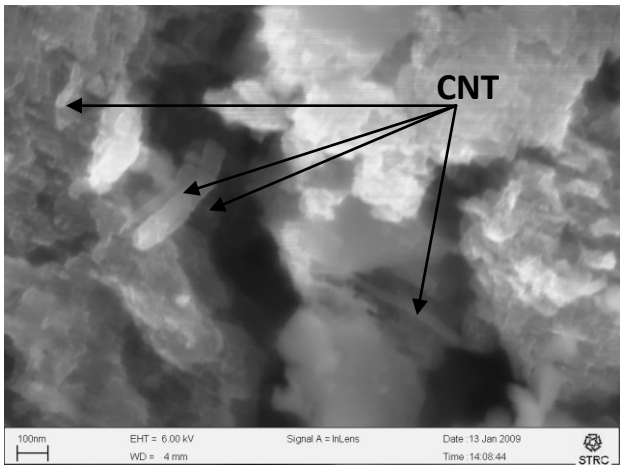

Figure 3. 22 FESEM micrograph of deep-etched spark plasma sintered 5 wt% CNT–Al samples showing nanotubes [43].

Kwon *et. al.,* used a similar process; in their study they processed their material by SPS followed by extrusion. They reported that their product exhibited tensile strength that is much higher than pure Al. They prepared the powder mixture using a nanoscale dispersion (NSD) method that was first used by Noguchi *et. al.,* [47] In this process natural rubber (NR) is used as a mixing medium for the dispersion of CNT with metal powder. The author used 99.8% pure gas atomized Al powder, 5 vol. % MWCNT with an average diameter of 20nm, and natural rubber in the process. In order to disperse the CNT in Al, the mixture is put in a furnace under argon at a temperature of 500° C for 2 hours to evaporate the NR. The obtained powder is then put in a carbon mold and sintered at 600° C for 20 min under 50MPa of pressure. Finally, the sintered billet (15mm diameter, 30mm length) is extruded at 400° C with an extrusion ratio ok 20:1. Figure 3.23 is a schematic representation showing the process steps [46].

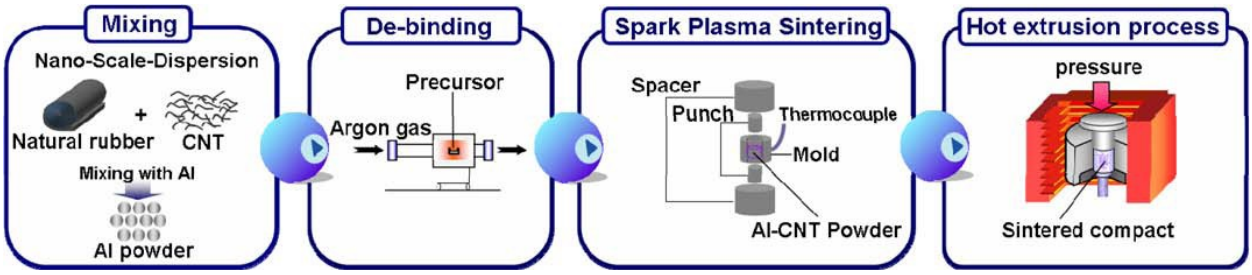

Figure 3. 23 Mixing, SPS, and hot extrusion steps [46]

Using FESEM the mixture was examined after the debinding process to determine whether there is full dispersion of CNT or not. Images shown in Figure 2.24 (b) shows that the CNTs were condensed on the surface of the Al particles by the capillary effect of the melting NR. Also, Figure 3.24 (a) shows that the Al particles preserved their spherical structure despite the heat treatment. Also, the author reported that there were some agglomerations of CNT on the

surface of the Al particles and this is clearly shown in Figure 3.24 (c). TEM images showed the presence of different phases at the grain boundary interface which were proven by EDS and SAD pattern to be CNTs, amorphous carbon, graphite, and Al carbide [46].

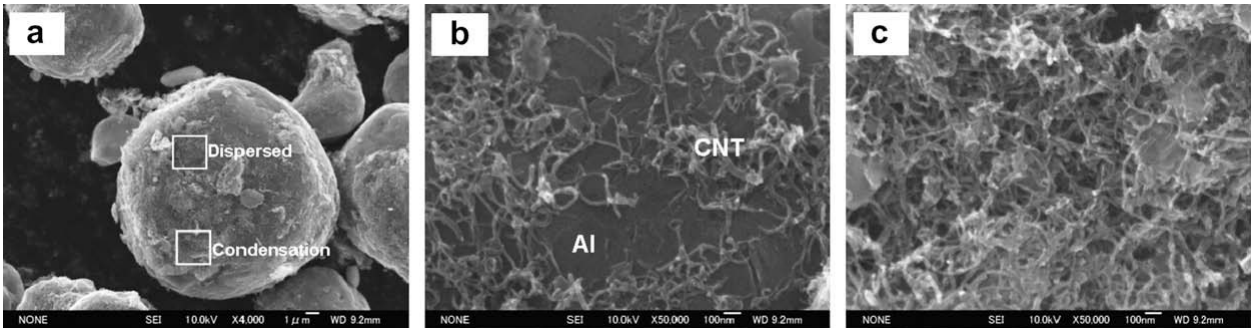

Figure 3. 24 (a) Al-CNT powder mixture, (b) uniformly dispersed Al-CNT phase, (c) agglomerations of CNTs on Al particles [46]

The author reported an ultimate tensile stress value of 190MPa at 11% elongation for the 5 vol % CNT sample, and 90MPa for the pure Al sample. The author claims that these results which were achieved without any work hardening are remarkable and outstanding compared to other reports, and he explains this enhancement to be due to the formation of Al carbide which enhanced the bonding between Al and CNTs [46].

3.1.10 The effect of varying the CNT content on Elasticity and Strength

In another study the author used 4 layers of pure Al foil of thickness 40μm, he then sprayed 60nm diameter ultra-sonicated CNTs on the surface of each layer. The layers were then stacked and cold rolled for 4 passes, then annealed at 523 for an hour. Finally, the sheet underwent five more cold rolling passes to reach a final thickness of 50 μm for a final reduction of 70%. Composites with different CNT volume concentrations (2, 7.5, 9) were produced in order to examine its effect on the elasticity and strength of the material. The author examined the surface of the Al foil after delaminating under the SEM for the 2, 9 vol.% CNT, and he

discovered that the 2% CNT sample had homogeneous dispersion of CNTs on the surface with some broken and damaged CNTs whereas the 9% CNT sample experienced some clustering of CNTs on the surface. Nano-indentation and tensile mechanical testing were performed for all samples and they revealed very interesting results. The 2 vol.% sample has the highest elastic modulus in all samples whereas the 9 vol.% sample had the highest UTS value of 98 MPa compared to 72 MPa for the 2 vol.% sample. As for the nano-indentation results, the author compared all the results to theoretical elastic modulus values calculated by the rule of mixture which was only true for the 2 vol% sample. The author explained this by claiming that the rule of mixture is only valid for the homogeneously dispersed reinforcement, and this was the case for the 2 vol.% sample but not for the 9 vol.% sample which experienced clusters of CNTs on the surface of the Al foil. The elastic modulus dropped for the 7.5 and 9 vol.% samples due to the presence of CNT agglomerates which creates CNT depleted regions causing plastic deformation to start at these regions at lower stresses than CNT rich regions and this is because the Al and CNT have totally different E values. As a result, the actual elastic modulus of the 7.5, 9 vol.% samples was much lower than their theoretical ones. In an attempt to explain the UTS of the samples, the author argued that CNT agglomerates inhibit the dislocation motion and result in an increased dislocation density with the increased CNT content. As a result the composite gets strengthened by the strain hardening effect [48].

3.1.11 Plasma spray forming of Al-Si, and CNT powders

The molten metal or alloy is sprayed against a revolving mandrel on which the desired shape is mounted. (Figure 3.25) [49].

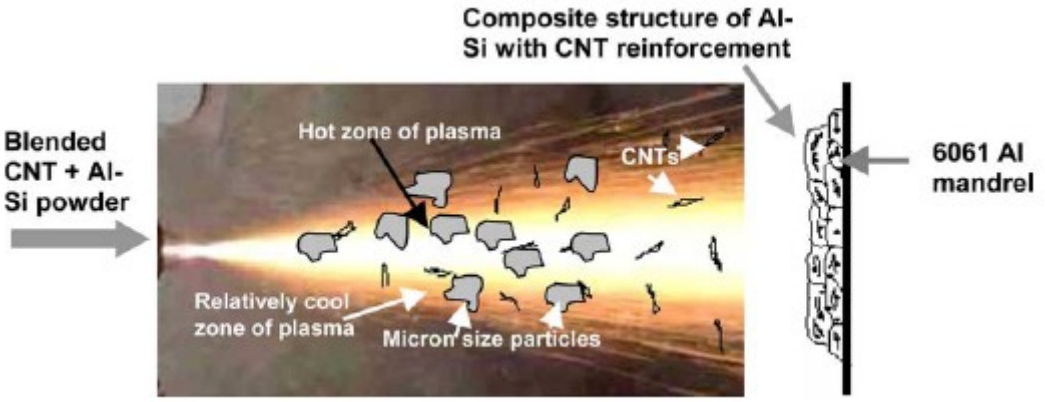

Figure 3. 25 Schematic of plasma spray forming of blended powders [49]

Some of the fine particles including the CNT don't reach the hot core of the plasma because of their light weight and get entrapped inside the deposition. In this case, the composite was sprayed on a 6061 Al mandrel [49].

Al-Si alloy, gas atomized spherical hypereutectic Al-23% Si by weight, prealloyed powder were the ingredients used. The alloy itself has the density of 2.61 gm/cm^3 and particle size ranging from 15-45µm. Coarse grains may not melt or may melt partially which won't achieve good adherence in the spray structure. 10% of CNT of 95% purity was utilized. The CNT diameter ranged about 40-70nm and length about 0.5-2µm and bulk density of 1.3-1.5gm/cm^3. The powder was mixed with the CNT in a ball mill for 48 hours. It's hard to spray light particles like CNT and small particles [43]. The alloy particles will act as a carrier to the CNT to be sprayed along. Even though the mixture was ball milled for 48 hours, some agglomerates could still be found in the mixture (Figure 3.26). However, CNT's can be observed on the surface of the alloy particles [49].

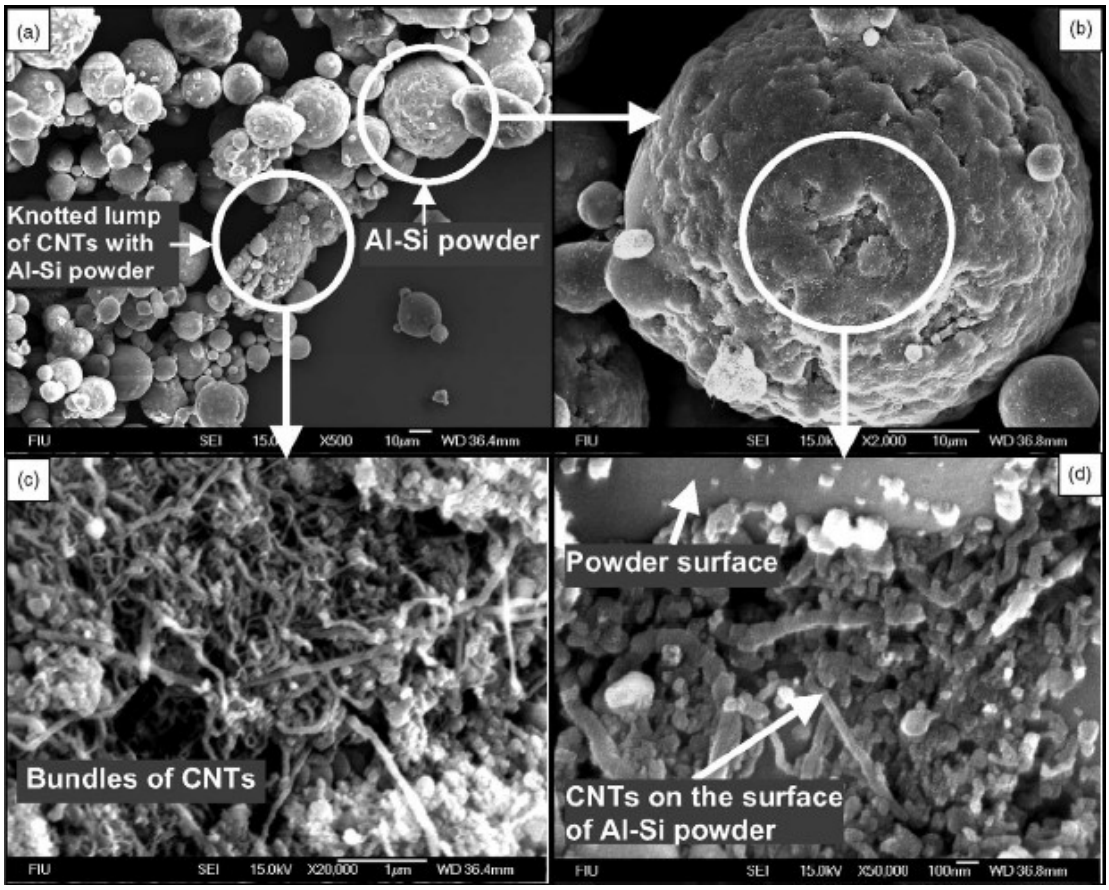

Figure 3. 26 SEM micrograph of homogeneously blended Al–Si powders and carbon nanotubes (a), showing CNTs residing on the surface of Al–Si powder (b and d) and bundles of entangled CNTs (c) [49]

The rough outer surface of the produced cylinder is a result of the pulsed powder flow during the spray, which is caused by massive clusters of particles. The black spots in the grey surface are indication of carbon phase (Figure 3.27). By examining the outer surface (Figure 3.28), the alloy particles and CNT clusters are very clear. The mixture of the alloy particles and the CNT's weren't subjected to melting due to their high melting point, the CNT presence, the powder large size and the pulsing attitude of the spray gun. The collisions of the mixture with the mandrel surface created fragmental structure (Figure 3.28). The inner wall had a smoother surface because it was shaped on the mandrel itself. A few pores were noticed on the inner wall. Temperature of the plasma spray forming is ranging from 10000-15000K which is more than the

boiling temperature of graphite. However, the large particle size and the plasma inconsistent flow conserved the CNT inside the composite [49].

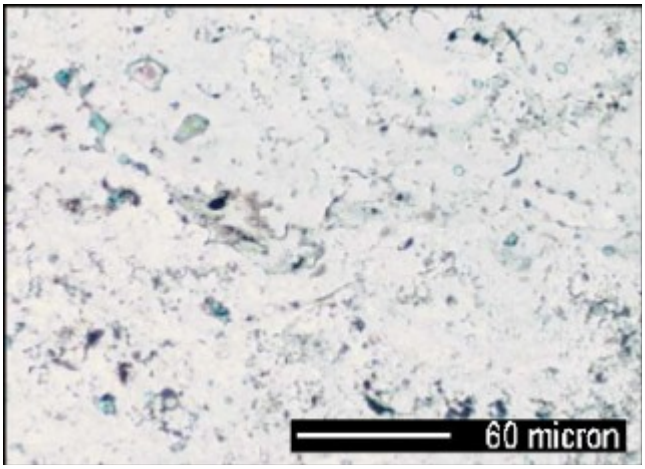

Figure 3. 27 Optical micrograph of the polished and etched composite showing the grayish-black phase of carbon allotropes [49]

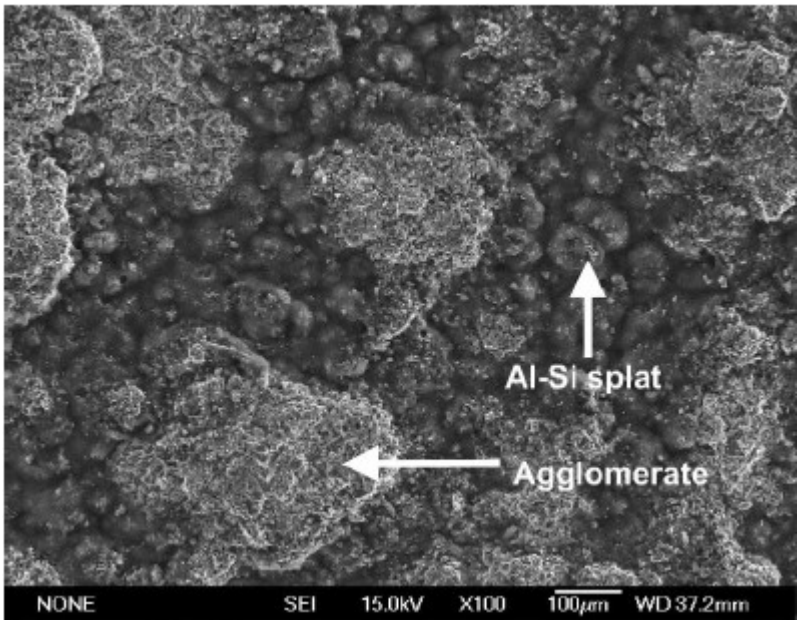

Figure 3. 28 SEM micrograph of spray formed unpolished outer plane of Al–CNT composite structure, showing the splitting of both individual Al–Si powder particles and powder–CNT agglomerates [49]

3.2 Summary of Literature

It was clear from the literature that the most efficient and easiest technique for dispersing CNTs in Al matrix is high energy ball milling. This technique as argued by many authors is successful in creating a sound powder composite. Also, recently published articles reported enhanced strengthening in composites manufactured using this technique. In addition, there was uncertainty about whether milling damages or amorphizes the CNTs or not.

Another very controversial issue is the interfacial bonding between Al and the CNTs. Many authors argued that it is practically impossible to wet the surface of CNTs using Al due to the large difference in surface tension coefficients. In order to produce bulk composite samples for testing purposes, hot extrusion, SPS, and SPE were used by the researchers. Carbide formation was reported in several occasions especially when high temperatures were used. It was argued that carbides may also form due to structural damage or amorphization of CNT.

CHAPTER 4

MATERIALS AND EXPERIMENTAL PROCEDURE

4.1 Materials

In this work, 99.7% pure Al with a particle size of 45 μm, and two types of CVD-MWCNT were used: 140 nm and 40 nm diameter. Concerning the pure Al, the powder was characterized to be non uniform in shape and size which was proven by SEM images (as shown in Figure 4.1(a, b)).

Figure 4.1(c, d) represents the 140nm diameter MWCNTs; they are characterized by their uniform straight shape. Figure 4-1(e, f) represents the 40nm diameter MWCNTs; which appear to be less rigid and more entangled. Table 4.1 summarizes the specifications of each type of CNTs employed in this study.

Table 4.1 Specifications of the CNTs used in the present study

Supplier	Purity	Density	Mean Diameter, D	Average Length, *l*	Aspect Ratio, *l*/D
Cheaptubes, Inc.	> 95%	2.1 g/cc	30-50 nm	10-20 μm	375
MER corporation, USA	> 90%	1.9 g/cc	140 +/- 30 nm	7 +/- 2 μm	50

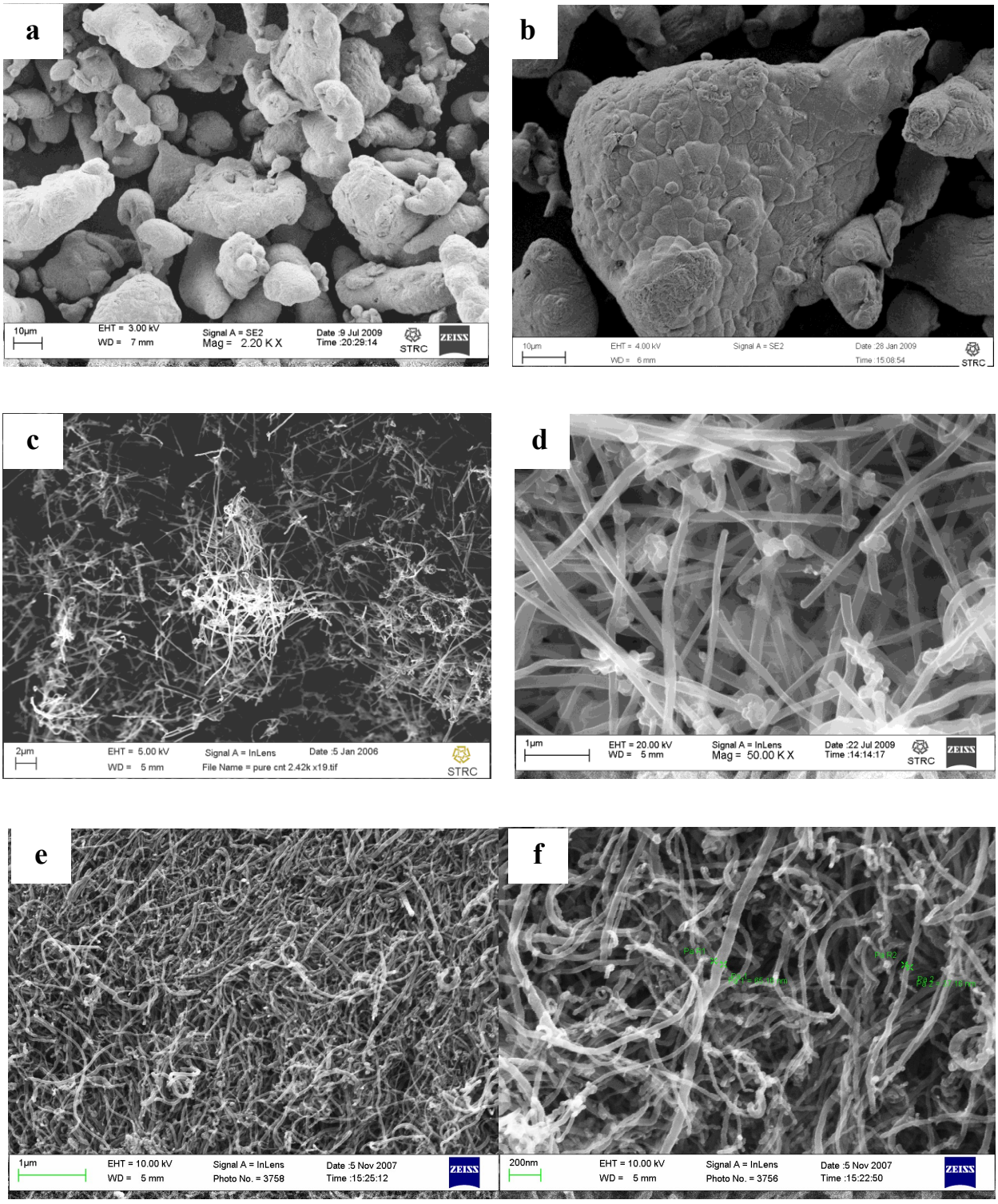

Figure 4. 1 (a, b) high and low resolution SEM images of as-received 99.7% pure Al, (c, d) 140nm MWCNT as received from MER Corporation (e, f) 40nm MWCNT as received from Cheap Tubes Corporation

4.2 Experimental Procedure

4.2.1 The Milling Process

4.2.1.1 Preliminary Milling Investigations

The first part of this research project was based on the work done by Esawi and Morsi [36] that is concerned with milling pure Al with and without the addition of 2 wt.% of the 140nm CNT supplied by the MER Corporation. At early stages in this work some parameters were subject to trial and error due to the lack of background information about the milling technique of Al with CNTs. As noticed from Esawi and Morsi work in Figure 3.16, the Al particles kept on welding together with time forming large spherical balls. These large particles would pose processing problems during their compaction and extrusion. Also, when Al is milled whether with or without the presence of CNT it tends to stick to the walls of the jars and to the steel balls. In order to avoid these problems a Process Control Agent (PCA) had to be added to the mixture in certain amounts in order to control the cold welding of particles. The PCA was chosen to be ethanol but there was no reference for the amount to be added. After several trials the exact amount of ethanol required was calculated, and it happened to be different depending on whether CNTs were added or not. This was due to the fact that CNTs themselves reduce the cold welding of Al particles and thus when CNTs are added the amount of ethanol required decreases.

The PCA was considered to be a problem if samples were required to be taken at some intervals during milling especially at the early stages of milling because the volatile methanol will vaporize leaving the mixture without a PCA for the rest of the process which will result in the particles excessive cold welding. That's why if samples are to be taken for investigation; their milling process is not to be continued after that. Moreover, it is very important to add the

PCA right before the milling starts and to close the jars immediately after adding it in addition to unifying the time taken for this process in order to make sure that the ethanol didn't escape the jar. Also, adding ethanol in such high energy milling environment must be done with care because if ethanol is added in excess it will make the powder very fine and strain hardened in addition to making the atmosphere inside the jar flammable.

Milling was more challenging in the second part of this work; different types of CNTs with different concentrations were used. The aim was to come up with the suitable milling time at the highest speed available (400RPM). The properties and shapes of the CNTs used were different. At the beginning of the process no PCA was added to any of the mixtures, and the powder was carefully examined every 5 min to evaluate the progress. Using the experience gained in the first part of the work and of course with some failed trials the exact amounts of ethanol were calculated for each type and concentration of CNTs. Moreover, the milling time at which a homogenous mix is formed was found to be 30 min.

Unaided eyes investigation of the powder after milling is very crucial for saving time required for characterization. The Al is shiny and silver in color whereas the CNTs are black and this is an advantage that made it easier to do a preliminary evaluation of the success of the milling process in dispersing the CNTs within the Al powders.

4.2.1.2 First set of experiments (140nm MWCNT, 200RPM, 3 and 6 hours)

In this part ball milling was performed with one type of CNT (the 140nm), and with only 2wt% concentration in addition to a pure Al sample as a reference. Milling was done in a Retsch PM 400 MA-type high energy planetary ball mill (3:1 sun to planet ratio) at 200 rpm using

stainless-steel jars and 10mm diameter steel balls weighing 4 grams each. 75 steel balls along with 30 grams of powder were to be used in all experiments giving a ball to powder ratio of 10:1. There were two different time intervals; 3, and 6 hours of milling. Powder handling was performed under an Argon atmosphere inside a glove box. A PCA had to be added to the 2wt% mixture and to the pure Al once at the beginning of the process; 300µl of ethanol in case of the pure Al, and 250 µl of ethanol in case of the 2wt% CNT. The mill had to be stopped every hour for 20 min to cool down the jars.

4.2.1.3 Second set of experiments (140 and 40nm MWCNT, 400RPM, 30min)

In this set of experiments; ball milling was done using the two types of MWCNT with different concentrations in addition to a pure Al to be used as a reference. Concentrations of 0%, 0.5%, 1%, 1.5%, 2%, and 5% were prepared for both types of CNTs, and the amount of PCA (ethanol) added were 400µl, 400µl, 350µl, 350µl, 300µl, and 0µl respectively for the 140nm MWCNT and 350 µl, 350µl, 300µl, 300µl, 250µl, and 0µl respectively for the 40nm MWCNT. The same ball mill of the first set with the same amount of powder (30 grams), and ball to powder ratios (10:1) in each jar were used. The RPM of the machine was set to maximum (400 RPM), and the milling time was reduced to 30 min. The mill had to be stopped every 10 min for 15 min for the jars to cool down. Powder extraction operations were handled with care inside argon filled glove box, and extreme safety measures were taken because the impacts of such high energy milling on such powders were not known.

4.2.2 Compaction, Sintering, and Extrusion processes

4.2.2.1 Compaction Pressure

The choice of the suitable compaction pressure was not an easy process. There were no references discussing the compaction pressure of AL-CNT composites. The closest hit was Al alloys compaction pressures. The Compilation of ASTM Standard Definitions introduced a curve (Figure 4.2) showing the compaction pressure versus the green density, % theoretical of a 601 AB Al alloy [19]. Based on this curve powder compaction pressure of 300, 400, 475, and 550MPa were examined. After careful density measurements for different samples with different milling conditions and CNTs concentrations, a 475MPa compaction pressure was chosen.

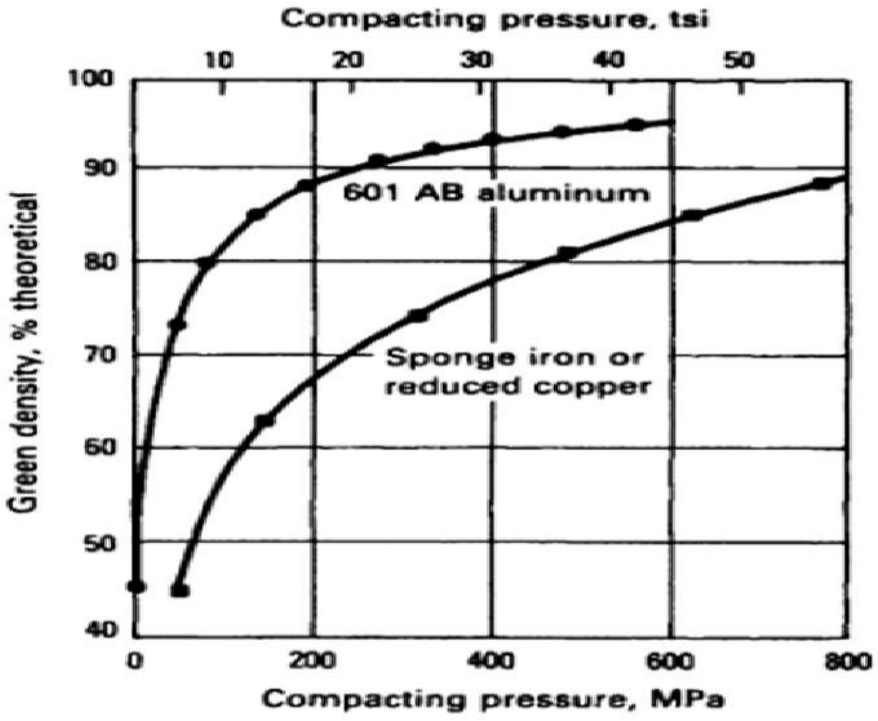

Figure 4. 2 Relationship between green density and compaction pressure of Al alloy [19]

4.2.2.2 Uniaxial Cold Compaction Processing

All the specimens processed in this work were subjected to uniaxial cold compaction. A 100 ton capacity ARMSTRONG hydraulic press was used to compact the specimens at 475 MPa for 30 min. Compaction was performed in a cylindrical die as shown in Figure 4.3 with a bore diameter 20mm. The die is made out of steel (AISI-H13) and is hardened at 55HRC with all its parts that are shown in the Figure below. Approximately 28 grams of powder are used in the process leaving about 2 grams from the powder specimen to be used in the characterization process. The compacted sample height is 30mm and it could be ejected intact from the die as illustrated in Figure 4.4.

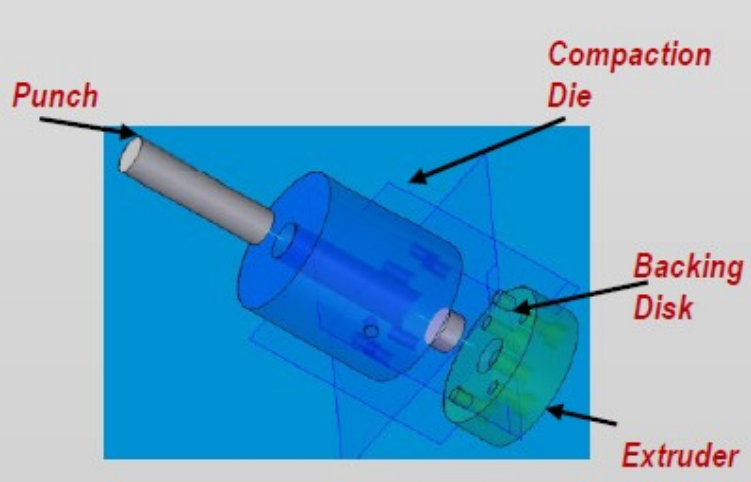

Figure 4. 3 Compaction and extrusion dies [50]

Figure 4. 4 green compact

4.2.2.3 Sintering and Extrusion

Sintering is done in the same die in Figure 4.3 after attaching the extruder by means of 4 M8 bolts. The extruder is machined with a bore diameter of 10mm so as to give an extrusion ratio of 4:1. The die is then heated at 500°C for 30 min in a custom made heating jacket. At that temperature the extrusion die is then subjected to uniaxial loading using the Armstrong 100 ton hydraulic press for extrusion. The observed extrusion pressure was about 800 MPa and varied slightly according to the properties of the sample. The extruded sample is about 100mm in length and 10mm diameter.

4.2.3 Annealing and Machining of the samples

All the sample sets in this work were annealed at 400°C and 500°C after machining and grinding using sand paper with grit sizes of 180, 240, 320, 400, 600, 800, and 1200. There are two machined tensile testing sample forms employed in this research; the ASTM E8 standard sample [51] used for producing samples for the second set of this work (presented in section 4.3.2.1), and a sample with special dimensions as shown in Figure 4.6 used for producing samples from the first set of experiments in this work (presented in section 4.2.1.2).

4.2.3.1 The notch sensitivity problem

Due to the straining imposed on the powder during milling for 3 and 6 hours in the first set of this work, tensile testing done for composite samples machined according to the ASTM standards was not successful. The Al-CNT samples always broke at the shoulders area yielding very low strain readings which made the results useless whereas the pure milled Al samples didn't suffer from the same problem; although they were also milled at similar conditions. Figure 4.5 shows a tensile tested sample which broke at the shoulders yielding unreliable results.

Figure 4. 5 A failed tensile sample

4.2.3.2 The modified tension sample and annealing

In order to solve the notch sensitivity problem a double action plan was made; machine the specimens in a modified form as shown in Figure 4.6 to reduce the stress concentration, and to anneal them at a suitable temperature that would relieve some of the internal stresses. In order to detect the suitable annealing temperature while saving time and effort, two extruded samples (2wt%Al-CNT, pure Al) were sectioned into discs with a height of 10mm each by means of Isomet 5000 linear precision saw cutting machine. Each pair of discs was subjected to annealing at the following temperatures: 200°C, 300°C, 400°C, and 500°C, in addition to a pair that was

not annealed to be used as a reference. The annealing times were: 2, 4, 6, 8, 10 hours for all the previously mentioned temperatures. After that, all the disc samples were subjected to a Vicker's micro hardness tests which were performed at room temperature using a Mitutoyo MH Series 810-128A, in order to detect the temperature and annealing time at which the stresses start to be relieved.

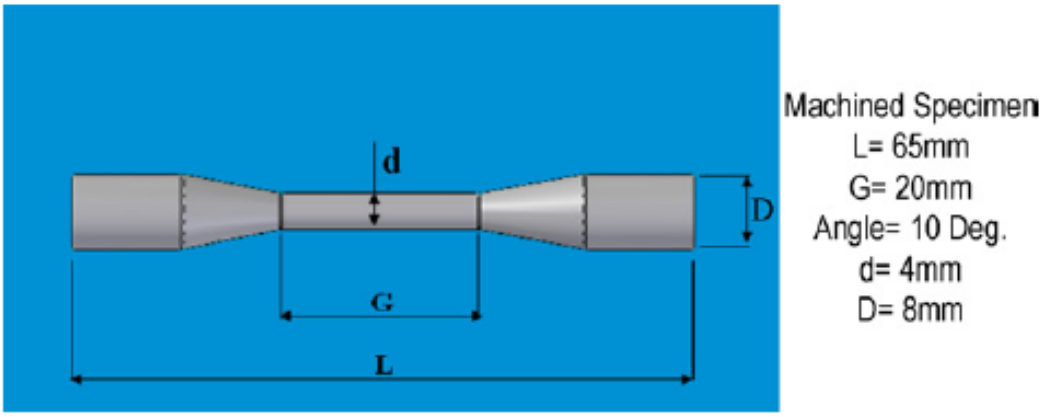

Figure 4. 6 A tension sample machined in special form [52]

4.3 Characterization and Testing Techniques

In order to investigate the properties and the quality of the produced samples, the physical, mechanical, and micro structural properties of the samples had to be investigated. The physical properties were determined by measuring the densities of the extrudates and comparing them to the theoretical density. The mechanical properties were determined by tension tests, micro hardness testing, and nano-indentation. The microstructures were investigated by employing optical microscopy, scanning electron microscopy, and transmission electron microscopy.

4.3.1 Density measurements

Equal sized discs are cut from the shoulders of the samples prepared for tension test after being annealed using a Buhler_Isomet4000 Precession Cutter at a speed of 10mm/min. Measurements are done using a Mettler Toledo XS 205 digital densitometer that employs the Archimedes principle. The sample is first weighed in air, and then it is immersed and weighed again in a liquid with a known density, and the density of the sample is finally calculated from equation 4.1 [53]. The process took place at room temperature, and the auxiliary liquid used was xylene (density = 0.862 g/cm^3 at T_R).

$$\rho_s = \frac{M_a \rho_l}{M_a - M_l} \qquad \text{.....(4.1)}$$

Where:

ρ_s is the density of the sample, ρ_l is the density of the auxiliary liquid, M_a is sample Mass in air and M_l is sample mass in the auxiliary liquid.

4.3.2 Mechanical Testing

4.3.2.1 Tensile Testing

The closest tensile testing sample dimensions to the size of the extrudate made the ASTM E8 [51] shown in Figure 4.7 the perfect choice. Another sample with special geometrical form and dimensions as shown in Figure 4.6 was machined to be used in testing the first set of this work, after the attempts to use the E8 standard shape failed due to the excessive notch sensitivity of the A-CNT samples. Testing was done at room temperature using an Instron 50KN capacity universal testing machine; for Young's modulus and strain measurements, resistance foil strain gauges of gauge length 2 mm and gauge factor 2.09 (Kyowa, Japan) were carefully bonded to the

cleaned tensile samples. A Kyowa data acquisition system was used to monitor and record the measured micro-strain (με), due to the unavailability of an extensometer. The crosshead speed was 1mm/min, and the data were recorded automatically for load and strain every second.

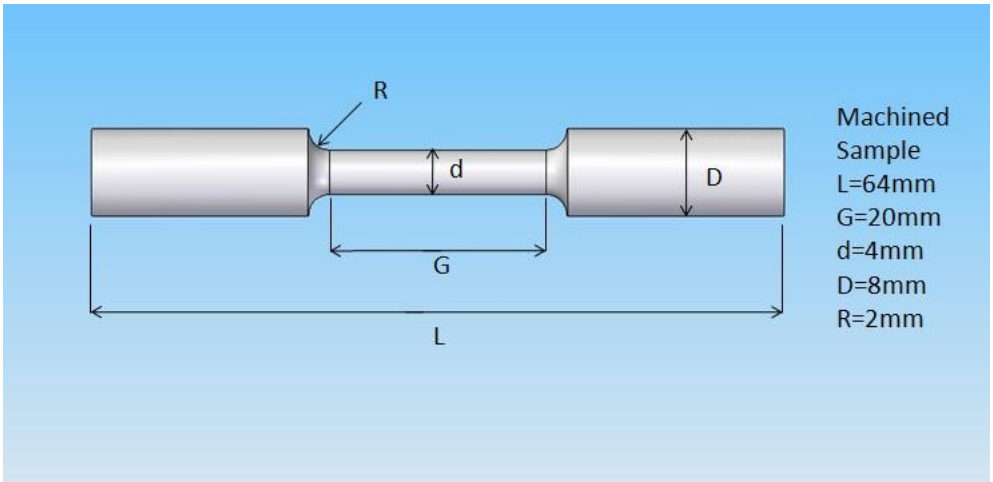

Figure 4. 7 ASTM (E8) tensile testing sample

4.3.2.2 Vickers Micro-Hardness Testing

Three different specimens are to be taken from each sample at different sections for testing to ensure the validity of the results. Samples are cut using the same machine and technique used for preparation of the density samples section 4.3.1. The surface of the specimens has to be grinded and polished to be ready for testing and this is done by the sample preparation technique described in section 4.3.3.2. The measurements were performed at room temperature using a Mitutoyo MH Series 810-128A, at 300 gf of load and 15 seconds of dwell time. All readings were taken in Vickers Hardness Number (VHN). Five different indentations are made at different sites on each of the samples as shown in Figure 4.8 and the average is taken as a final result.

Figure 4. 8 Indentations on an extruded and polished sample

4.3.2.3 Nano-Indentation

Nano-Indentation was done using a Nanoindenter XP (MTS systems Co., Oak Ridge, TN, USA) testing under the Continuous Stiffness Module (CSM). The module enables dynamic measurements of Young's Modulus and Hardness throughout the depth of indentation. This makes it beneficial for composite materials where dispersion of the filler phase is directly related to the uniformity of the measured mechanical properties. This is implemented by imposing an oscillation of known amplitude and frequency on the linear force applied by the indenter.

Two 4x5 arrays of indentations are made for each sample. Although, CSM is a displacement-based module (i.e. the indenter goes into the surface till it reaches a predetermined depth) , the depth of indentation is set to unrealistic value (10μm) in order for the indenter to go for the maximum possible depth at the maximum indentation load (700 mN); therefore, allowing mapping of the measured properties along a representative depth. The distance between adjacent indentations was set to 100 μm to avoid the effect of interaction. The test is not allowed to start until the thermal drift rate is stabilized below 0.05 nm/s.

The indentation test starts by loading the indenter into the sample at a constant rate till it reaches the maximum possible depth (at the maximum load). The indenter is then held at its maximum load for 10 sec. After that, the indenter is unloaded at the same rate till 90% of the indentation load. Then, the indenter is held again for 60 seconds for thermal drift correction. This is followed by full unloading till the indenter is drawn out of the sample. Depths of indentation varied from 4000 nm to 5000 nm. Therefore, the measured properties are averaged between depths of 2000 and 4000 nm.

4.3.3 Microstructure Characterization Techniques

4.3.3.1 X-ray Diffraction

X-ray diffraction (XRD) (using Cu-Kα, Panalytical Xpert Pro diffractometer) is used for phase analysis. X-ray Diffraction tests are employed for both bulk and powder samples. Crystallite size is calculated from diffraction peaks by means of Sherrer equation as shown in equation 4.2 [54]:

$$\beta \cos\theta = \frac{K\lambda}{D} \quad \text{.....(4.2)}$$

Where:

β = Full Width at Half Maximum (FWHM)

θ = Diffraction angle

λ = Wavelength

D = Particle (crystallite) size

K = Scherrer constant (= 0.91)

4.3.3.2 Sample Preparation for SEM Imaging

This technique was used in order to obtain sound polished and etched specimens. The same specimens used for the density measurements are then used in this process. Specimens are grinded directly using ascending grinding steps with grit sizes as follows: 180, 240, 320, 400, 600, 800, and 1200. After the samples are ground they are subjected to polishing using alumina solution of 0.5 followed by 0.3 particle sizes. Finally, the samples are etched using (95ml distilled water, 2gms NaOH, and 4gms Na_2CO_3) for 1 min.

4.3.3.3 Scanning Electron Microscopy

Powder morphology as well as fracture surfaces were characterized using a field emission scanning electron microscope (FESEM) (LEO supra 55). The device is capable of reaching very high magnifications, thanks to the field emission source, the high pressure vacuum chamber, the 30KV power, and the vibrations damping table and supports, it can reach a resolution down to 1 nm. It was very useful in investigating post-tensile fracture surfaces and obtaining an insight regarding the nature of failure, degree of ductility and interface bonding for milled composites. Moreover, it was very effective and useful in investigating the presence and degree of damage concerning the 40nm MWCNT employed in the second set of this work which was very hard to capture due to its small size and the effect of milling on the CNTs. In addition, the Energy Dispersive Spectroscopy was used in parallel with SEM imaging to identify the nature of particles and different regions on the surface.

4.3.3.4Transmission Electron Microscopy

For TEM examination, the specimens were prepared by dual focused ion beam (FIB) and were examined at 200kV on a JEOL 2010 equipped with a high resolution pole piece. Although

TEM analysis is very expensive and took too much time to be done outside the country, it is considered to be a valuable characterization tool that provides a wealth of information about the internal structure of Al-CNT composites, and was very helpful in detecting the presence of nanostructures, and any carbides structures.

CHAPTER 5

RESULTS AND DISCUSSION

5.1 Synthesis of 2wt % Al-CNT Nano composite Milled at 200RPM for 3 and 6hrs with BPR10:1

5.1.1 Powder blending of Al-CNT Nano composites (200RPM, 3 and 6hrs)

In this set of experiments, only one concentration of Al-CNT powder was synthesized (2wt.% CNT) using 140nm diameter MWCNTs. The mixture is milled for three and six hours with the conditions previously mentioned in section 4.2.1.2. Powders synthesized using the same conditions used here were previously investigated in the work done by Esawi and Morsi [36], the only difference is in using a PCA which helped in keeping the particle size of the composite powders within a certain range, suitable for processing.

5.1.2 SEM and TEM analysis of powder and bulk samples morphology and distribution for 2 wt% Al-CNT and pure Al

Figure 5.1 shows the clear distinction between the three and six hours milled Al-CNT samples concerning the particle size distribution. The sample milled for six hours showed a bi-modal particle size distribution; this could be explained by the fact that the PCA (methanol) lubricates the particles surface, which in turn minimizes re-welding, leading to particle size refinement. Adding more methanol will result in further particle refinement, but this will be at the expense of ductility. Methanol also helped in avoiding the sticking of the Al powder to the walls of the milling jars.

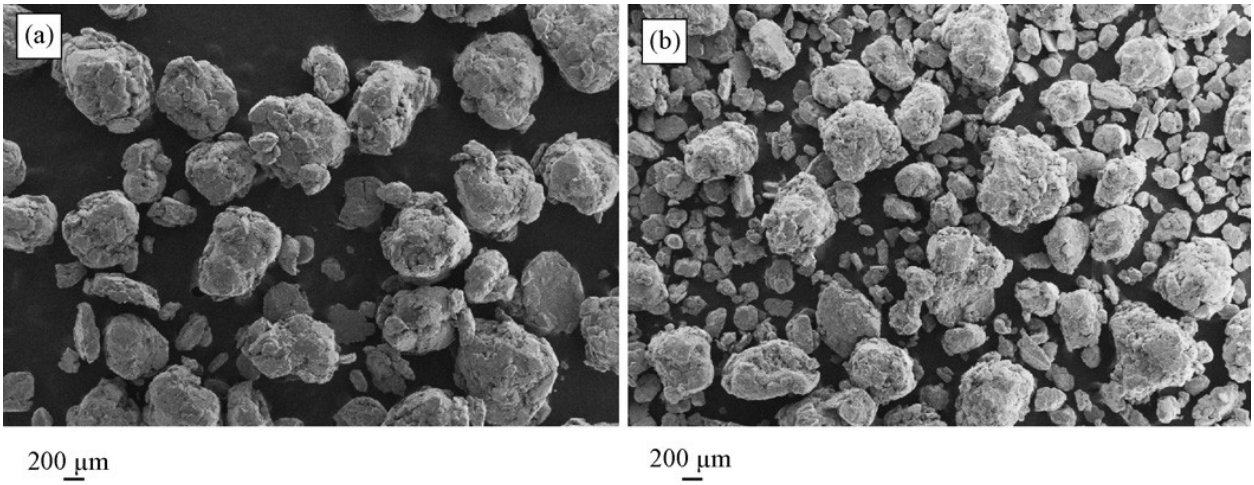

Figure 5. 1 Ball milled 2wt.% Al-CNT (a) 3h, (b) 6h [52]

Upon comparing this with the work of Esawi and Morsi [36] which was performed under the same conditions without adding ethanol or methanol as shown in Figure 5.2, it is clear that the particles went through welding instead of fracturing when further milling from three to six hours is performed. It is very important to fix and maintain an adequate amount of methanol due to its direct effect on ductility. Increasing the amount of methanol could cause the particles to become excessively brittle creating difficulties in the after milling processes. The average particle size that was considered suitable for processing is shown in Figure 5.1. SEM was very helpful in determining the presence of CNTs after milling. During the preliminary investigations samples were taken at different time intervals for SEM characterization. Figure 5.3 shows that the ball milling technique was effective in dispersing CNTs on the surface of the particles at the beginning of milling, and within the particles after several hours of milling. Also it is obvious that most of the CNTs preserved their tubular structure and didn't degrade into amorphous carbon.

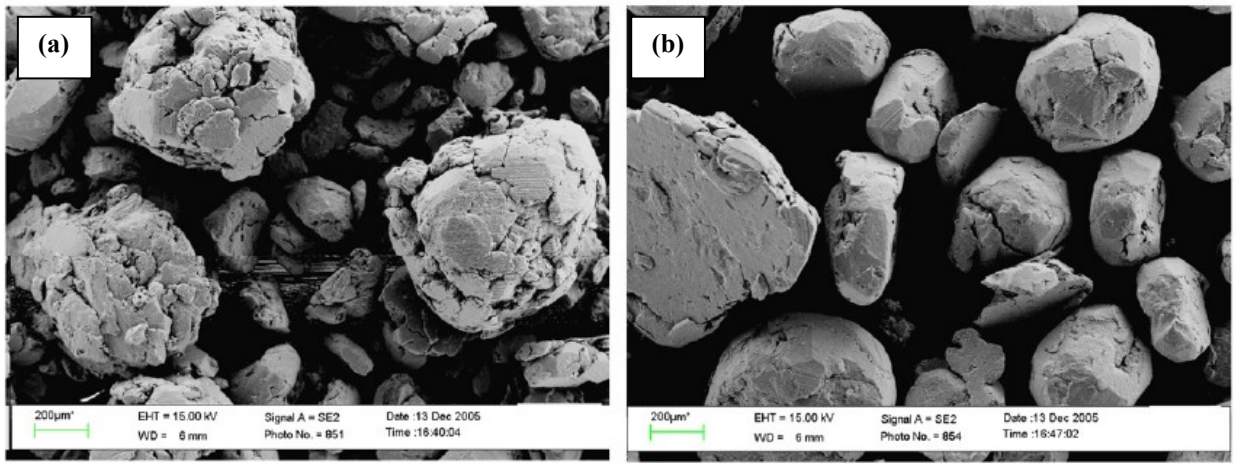

Figure 5. 2 SEM micrographs of mechanically alloyed 2 wt% Al-CNT powder after (a) 3 hrs, (b) 6 hrs [36]

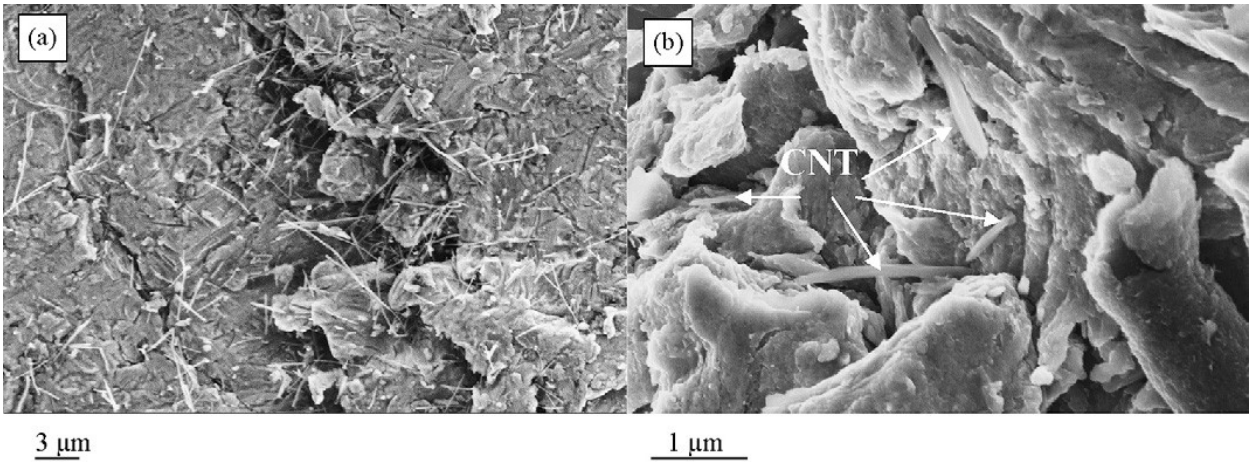

Figure 5. 3 (a) CNTs on the surface of Al particles after 0.5 hrs of milling, (b) CNTs embedded between the re-welded particles after 3 hrs of milling [52]

Figure 5.4 shows a TEM micrograph grains, Al-oxide particles, and dislocations activity in a pure Al sample milled for 6hrs. Preparing 2 wt.% Al-CNT samples for TEM imaging was not possible due to the difficulty of producing wafer thin slices with the 140nm CNTs without the CNTs flying off because of their considerably large size. This limitation along with the XRD inability to identify any carbide peaks (as it will be discussed later), made it difficult to ascertain whether or not any carbide structures are present when using the large diameter 140nm CNTs.

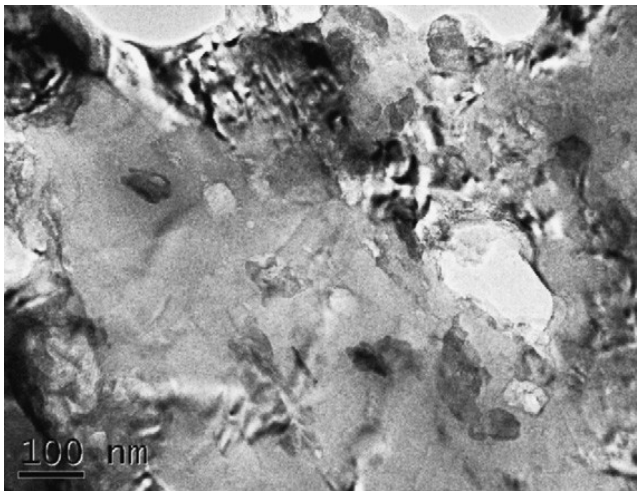

Figure 5. 4 TEM micrograph taken for a pure 6hrs milled Al sample [52]

Figure 5.5 shows that CNTs are still present and well dispersed in the composite. It is noticeable that there are voids around the CNTs; these voids initiated around the CNTs and grew bigger during the tensile testing which is proven in Figure 5.6. Also, CNTs pullout observed in Figure 5.5 is a sign of poor interfacial bonding between CNTs and the Al matrix. It is evident that the sample shown in Figure 5.5 (c) has the highest ductility because it represents the deepest dimpled structure in the 3 samples represented in the Figure 5.5. This is because that sample was annealed at high temperature and subjected to the least straining by milling.

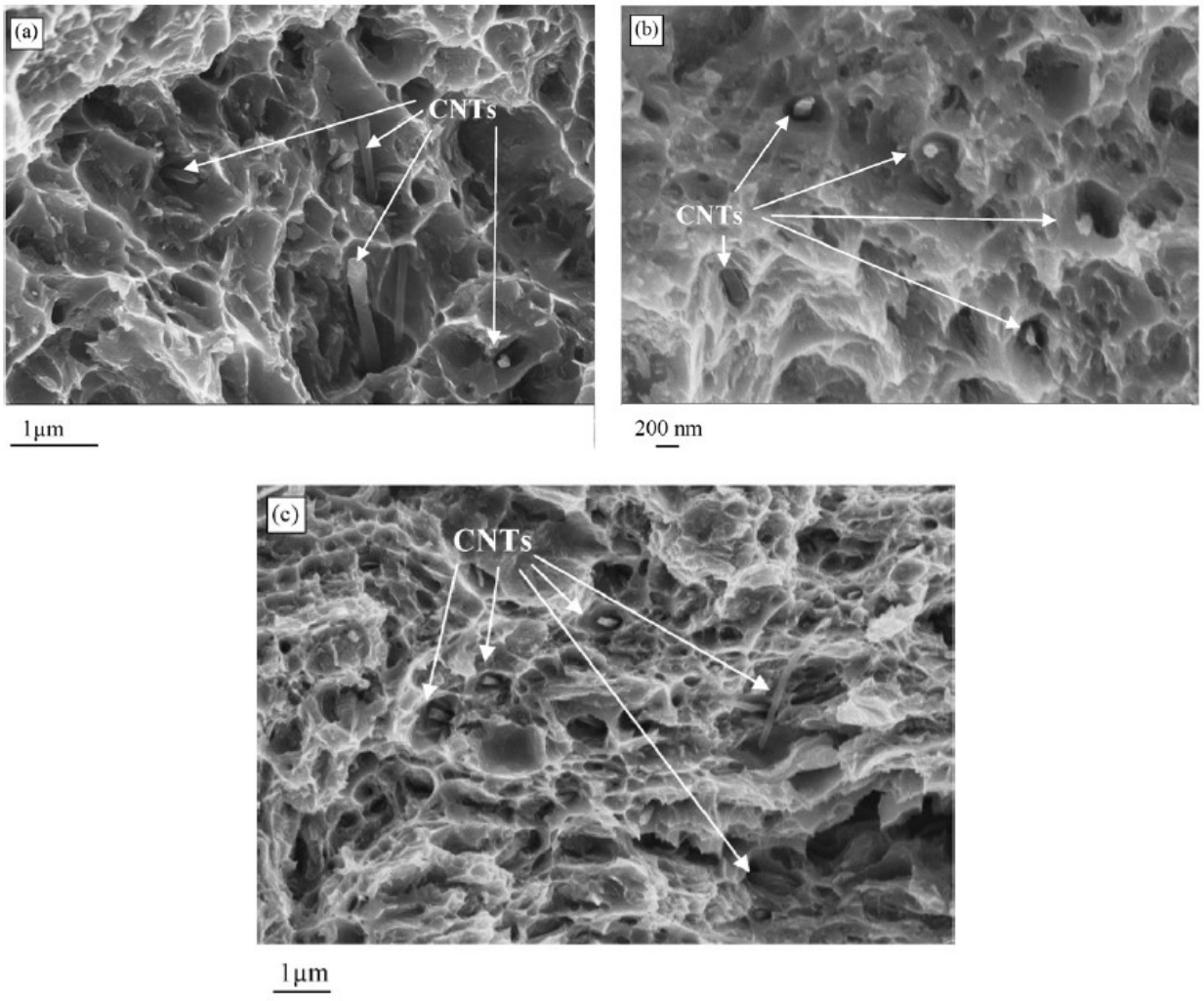

Figure 5. 5 Fracture surfaces of 2wt.% Al-CNT sample showing individual CNTs dispersed in the matrix (a) un-annealed ball milled for 6hrs (b) annealed at 500°C ball milled for 6hrs, (c) annealed at 500°C ball milled for 3hrs. [52]

Figure 5.6 (a,b) shows a heavily etched composite bulk sample that was not subjected to tensile testing. CNTs are aligned in the extrusion direction which may result in anisotropic properties in the final composite. The voids formed around the CNTs are not present in this sample which proves that they are due to tensile testing (see Figure 5.5). Figure 5.7 shows a MWCNT with its inner layers slipping, a kind of defect which might be due to milling or the tension test. If that kind of defect is an outcome of tensile testing, it is considered to be a sign of weakness of multi-wall CNTs.

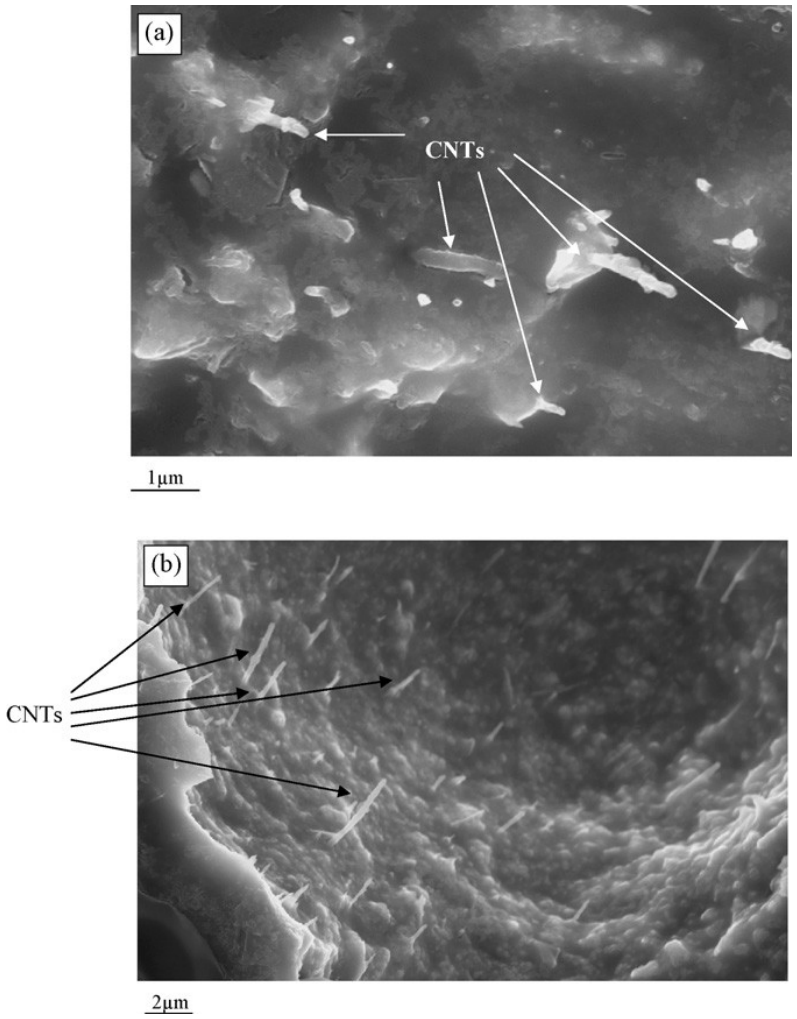

Figure 5. 6 (a,b) a cross section of a 2 wt.% Al-CNT extruded sample not subjected to tensile testing and deeply etched showing individual CNTs aligned in the extrusion direction at different magnifications [52]

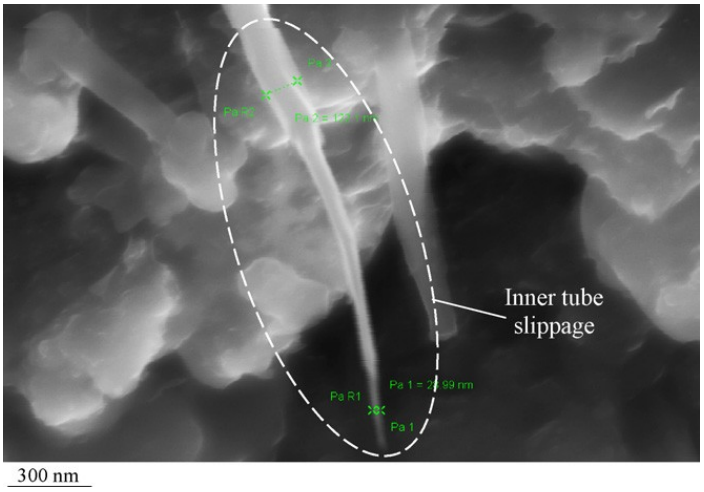

Figure 5. 7 FESEM micrograph of a fracture surface showing MWCNT with a layer slippage defect [52]

5.1.3 X-Ray Diffraction of the 2 wt.% Al-CNT Milled Powder and Bulk Samples **(scans and analysis of all samples were performed by the research team members at SDSU)**

XRD is done at SDSU to investigate the presence of graphite peaks and the formation of any carbides in the composite. The resulting peaks were also used for phase analysis and crystal size determination using the Scherrer equation [54], and excluding the instrumental effects on broadening. XRD scans of CNT powder presented in Figure 5.8 show a predominant peak at 26^{o} indicating the presence of graphite (002).

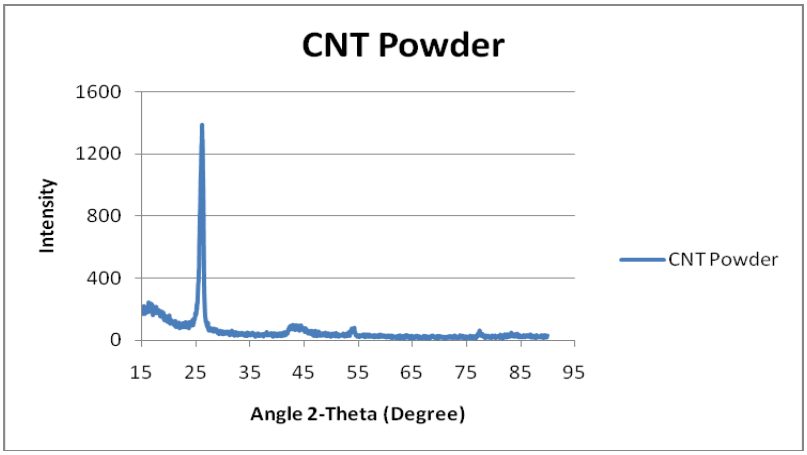

Figure 5. 8 XRD scan of 140nm CNT powder sample

Figure 5.9 shows XRD scans for the 2wt.% milled Al-CNT powders milled for 3, and 6 hrs. It could be observed that there is a small peak at 26^{o} in the 3h sample curve indicating the presence of graphite (CNT) which then disappears in the 6h sample. These results are in line with other published work of George *et. al.,* [27] where 2 vol.% of CNT were milled for just 5 min and there were no carbon peaks identified, despite that the TEM micro graphs indicated the presence of CNT. A reasonable explanation for this is the limitation of XRD resolution. Another explanation could be that the carbon peak is only observed when CNTs are clustered (in case the clusters are well dispersed that peak diminishes). After extrusion, samples are annealed at 400,

and 500 °C and XRD is performed on samples cross sections after mounting. The resulting curves shown in Figure 5.10 indicate no graphite peaks in any of the bulk samples. This could be due to a number of reasons including: the good dispersion of CNTs within the matrix, the small amount of CNTs used, unfavorable strain/CNT effect (CNTs deformation), or amorphization of CNTs. It is also worth mentioning that the unidentified peaks in Figure 5.10 that are quite obvious especially in the 3h sample between 10 and 20 degrees comes from the mounting material used.

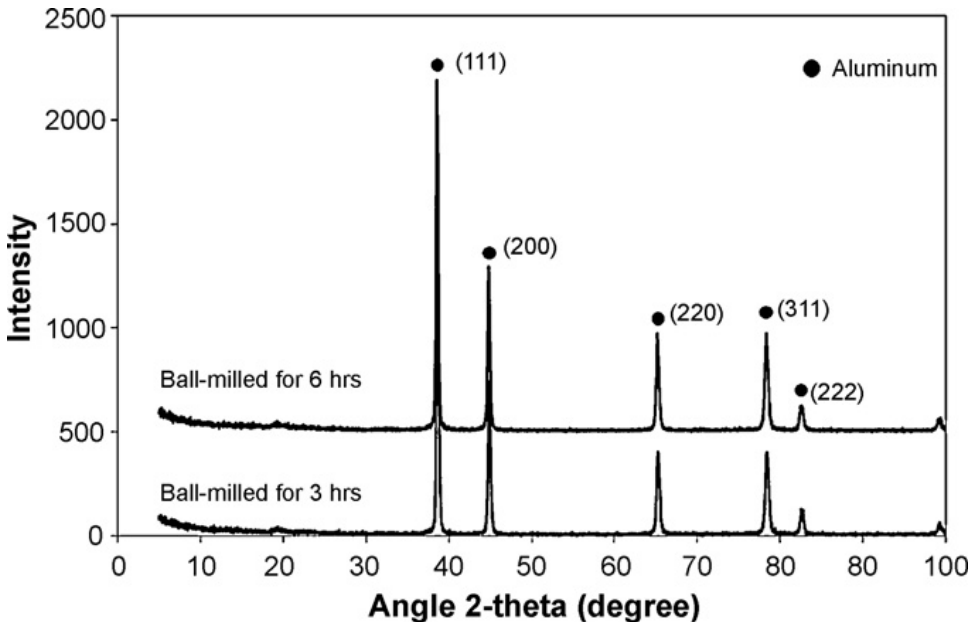

Figure 5. 9 XRD scans for 2wt.% Al-CNT milled for 3, and 6hrs [52]

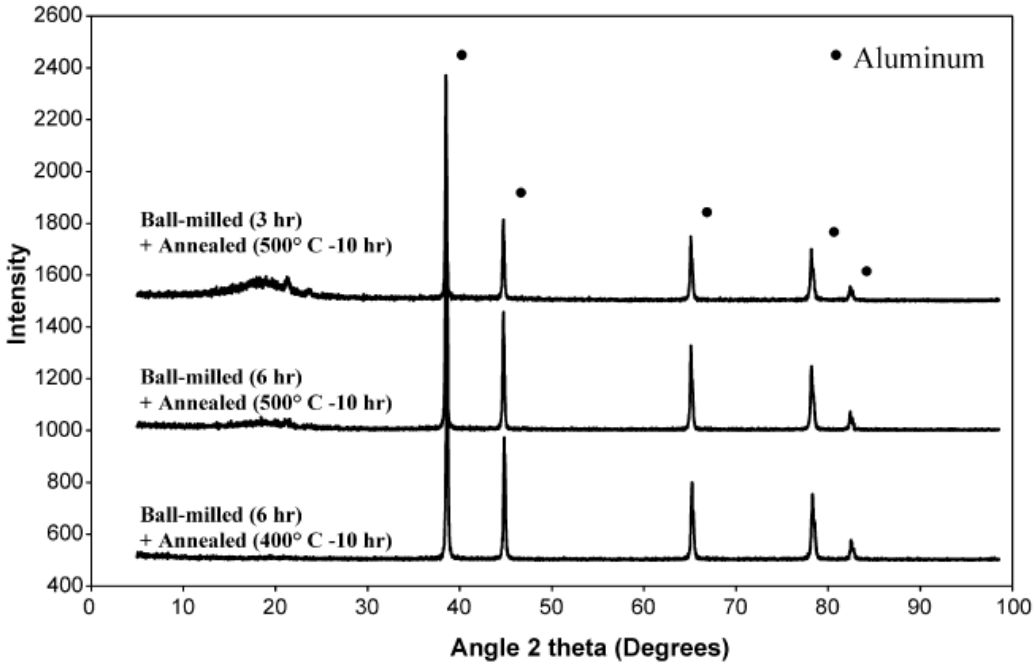

Figure 5. 10 XRD scans for extruded bulk 2wt.% Al-CNT sample milled for 3, 6hrs at different annealing temperatures [52]

All the XRD scans conducted on the 2wt.% Al-CNT powder and bulk samples didn't indicate the presence of any carbides. This doesn't rule out the formation of carbides because simply the amount, structure, and size of the carbides formed might be out of the detector resolution range. Thus, previous investigations of carbide formation in similar composites are inconclusive. A TEM investigation would provide a more definitive conclusion. For example, Deng *et. al.,* [31] reported the formation of Aluminium Carbide at 656 $^{\circ}$C, whereas others [3, 32] reported that carbides were absent. This contradiction could be neutralized by the hypothesis and outcomes of Ci *et. al.,* who investigated various annealing temperatures ranging between (450 - 900 $^{\circ}$C) as described in section 3.1.3 and suggested that the formation of carbides is subject to the processing or sintering temperatures, and that only processing temperature exceeding 650 $^{\circ}$C favors the formation of carbides [28].

It is evident that the variation in grain size is directly related to the milling energy imposed on the powders, i.e. milling parameters (MT, RPM, BPR, and PCA). For example, Choi *et. al.,* who milled Al powders for prolonged times (up to 48hrs at 550RPM) reported that there is a dependence of grain size on milling time. His results showed that Al grain size went from 150nm to 48nm when the MT is increased from 8 to 48hrs, respectively [39]. Table 5.1 summarizes the mean crystal size calculated from the XRD scans. The results show a small increase in mean grain size for both the three and six hours milled samples before and after annealing. Also, it is remarkable that reducing the milling time from 6hrs to 3hrs had an effect on the grain size which increased from 45nm to 87nm, respectively. The preservation of the reduced grain size throughout the processing steps resulted in the enhanced tensile strength which will be presented and discussed later.

Table 5. 1 crystal size (in nm) of powder, un-annealed, and annealed extruded 2wt.% Al-CNT samples

Milling Time	Powders	Bulk (no annealing)	Bulk (10h annealing)
3hours	87	-	93
6hours	45	56.5	72

5.1.4 Nano Indentation and Vickers Micro Hardness Testing of the pure Al, and 2 wt % Al-CNT Composite

The main reason for conducting hardness testing on both micro and nano levels was to help solve the consistent problem of notch senstivity. Also, the efforts were focused to try to determine the appropriate annealing temperature at which the stresses are relieved in a trial to pinpoint the effect CNTs on the mechanical properties of the composite and not the effect of strain hardening. Figure 5.11 shows the nano indentation and vickers hardness results which are consistent together to a great extent. There is a significant increase in hardness approximately

three times when the unmilled Al is compared to its milled counterparts. These results show the strain hardening caused by milling on the Al matrix which will made it very difficult to isolate the effect of CNTs on the mechanical properties when added to the Al as reinforcement. The similar hardness results for pure and composite samples in Figure 5.11 prove this argument. In addition, the presence of Al oxide might have had played a role in hardening the Al matrix as well. Figure 5.12 shows the young's modulus for pure milled and un-milled Al in addition to the 2 wt % Al-CNT sample. These results prove the point by showing that CNTs didn't enhance the stiffness when added to a strain hardened Al matrix.

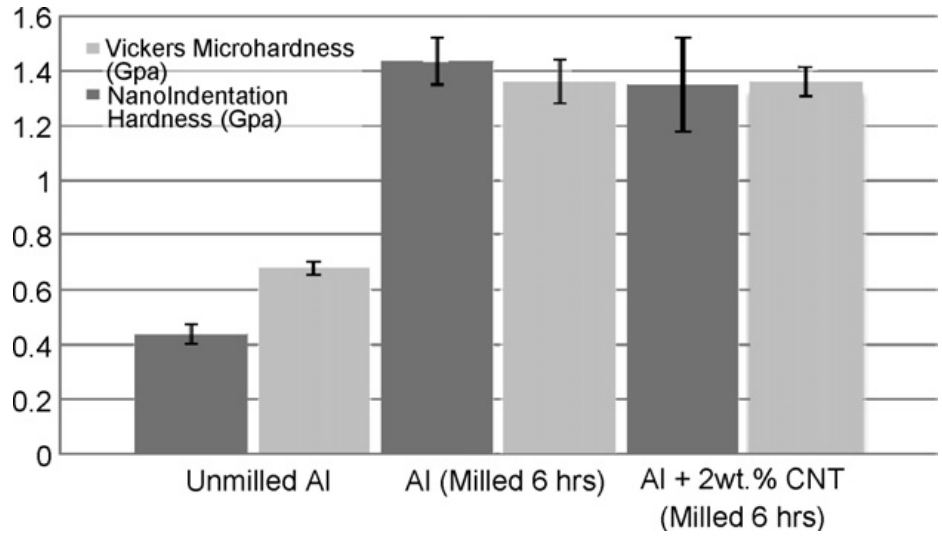

Figure 5. 11 Vickers micro hardness and nano indentation hardness in GPa for un-milled and milled pure Al and 2 wt.% Al-CNT extruded samples cross sections [52]

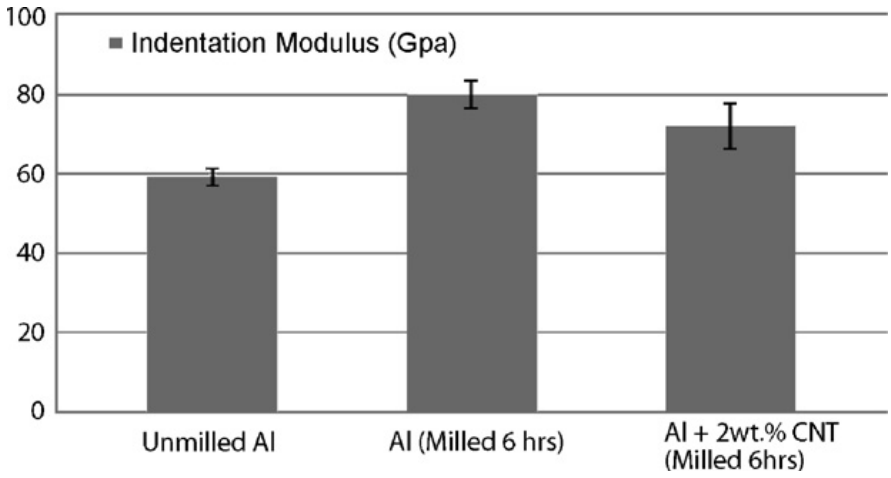

Figure 5. 12 Young's modulus calculated from nano indentation testing [52]

VHN was done on extrudates cross sections for un-annealed, and annealed (200°C, 300°C, and 400°C) pure Al samples in order to determine the point where stresses start to be relieved. Figure 5.13 shows VHN readings for sample cross sections versus different annealing times for annealing temperatures of (200°C, 300°C, and 400°C). Also, the hardness of unannealed milled and unmilled pure Al is shown as thin dotted lines. From the results presented in this Figure, it is clear that the sample annealed at 400°C for different durations experienced a noticeable stress relief.

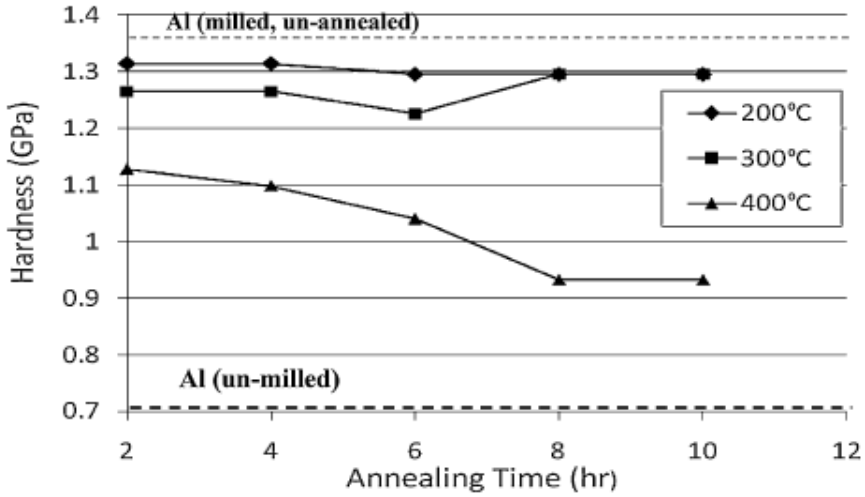

Figure 5. 13 VHN (GPa) for pure milled extruded Al cross-sections at various annealing temperatures [52]

Using the hardness results for guidance, tensile annealed samples at 400°C, 500°C were prepared for testing. It should be noted that ductility is directly proportional to temperature increase, but there will be drawbacks to increasing temperature above a certain limit. As mentioned before in section 5.1.3 increasing the processing temperature of the composite to 650°C and above might cause the formation of unfavorable interfacial reactions, which might be excessive in the presence of amorphous carbon regions. That's why in all this research work the annealing temperature didn't exceed 500°C, but this didn't rule out the formation of carbides as it will be demonstrated later on.

5.1.5 Tensile Testing of the pure Al, and 2 wt.% Al-CNT Composite

Tensile testing was performed using an Instron 50KN universal testing machine. A 1mm/min crosshead speed was maintained in all tests. Figure 5.14 shows the tensile strength vs. strain% for 2 wt % Al-CNT tensile samples milled for 6hrs and annealed at 400, and 500°C for 10 hrs after extrusion. The Figure shows that the pure Al sample annealed at 400°C has the highest UTS yet the lowest ductility in all samples. Also, it is obvious that increasing the annealing temperature had an effect on the ductility of the milled samples where the strain% increased from 5.9% to 8.4% in case of pure Al, and from 6.9% to 7.9% in case of 2 wt% Al-CNT when the annealing (refer to section 4.2.3 on annealing) temperature was raised from 400°C to 500°C, respectively. Table 5.2 summarizes the mechanical properties of the composites where Young's Modulus happens to have the same trend of the data calculated from the nano indentation results.

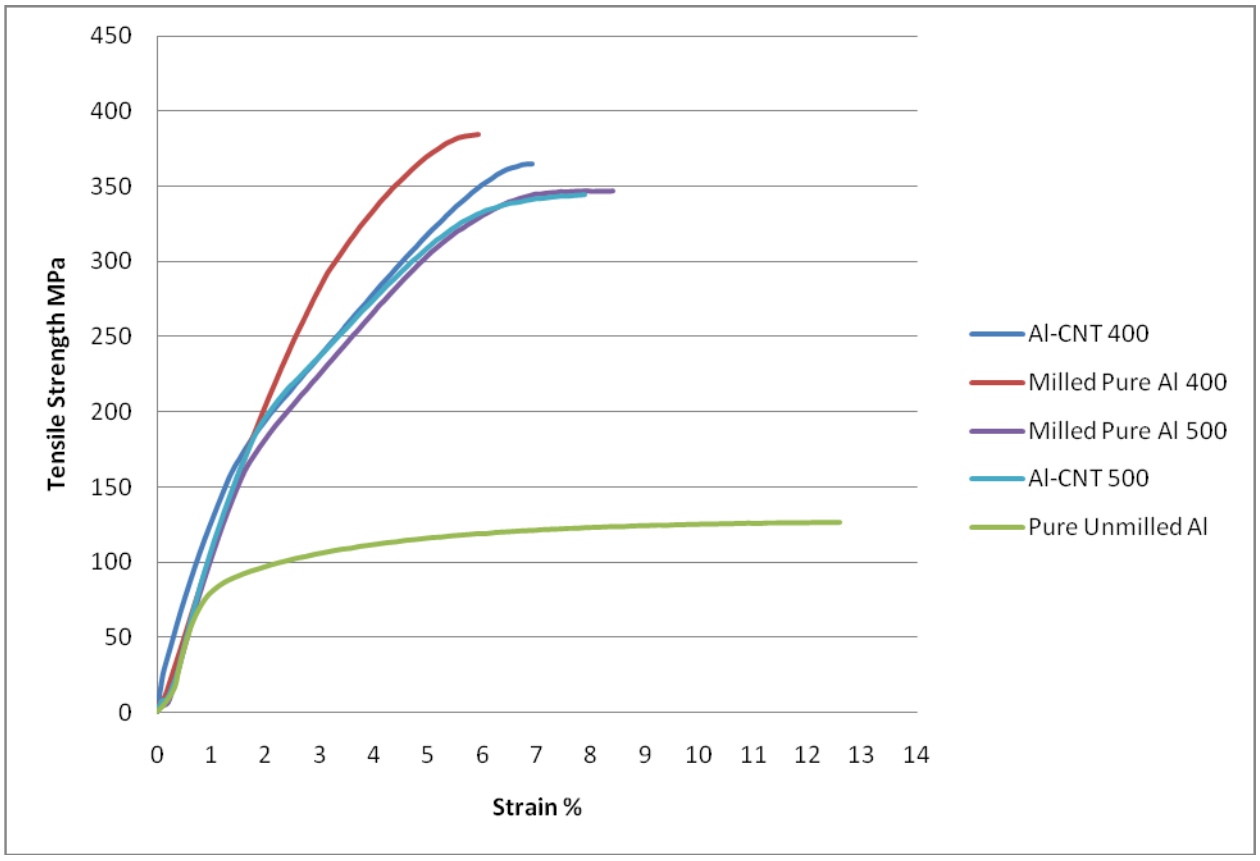

Figure 5. 14 Stress-strain curves for representative tensile samples milled for 6hrs

Table 5. 2 Mechanical properties of pure and 2 wt.% Al-CNT milled for 6 hrs annealed at different temperatures for 10 hrs

Sample	Unmilled Pure Al	Milled pure Al annealed at 400°C	2 wt.% Al-CNT annealed at 400°C	Milled pure Al annealed at 500°C	2 wt.% Al-CNT annealed at 500°C
UTS (MPa)	130	377.4	365.5	348.5	348
YS (MPa)	70	185	200	160	180
Young's Modulus (GPa)	56	82	81	78	70
Elongation (%)	15	5.9	6.9	8.4	7.9

Figure 5.15 shows the tensile strength vs. strain% for 2 wt % Al-CNT tensile samples milled for 3hrs and annealed at 500°C for 10 hrs after extrusion. The Figure shows that the 2wt % Al-CNT sample possesses higher UTS yet the lower ductility than the pure sample. Also, it is obvious that there is a high variability in ductility between the two samples; the composite sample failed at 5.7% strain whereas the pure sample failed at 8.4% strain.

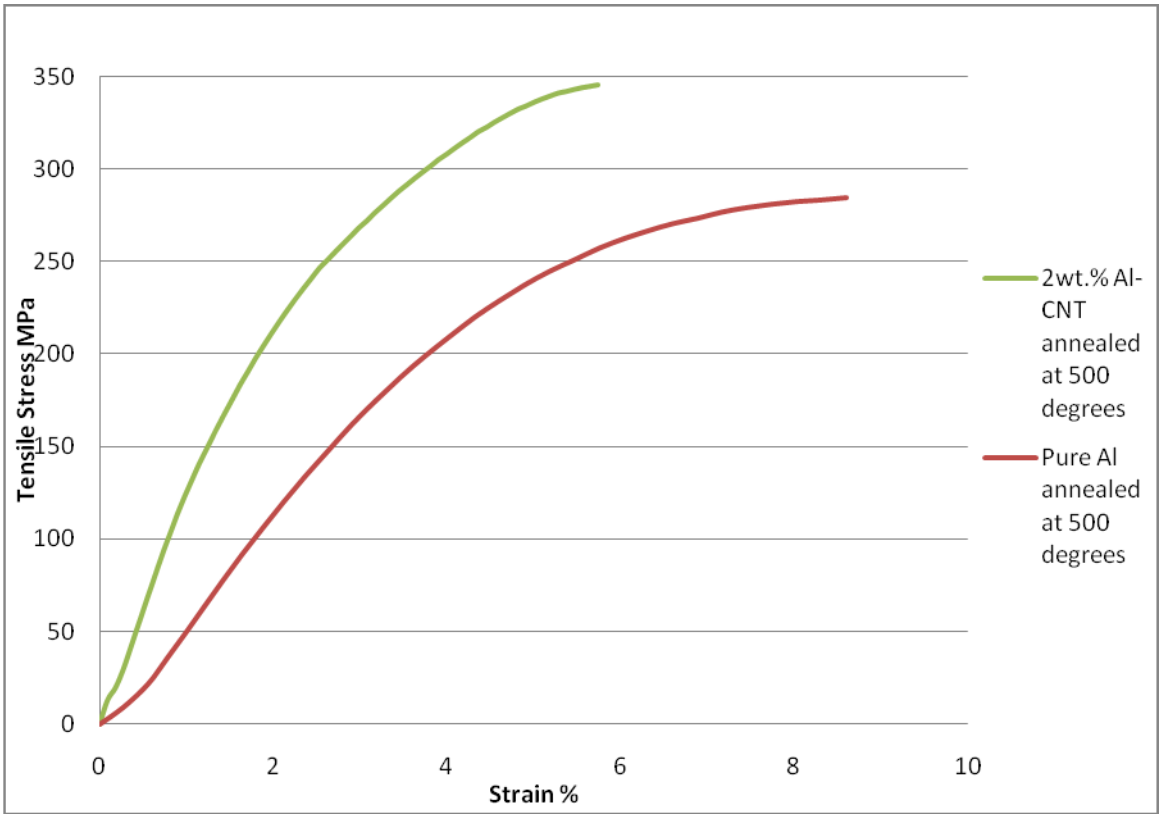

Figure 5. 15 Stress-strain curves for the bulk tensile samples milled for 3hrs

Table 5. 3 Mechanical properties of pure and 2 wt.% Al-CNT milled for 3 hrs annealed at 500°C for 10 hrs

Sample	Un-milled pure Al	Milled pure Al annealed at 500°C	2 wt.% Al-CNT annealed at 500°C
UTS (MPa)	130	284.5	345
YS (MPa)	70	150	200
Young's Modulus (GPa)	56	70	80
Elongation (%)	15	8.6	5.7

Unfortunately, no XRD scans were made for the pure milled samples, so it is not possible to calculate the average grain size before and after annealing which seem to have changed remarkably in this case. It could be argued that the decreased milling time and absence of CNTs facilitated the relieving of the amount of strain hardening induced in the pure sample whereas in case of the composite sample the CNTs prevented this relieving action. This argument is supported by the outcomes of Kuzumaki *et. al.,* shown in Figure 3.1 which demonstrate that CNTs prohibit the deterioration of tensile strength and prevent the increase in ductility when samples are annealed [25]. Furthermore, the UTS results of compression testing of milled samples presented by Choi *et. al.,* show that CNTs retained the strength of the composite when heating is applied whereas the pure Al sample didn't [39]. Table 5.3 summarizes the mechanical properties calculated from Figure 5.15 curves.

The reason for performing annealing was the notch sensitivity of the failed samples. Succesful results were obtained first from the 400°C annealed samples which possessed increased ductility than its failed un-annealed counterparts. Additionally, annealing at 500°C was performed for the purpose of studying the effect of annealing on strength and ductility. All samples that were milled at 200 RPM discussed in this section exhibited approximately three

times higher UTS values when compared to un-milled pure Al processed with the same technique. This was mainly due to the grain size reduction (proven by XRD) and crystallographic defects imposed by the milling process. From all the results mentioned in this section, it is found that only the 500°C annealed Al-CNT sample that was milled for 3hrs had mechanical properties that were significantly different than its pure Al sample counterpart for the reasons mentioned in the previous paragraph. For all other samples the addition of CNTs didn't change the mechanical properties of the material significantly.

If the tensile values reported here are to be compared, they are found significantly higher than other previously published work. For example, Esawi and Borady [55] reported a tensile strength of 62MPa for the same CNT content, Kwon *et. al.,* [46] reported a tensile strength of 194MPa for the process and testing described in section 3.1.9. However, in those studies ball milling and MA techniques were not used, which directly relates the enhancement made in this study to the good dispersion of CNTs in the Al matrix demonstrated clearly in the SEM micrographs, and the strain hardening of the powders that is considered to be a strengthening mechanism relating directly to the final strength of the composites. George *et. al.,* [16] whose process was described earlier in section 3.00 used the ball milling technique to mill 2 vol.% Al-CNT but only for 5 min and reported 138MPa UTS which is still significantly lower than the values reported here. A recent study by Choi *et. al.,* reported UTS compression values of 380MPa, 405MPa for 4 vol.% Al-CNT after milling for 6, 12hrs, respectively [39]. These results that are very close to ours reinforce our outcomes.

The results presented in section 5.1 were conclusive, and the outcomes were quite interesting. The main obstacle in this set of experiments was the strain hardening which was a

problem that actually took a lot of time to be solved. In an effort to eliminate or diminish this problem, a new set of experiments is designed with a much higher milling speed of 400RPM but, keeping the milling time to a minimum of 30 min. The aim behind this is to reduce the amount of cold working of the powders by decreasing the time they are subjected to ball impacts. In addition, two types of MWCNTs will be used for comparison purposes; the one used in the previous set of experiments (140nm diameter MWCNT), and a new 40nm diameter MWCNTs with a higher aspect ratio; and thus having a higher potential for strenghting and stiffening.

5.2 Synthesis of (0.5, 1, 1.5, 2, 5) wt % Al-CNT Nano Composites Milled at 400RPM for 30min with BPR10:1

5.2.1 Powder blending of Al-CNT Nano composites (400RPM, 30min)

In this set of experiments, five concentration of Al-CNT powder are synthesized (0.5, 1, 1.5, 2, 5 wt.% of CNT) using two different types of CNTs; 140nm diameter MWCNTs, and the 40 nm MWCNT with high aspect ratio. The mixture is milled for 30 min with the conditions previously mentioned in section 4.2.1.3 Powders milling is done in the presence of a PCA for particle size control and the amount of PCA added is calculated using the same technique described in section 5.1.1.

5.2.2 SEM and TEM analysis for powder and bulk samples for the various concentrations and CNT types of Al-CNT composites

The 140nm MWCNTs supplied by MER Corporation used in the previous set of experiments have a fairly straight tubular structure, as shown in Figure 5.16(a). The 40nm MWCNT supplied by Cheap Tubes Inc. that are going to be employed in this new set of experiments were found to be curvilinear and entangled as shown in Figure 5.16(b). Also, it is

worth mentioning that the aspect ratio of the 40nm MWCNT is more than 7 times that of the 140nm MWCNT.

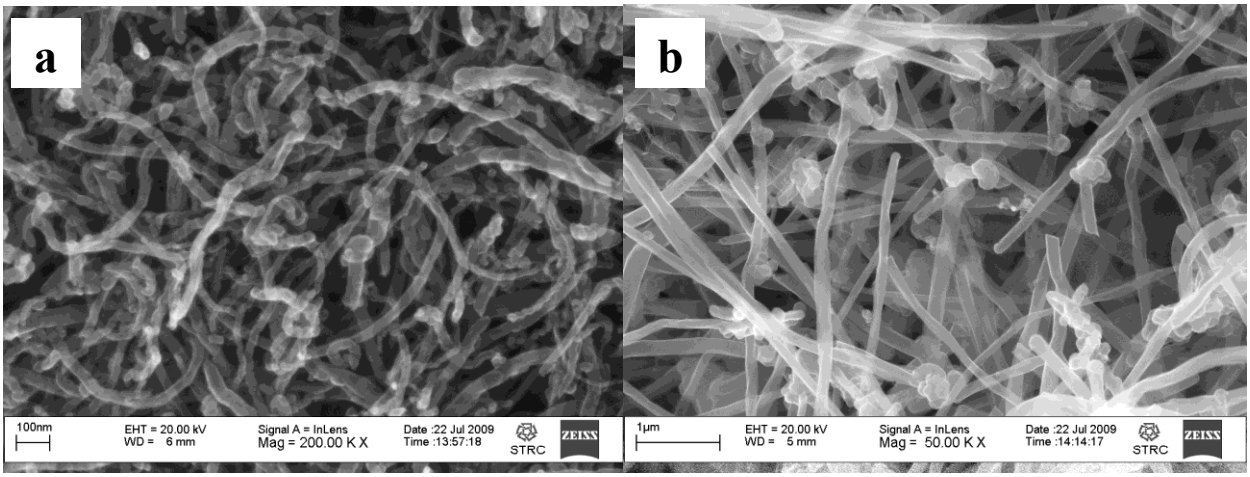

Figure 5. 16 SEM micrograph of (a) the 40nm MWCNT supplied by Cheap Tubes [56] (b) the 140nm MWCNT supplied by MER Corporation [57]

Following milling, examination of the composite powders with different types of CNTs but having same CNT concentrations was conducted. Some differences concerning particle size are observed. Figure 5.17 shows SEM micrographs for representative Al-CNT composite powders with different CNTs types and concentrations (0.5, 2, 5 wt %) milled for 30 min. It is clear that for micrographs a, c, e of composites prepared using the 40nm CNTs; particle size is smaller than those in micrographs b, d, f of composites prepared using the 140nm CNTs, respectively. This is very obvious especially for the 2, 5 wt % samples. This confirms that CNTs acts as a strain hardener when added to Al because as the surface area of CNTs increase (in case of the 40nm CNTs), the particle size decreases. This observation agrees with Wang *et. al.,* [42] who pointed to the strain hardening effect of CNTs.

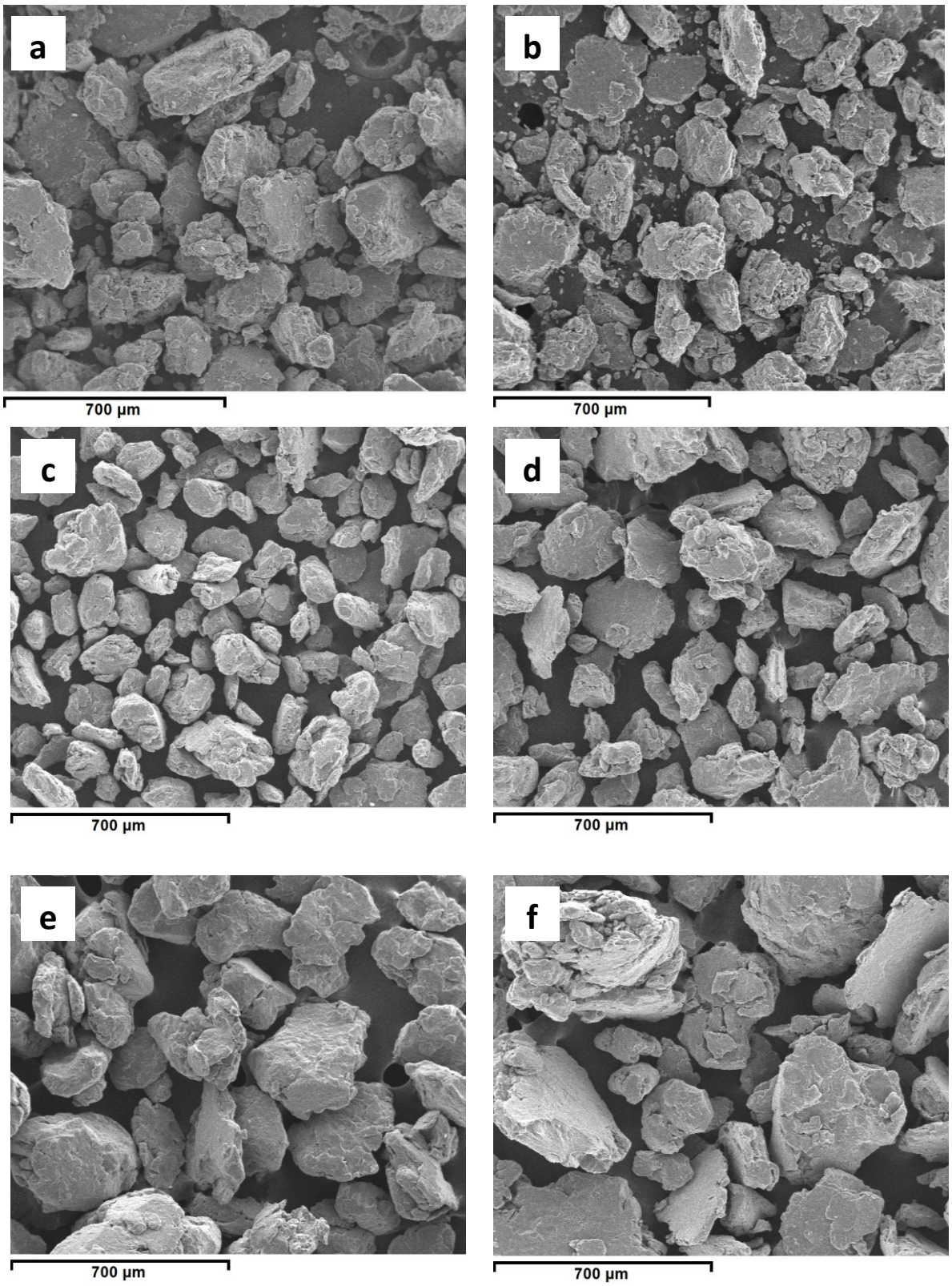

Figure 5. 17 SEM micrographs showing particle size and morphology for 0.5, 2 and 5 wt% 40nm MWCNT (a, c and e) and 0.5, 2 and 5 wt% 140nm MWCNT (b, d and f) [57]

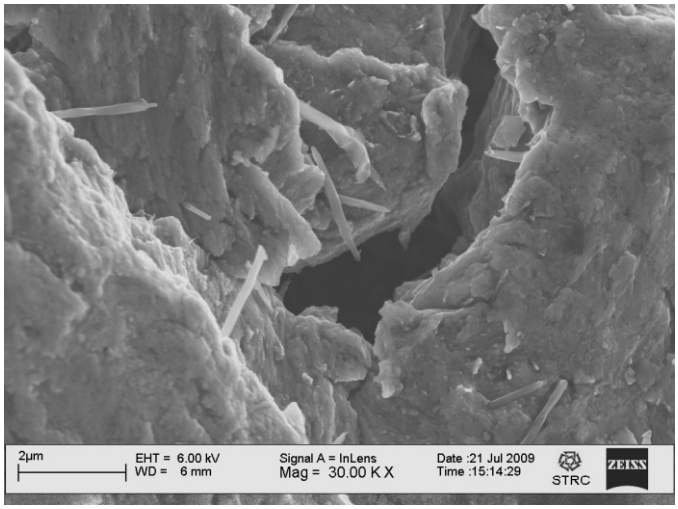

Figure 5. 18 2 wt % Al-CNT140nm composite powder [57]

Figure 5.18 shows the effect of milling 2 wt % Al-CNT_{140nm} for 30 min; it is clear that CNTs preserved their tubular structure, and are well dispersed and embedded in the Al particles. If this Figure is compared to Figure 5.3(a), it will be clear that increasing the RPM from 200 to 400 accelerated the mechanical milling process of the composite for the same milling duration, by increasing the milling energy.

It has been reported in several studies that increasing the concentration of CNTs above a certain limit results in the deterioration of the composite properties mainly because of the clustering problem. SEM investigations confirmed the presence of clusters of CNTs in the 5 wt % Al-CNT_{40nm} samples as shown in Figure 5.19 (b). On the other hand, SEM examination of the 5 wt % Al-CNT_{140nm} didn't confirm the presence of clusters.

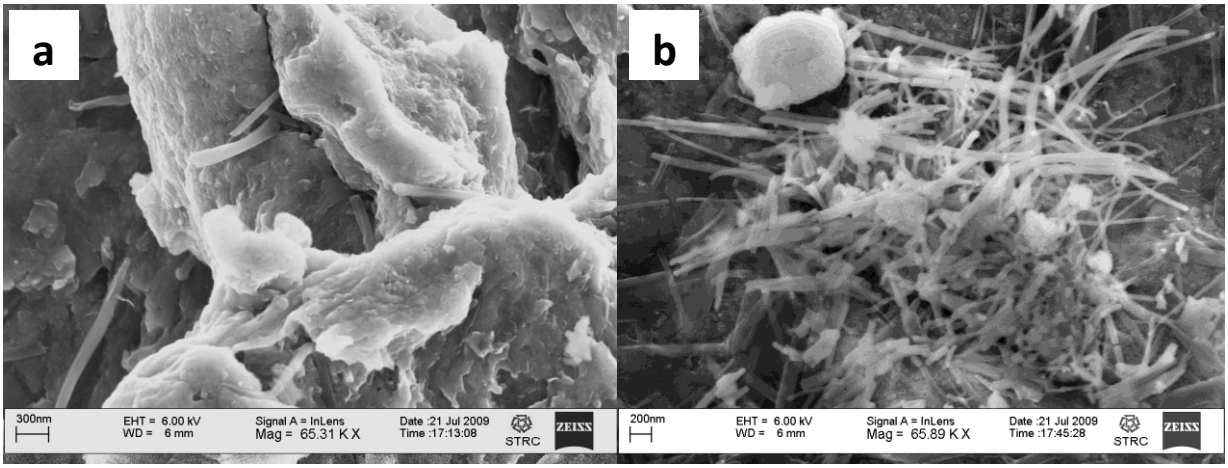

Figure 5. 19 5 wt % Al- CNT40nm composite powders showing (a) well dispersed, (b) clustered CNTs [57]

Figure 5.20 shows the fracture surfaces of Al-CNT_{140nm} composites with different CNTs concentrations. It can be seen in both micrographs that CNTs are present individually throughout the matrix, and that there are voids surrounding the CNTs because of the tension test that the sample went through as discussed earlier in section 5.1.2. In addition, the depth of the dimpled structure representative of ductile failure is decreased when the CNT wt % increases.

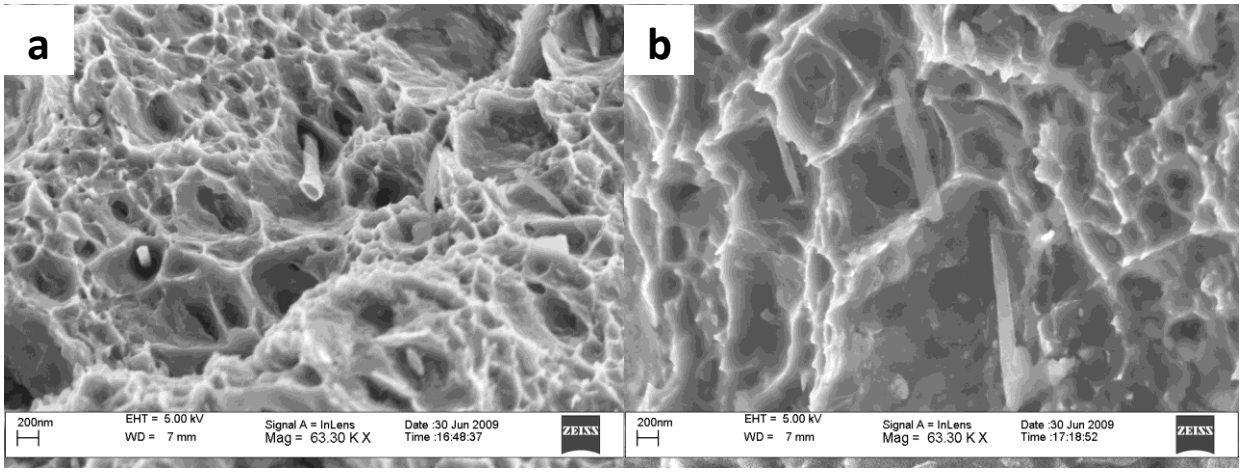

Figure 5. 20 Fracture surfaces of (a) 1.5 wt %Al-CNT_{140nm} and (b) 5 wt % Al-CNT_{140nm} [57]

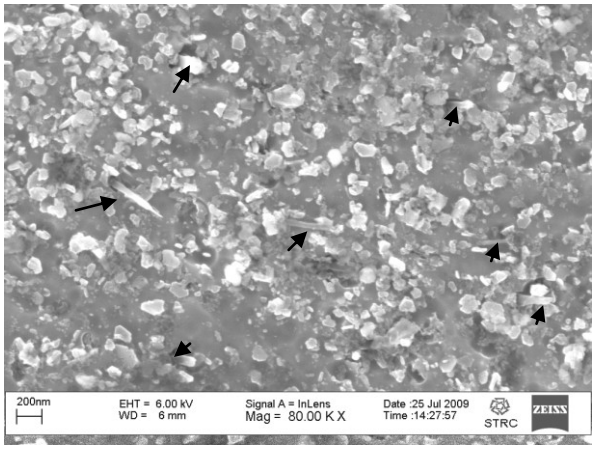

Figure 5. 21 Etched 5 wt % Al- CNT40nm sample showing several CNTs (indicated by arrows) [56]

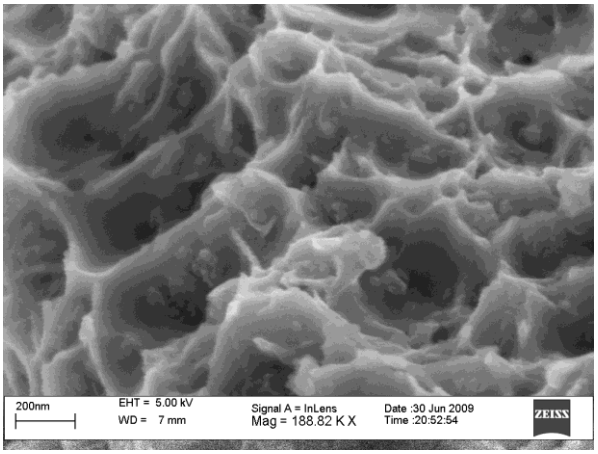

Figure 5. 22 Fracture surface of a 1.5 wt % Al-CNT40nm sample [57]

Figure 5.21 shows an SEM micrograph of a 5 wt % Al-CNT_{40nm} sample that was ground and heavily etched to expose the CNTs. It indicates the presence of CNTs on the surface. Figure 5.22 is a fracture surface of an Al-CNT_{40nm} composite; the dimpled matrix structure indicating a ductile failure is present, but CNTs are not easily seen throughout the surface although the magnification is three times higher than that used in investigating the 140nm CNTs.

There was no point of trying to prepare Al-CNT_{140nm} diameter samples for TEM imaging because the large CNTs fall-off the surface of the wafer, so only 40nm CNTs were investigated using TEM. Figure 5.23 represents a low resolution TEM micrograph of a 2 wt % Al- CNT_{40nm}

sample showing the well dispersed nanostructure and the matrix grains. Figures 5.24 and 5.25 are higher magnification micrographs to reveal details of the nanostructures observed. In Figure 5.24 CNTs of different diameters are observed though the typical CNT sidewall lattice structure is not clear. Also, the Figure proves that the interfacial region between the CNTs and the Al matrix is free of pores for samples not subjected to tensile testing as discussed earlier, thus confirming that point. Figure 5.25 shows a structurally damaged CNT, and a CNT that has been converted completely into a carbide rod like structure having the shape of a CNT, a phenomenon that was also observed by Poirier *et. al.,* [38] as discussed in section 3.1.5. Wang *et. al.,* have suggested that smaller diameter CNTs are more likely to deform under the impact of milling balls due to their lower bending stiffness and critical buckling volume compared to larger diameter ones [42]; a theory that couldn't be proven in the current study, since we could only prove damage due to milling by TEM analysis for the 40nm diameter CNTs.

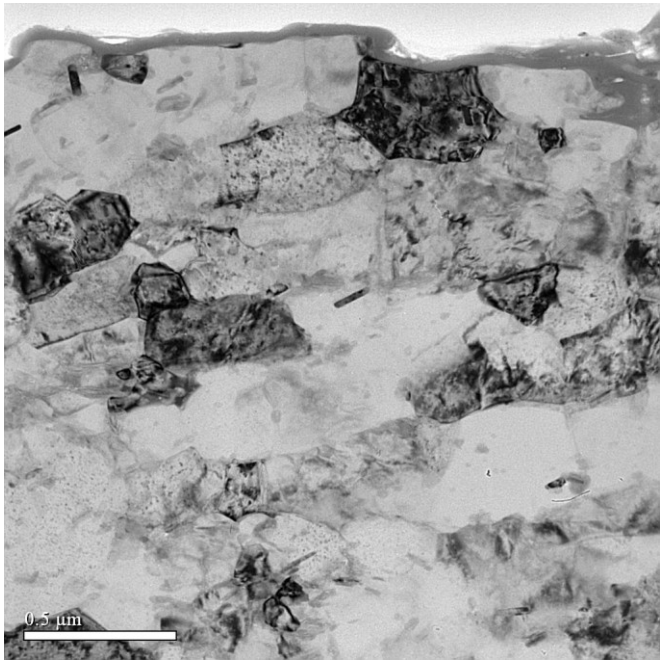

Figure 5. 23 Low magnification TEM micrograph showing the strain hardened aluminium matrix grains as well as dispersed rod-like structures [56]

Figure 5.26 represents a TEM micrograph showing different nanostructured regions marked by sites from 1 to 3. Energy Dispersive Spectroscopy (EDS) analysis is performed at the different sites on the sample confirming that both nano-sized aluminium oxide particles and nano rods of aluminium carbide are present within the sample, which is confirmed by the XRD analysis results that will be shown and discussed later in the coming section.

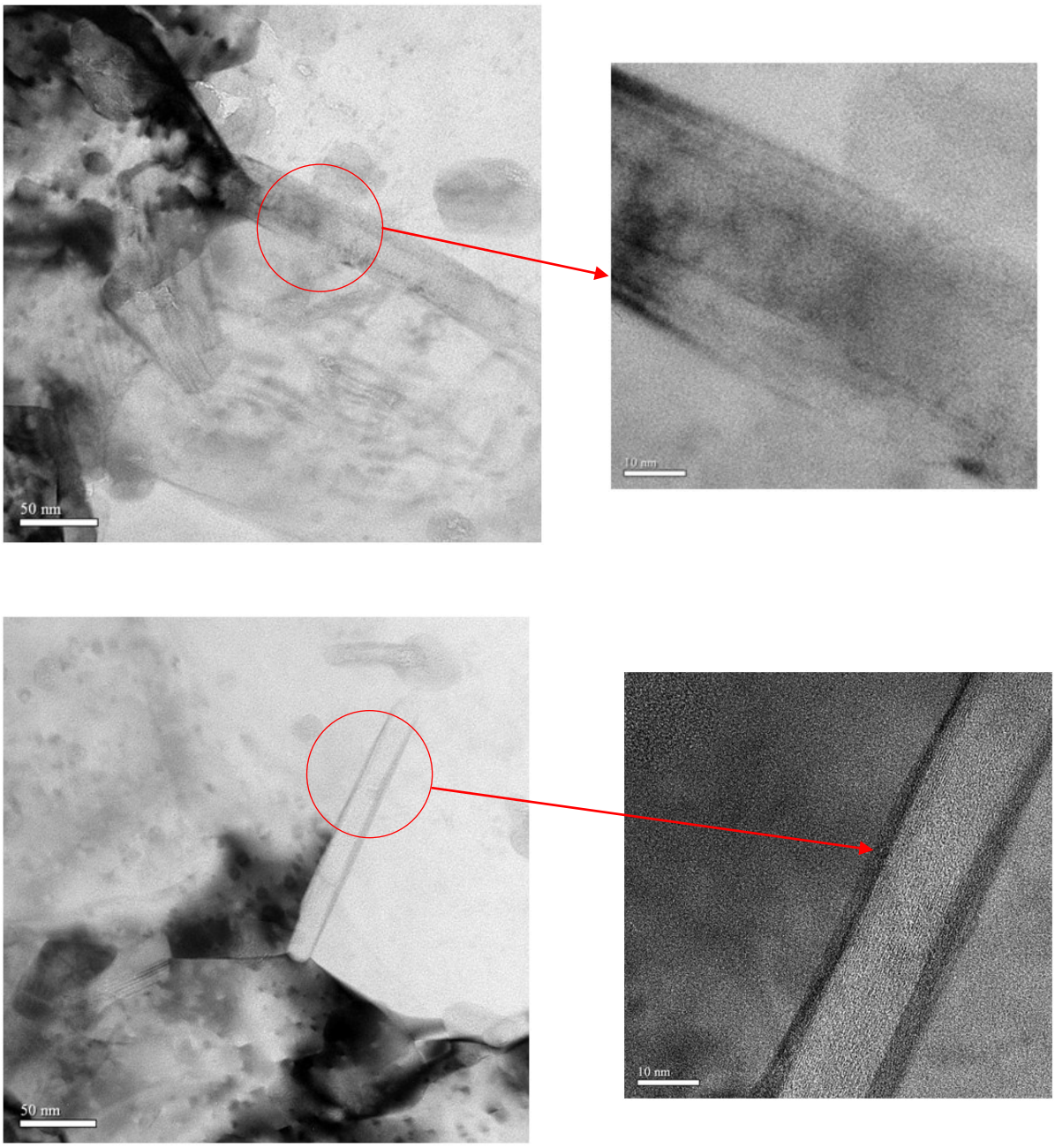

Figure 5. 24 High magnification TEM micrographs of some rod-like structures showing different CNT configurations. The insets are high magnification images of the same structures (on the left) [57]

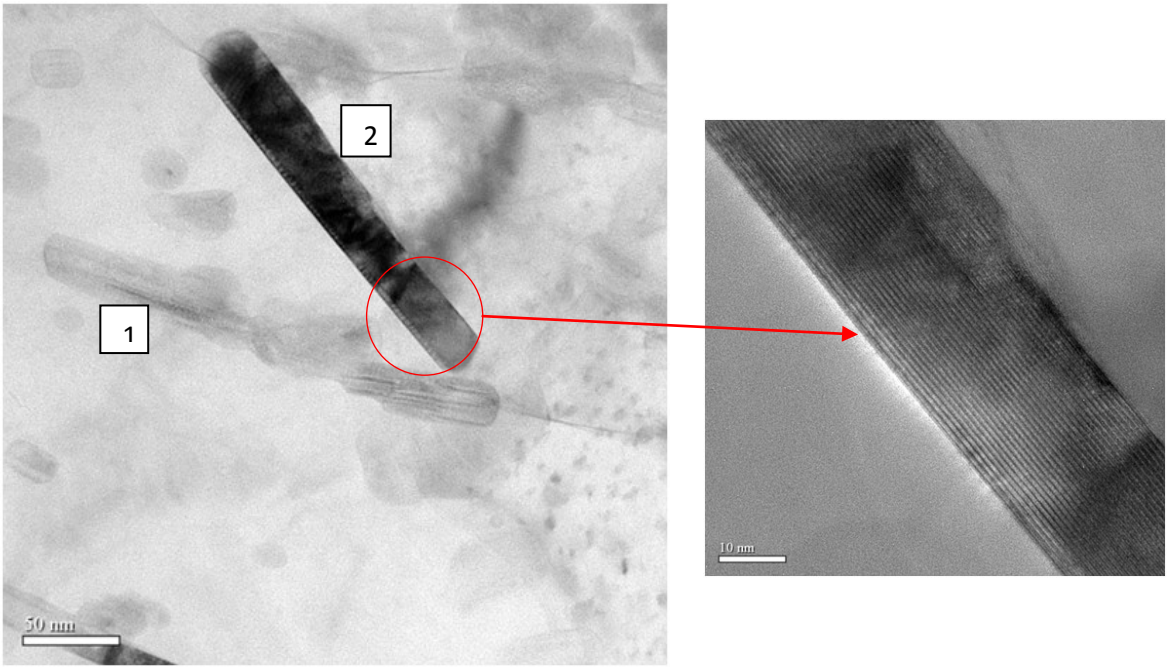

Figure 5. 25 High magnification TEM micrographs showing two rod-like structures. One of them is a damaged CNT (1); the other one is a CNT which has been transformed to a carbide rod (2). The inset is a high magnification micrograph of the carbide rod like structure [57]

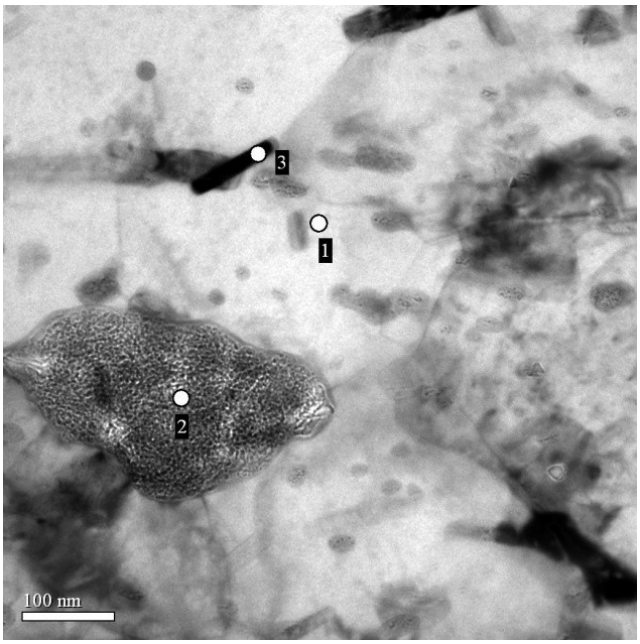

Figure 5. 26 TEM micrograph showing regions where EDS analysis was performed at three sites. Site 1: pure Al, site 2: Al and oxygen and site 3: Al and carbon [57]

5.2.3 XRD Analysis of Al-CNT composites Bulk Samples (scans and analysis of all samples were performed by the research team members at SDSU)

Figures 5.27 and 5.28 represents XRD scans of annealed extrudates of both types of 1.5 wt % and 5.0 wt % CNTs, respectively. The Figures show that the smaller diameter CNTs form more pronounced carbide peaks even at smaller CNT contents maybe because that type of CNT was more susceptible to damage which would encourage it to react with Al. For the 5 wt %, aluminium carbide is clearly observed for both types of CNTs. XRD analysis of the milled powders performed at SDSU but not available for this study doesn't reveal any carbide formation for all CNT contents. So, it is believed that the extrusion and sintering processes which took place at 500°C were responsible for carbides formation. In addition, no peaks for CNTs appears in either powder or extrudate scans; an observation which has also been reported by other researchers [27].

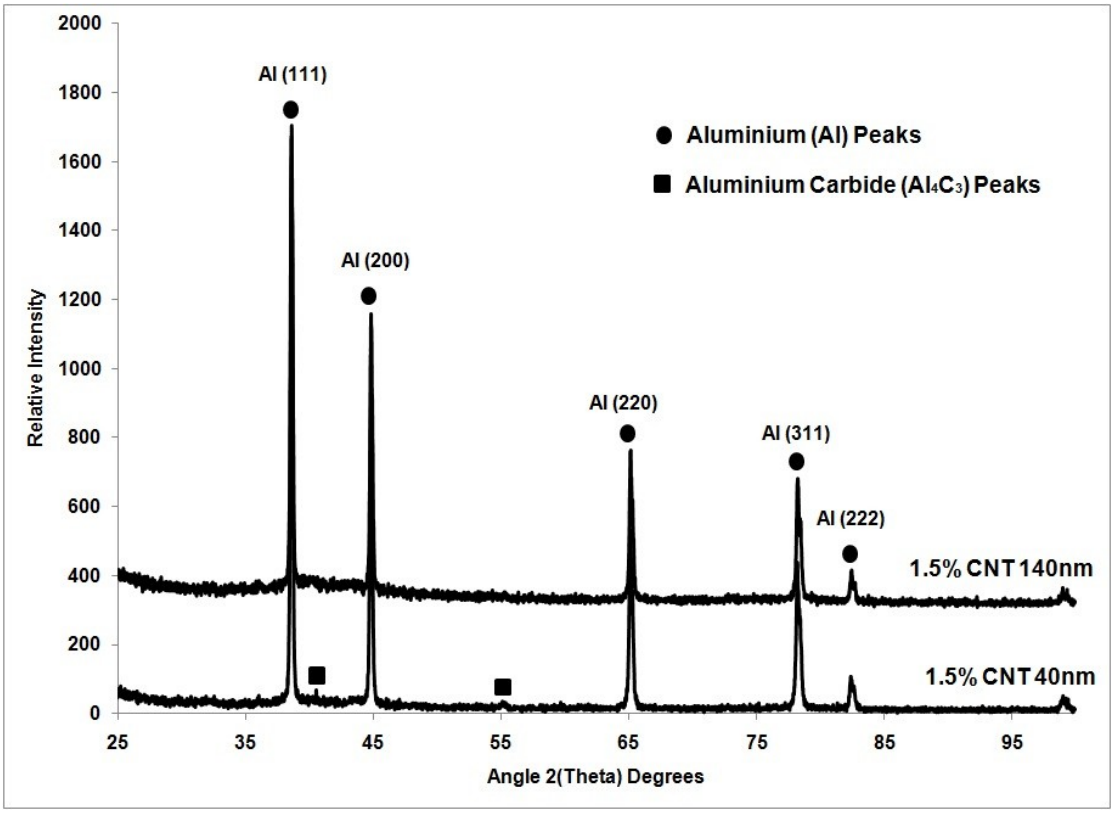

Figure 5. 27 XRD scans of Al- 1.5 wt % CNT extrudates for the two types of CNTs used [57]

Figure 5.29 shows the average grain sizes (measured from XRD) of milled powders of both CNTs at different volume fractions, namely (0.5, 1, 1.5, 2, and 5) wt%. Evidently, the average grain size decreases as the CNT content increases for both CNTs. One possible explanation is that the distribution of the CNTs within the powders hinders dislocation motion as discussed by Tokunaga *et. al.,* in reference to other researchers [41], as well as their strain hardening effect which minimizes powder welding during milling.

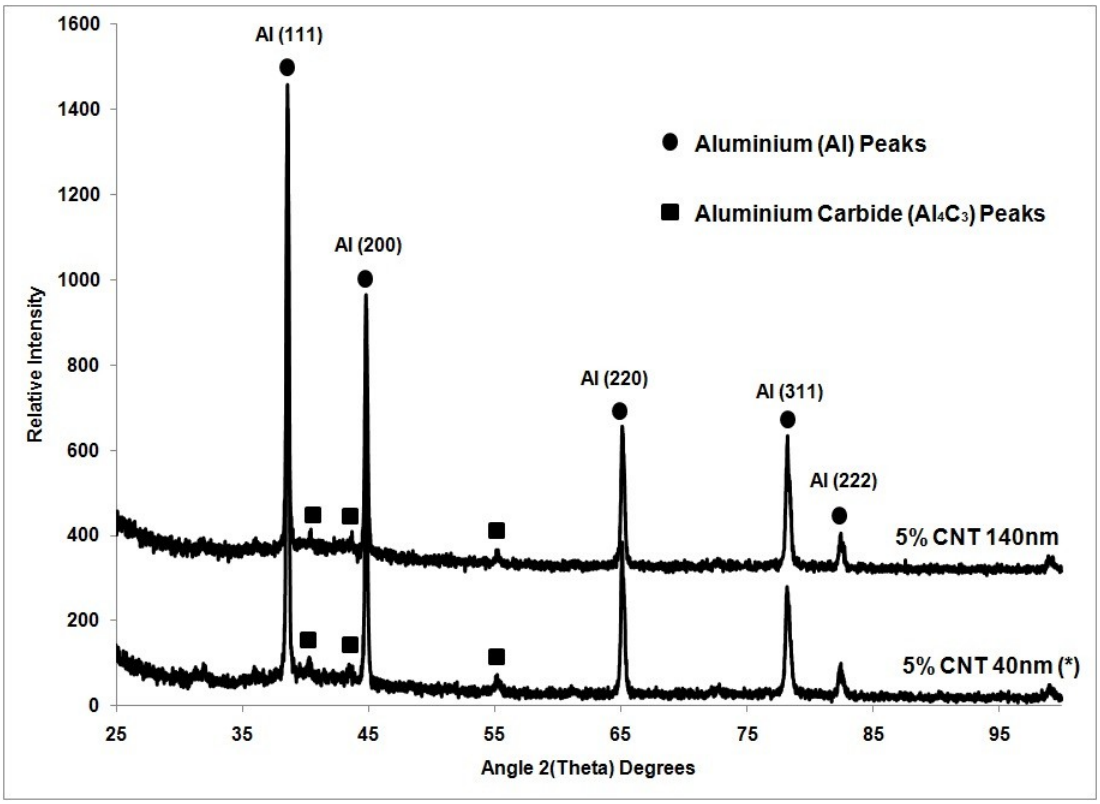

Figure 5. 28 XRD scans of Al- 5 wt % CNT extrudates for the two types of CNT used [57]

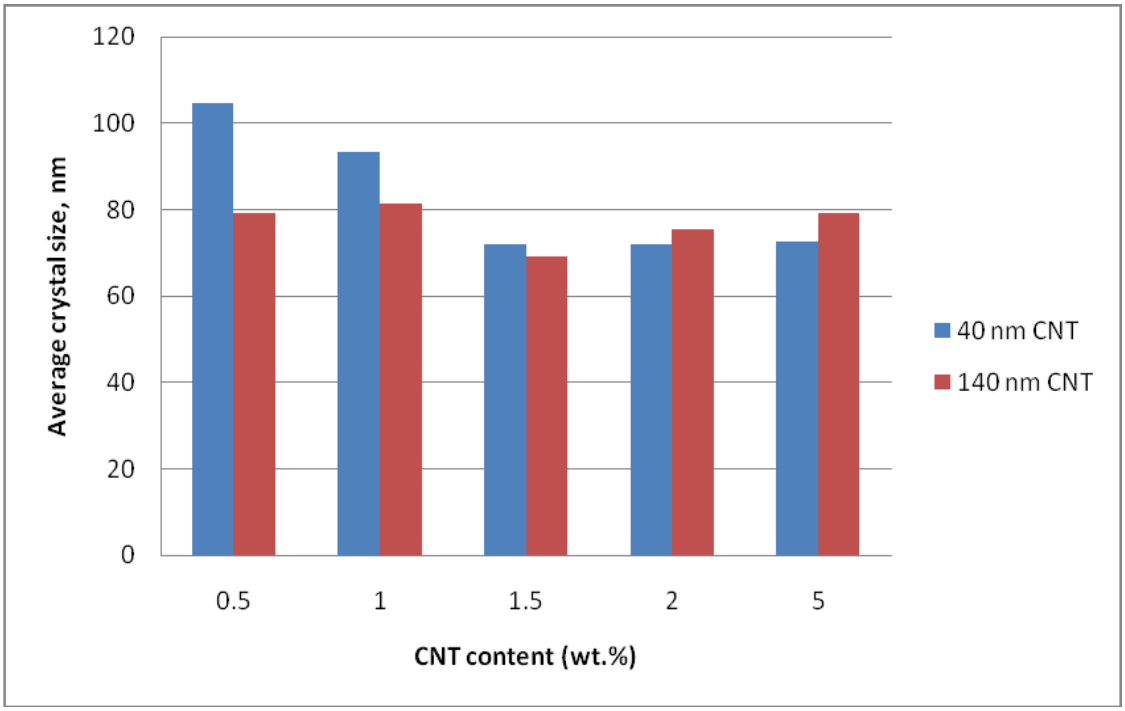

Figure 5. 29 Average crystal size in (nm) of milled powders based on the two types of CNTs [57]

5.2.4 Tensile Testing of the pure Al and (0.5, 1, 1.5, 2, 5) wt % Al-CNT Composites milled at 400RPM for 30min

Figure 5.30 shows the tensile strength of composite and pure samples for both types of CNTs milled at 400RPM. Error bars indicating the standard error based on a minimum of three samples for each composition is added to the bar chart to indicate the variation. Overall, the composite containing 2 wt % Al-CNT140nm provides the most significant strengthening (+96%). However, this is followed by a drop in strength, but still the values are higher than the unreinforced Al by approximately 49 to 72 % for the 40nm CNTs and the 140nm CNT, respectively. The Figure shows that the 40nm CNTs provide more strengthening than the 140nm CNTs up to a certain concentration limit (~1.5 wt %) after which the 40nm Al-CNTs composite strength starts declining. This could be due to clustering of CNTs when higher concentrations are used in the composite; the SEM micrograph of a 5wt% Al-CNT_{40nm} powder sample in Figure 5.19 (b) supports this claim. Also, the TEM micrograph of a 2wt% Al-CNT_{40nm} bulk sample in Figure 5.24 shows several CNTs present very close together which might be an agglomeration. The same strength dropping trend occurred for the 140nm CNT composite but at higher CNT concentration; the strength decreased for the 5 wt % Al-CNT_{140nm} composite samples. The reason for the difficulty of dispersion of CNTs in the Al matrix at higher CNT concentrations causing deterioration in the mechanical properties is the large surface area of CNTs and the Van der Waal's forces present. This was very clear especially for the 40nm CNTs (characterized by their small diameter and entanglements) which experienced this problem at lower concentrations than the 140nm CNTs.

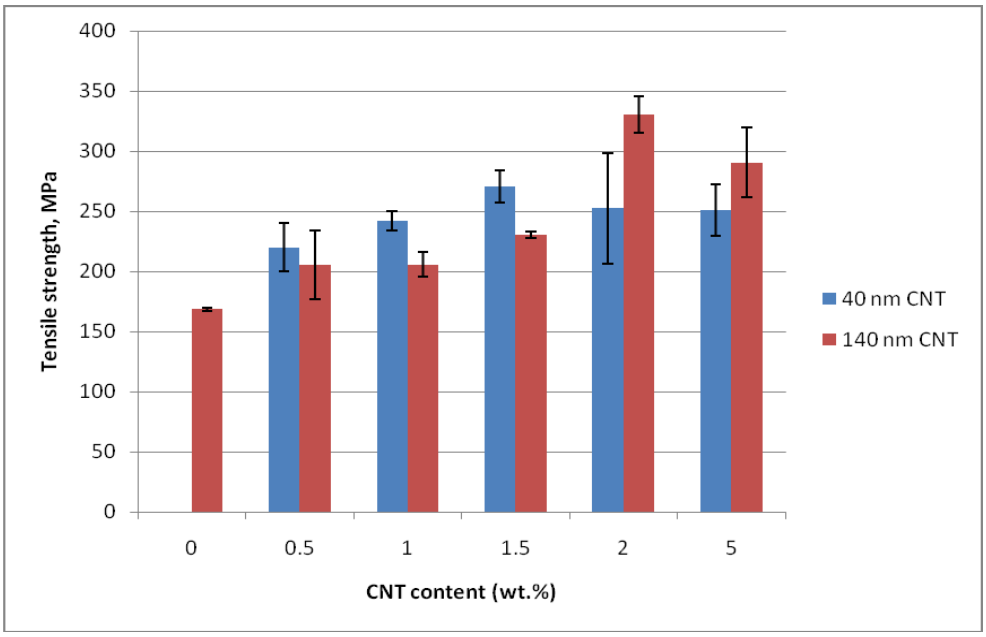

Figure 5. 30 Tensile strength Vs. CNT wt % for composites based on the two types of CNT [57]

Figure 5.31 shows the generally declining ductility with increasing the CNT wt% for both types of CNTs by presenting the amount of strain-to-failure at each concentration obtained from the strain gages with the specifications mentioned in section 4.3.2.1. This trend is expected because of the strain hardening effect that the CNTs have on the composite.

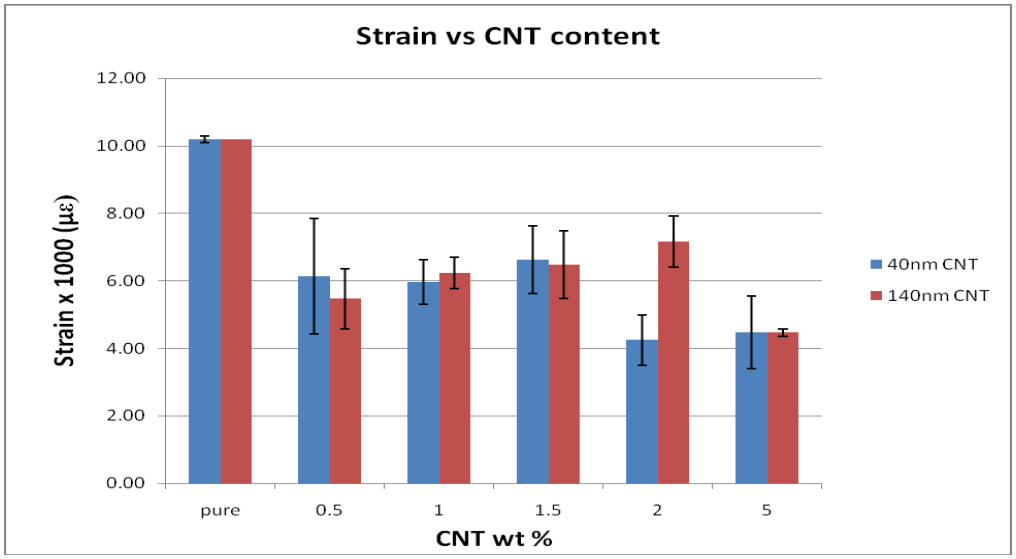

Figure 5. 31 Variation of strain-to-failure with CNT wt % for the 2 types of CNTs obtained from strain gauges

5.1.5 Nano Indentation of the pure Al and (0.5, 1, 1.5, 2, 5) wt % Al-CNT Composites milled at 400RPM for 30min

Figure 5.32, and 5.33 represents the variation of the elastic modulus vs. the CNTs wt% and the nano-indentation values for both types of CNTs. Compared to the tensile strength values, a different trend is observed for the Young's modulus and nano-indentation hardness measurements with the larger CNTs providing more effective stiffening and higher hardness compared to the smaller ones at all CNT wt% (up to +33 % and +119 % compared to pure Al). Similar to strength, Young's modulus and nano-indentation hardness values are observed to drop at 5 wt%. The modulii represented in Figures 5.32 was calculated from nano-indentation results. Theoretically, the elastic modulus should increase with the increasing CNT content if the rule of mixture is applied. However, this is not the case in this study where the elastic modulus is decreased at the highest of CNT content. This behavior is explained by Lahiri *et. al.,* who claimed that the rule of mixture is only valid for the homogeneously dispersed reinforcement which is not the case for the 5wt% Al-CNT composites. The author claims that the elastic modulus didn't increase as expected for the high CNT content samples due to the presence of CNT agglomerates which creates CNT-depleted regions causing plastic deformation to start at these regions at lower stresses than CNT-rich regions and this is because the Al and CNT have totally different E values [48].

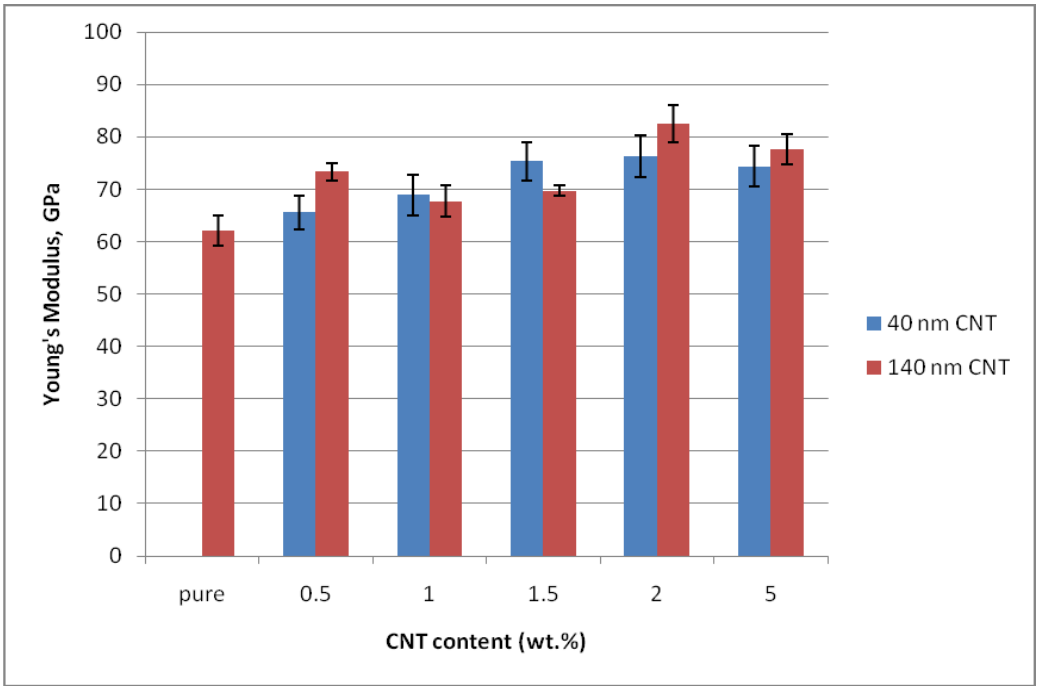

Figure 5. 32 Young's modulus calculated from nano indentation testing Vs. CNT wt % for composites based on the two types of CNT [57]

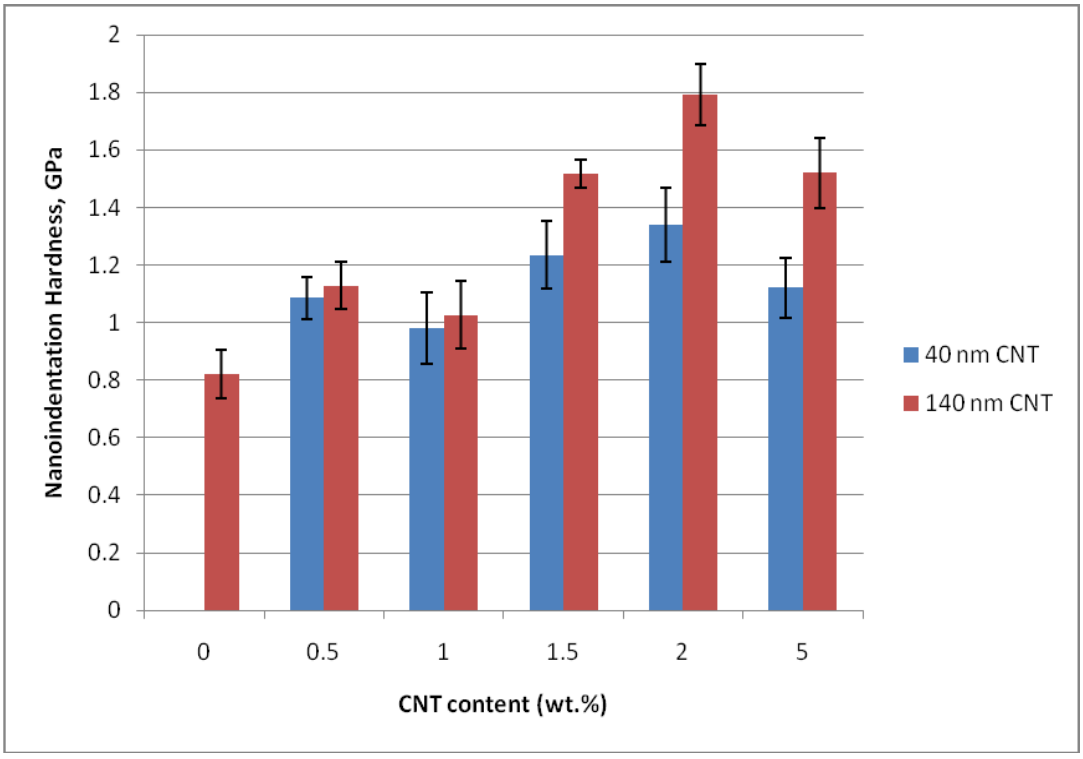

Figure 5. 33 Nano-indentation hardness vs CNT wt % for composites based on the two types of CNTs [57]

5.1.6 Relative Densities of the pure Al and (0.5, 1, 1.5, 2, 5) wt % Al-CNT Composites milled at 400RPM for 30min

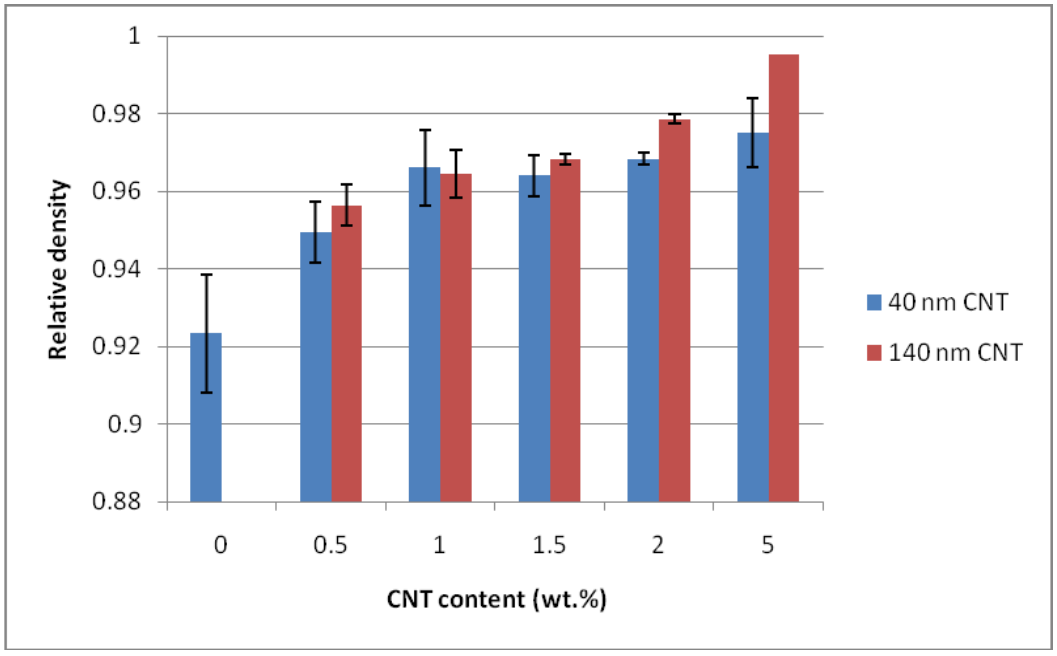

Figure 5. 34 Relative density (bulk density/theoretical density) as a function of CNT content (wt.%) for the two types of CNTs [57]

Figure 5.34 shows that the 40nm CNTs have somewhat smaller densities than the 140nm CNTs for most of the CNT concentrations tried. Moreover, Table 5.4 suggests that the effective volume fractions for the 40nm CNTs are slightly smaller than those of the 140nm CNTs for similar weight fractions. Thus we may conclude that in general, the relative density correlates with the CNT content, which in turn suggests that higher CNT concentration enhances the consolidation of the samples; owing to their lubricating effects during extrusion and reduction of particle size with the increase in CNT content [37]. The low relative density for the pure Al samples (0.92) clarifies why the measured Young's modulus (presented in Figure 5.32) was lower than 70 GPa. Similarly, the porosity reduction as CNT content rises enhances the modulus as reported earlier for all Al-CNT samples. Moreover, starting at 2 wt%, the relative densities for all

140nm Al-CNT samples are distinctly higher which hint at better dispersion. This in turn, explains the better mechanical properties and the SEM micrograph (Figure 5.19(b)).

Table 5. 4 Equivalent volume fractions for the two types of CNT used.

CNT wt.%	Equivalent Volume %	
	CNT_{140}	CNT_{40}
0.5	0.71	0.64
1	1.42	1.28
1.5	2.12	1.92
2	2.82	2.56
5	6.96	6.34

CHAPTER 6

CONCLUSIONS

1. Ball milling has been proven to be a very promising technique for the dispersion of CNTs in Al matrix. It has also been noticed that this technique excessively strain hardens the matrix as the milling time increases.

2. Ball milling pure Al for 3hrs and 6hrs at 200RPM almost tripled the UTS value, and noticeably decreased the ductility. Ball milling 2 wt % Al-CNT for 3hrs and 6hrs at 200 rpm caused the notch sensitivity problem which required the machining of a modified tensile testing sample geometry (to reduce stress concentrations), and post-processing annealing.

3. Ball milling 2 wt % Al-CNT_{140nm} at 200RPM enhanced the tensile strength by ~21% when compared to its milled pure Al counterpart. This enhancement in mechanical properties was only noticeable when the cold working effect was reduced by limiting the milling time to 3hrs instead of 6hrs and by subjecting the samples to a post-processing annealing treatment.

4. It was proven by SEM that CNTs were aligned in the extrusion direction.

5. Both XRD and TEM analysis showed that in all composites in this study the matrix conserved its nanostructure after extrusion and annealing with a minor increase in the mean crystal size which in turn contributed to the enhanced strength observed in all milled samples compared to un-milled ones.

6. For the two CNT types employed in this study under the investigated processing conditions, the larger diameter CNTs were found to be easier to disperse in the Al matrix than the smaller diameter ones which had a stronger tendency to agglomerate.

7. Both types of CNTs employed in this study were found to act as nucleation sites for voids that form during tensile testing. These voids were present on the fracture surfaces, and they imply that the bonding between the matrix and the reinforcements is not strong enough.

8. Both types of CNTs were found to experience damage due to milling at 200 and 400RPM. For the 140nm CNTs, CNT pull-out and CNT inner tube slippage were observed by SEM on fracture surfaces whereas for the 40nm CNTs, CNT structural damage was observed by TEM investigation.

9. XRD scans for all bulk Al-CNT composites in this study didn't reveal any clear CNT peak at ~26^{o} corresponding to the (002) plane although CNTs were observed in all samples by SEM and TEM investigations. This observation was also reported by other researchers in the field.

10. Reducing the milling time from 3 and 6hrs to 30 min even though the RPM was doubled had a very noticeable effect on the mechanical properties of the material. For pure milled Al the UTS value was decreased to half its value, which effectively paved the road for CNTs to excel in showing their remarkable strengthening effect when added to the Al matrix.

11. Nano-indentation hardness and Young's modulus of the 140nm CNT composites were significantly higher than composites with the 40nm CNT composites despite that the 140nm CNTs have the lower aspect ratio; this is primarily due to the better dispersion of the 140nm CNTs.

12. The elastic modulus of both types of CNTs didn't increase as expected for the high CNT content samples due to the presence of CNT agglomerates which creates CNT-depleted regions causing plastic deformation to start at these regions at lower stresses than CNT-rich regions because the Al and CNT have totally different E values.

13. Carbide formation was observed even at low concentrations of the 40nm CNT composites only, and this is attributed to their larger interfacial contact area. For the 140nm CNTs, carbides were observed at high concentrations only. In addition, Nanosized aluminium oxide particles and nano-rod carbide structures were observed by TEM analysis which is believed to contribute to the observed mechanical enhancement over Al. Enhancements of 96% in tensile strength and 33 % in Young's modulus were observed.

14. No carbide formations were observed by XRD for all powder samples which indicate that the extrusion and annealing temperatures contributed to their formation.

Chapter 7

Future Work and Recommendations

1 Focusing our research on the promising CNT content that yielded best results and study the effect of varying other parameters at that concentration.

2 Investigate the effect of ball milling on different types of CNTs through milling of CNTs alone.

3 Investigate the effect of aluminium carbide on the mechanical properties of Al-CNT composite.

4 Investigate the dual matrix microstructural design for improving the toughness and wear resistance of CNT-reinforced aluminium.

REFERENCES

1. W. Callister. "Materials Science and Engineering," John Wiley & Sons, Inc (2007); pp. 282-363

2. Serope Kalpakjian, Steven R. Schmid "Manufacturing Engineering and Technology," 4th international edition, Prentice Hall, Inc., 2001, pp. 315-510

3. R. P´erez-Bustamante, I. Estrada-Guel, W. Ant´unez-Flores, M. Miki-Yoshida, P.J Ferreira, R. Mart´ınez-S´anchez: "Novel Al-matrix Nanocomposites Reinforced with Multi-Walled Carbon Nanotubes," Journal of Alloys and Compounds (2006),Vol 450, pp.323–326

4. V. Viswanathan, T. Laha, K. Balani, A. Agarwal, S. Seal. "Challenges and advances in nanocomposite processing techniques," Materials Science and Engineering (2006) Vol R54; pp.121–285

5. http://www.wikipedia.com, Feb. 15th, 2010

6. http://Physicsweb.com, March 20th, 2010

7. Y. Gogosti, "Nanomaterials handbook", CRC press, 2006

8. Amal M. K. Esawi and Mahmoud M. Farag, "Chapter 15-Polymer nanotube composites: promises and current challenges", in Polymer nanotube Nanocomposites: Synthesis, Properties and Applications, Vikas Mittal (editor), M M Scrivner Press, MA, USA (In Press).

9. Carreno-Morelli. E. Yang. J. Couteau, E. Hernadi, K. Seo, J.W. Bonjour, C. Forro, L. Schaller, R. "Carbon nanotube/magnesium composites. Physica Status Solidi (A) Applied Research (2004) , Vol.201 (8), pp. R53–R55

10. Schey, John; "Introduction to Manufacturing Processes". McGraw Hill, 20073rd edition

11. http://www.b2b-powder-metallurgy.com/rimages/317/automobile-motorcycle-parts-B.jpg, April 15th, 2010

12. Dowson, Gordan: "Powder metallurgy: the process and its products," 1st edition, Adam Hilger, Bristol and Newyork, 1990; pp.1-3

13. M.E. Fayed, L. Otten. "Handbook of Powder Science and Technology," Van Nostrand Reinhold Company Inc., 1984

14. H.H. Hausener, “Bibliography on the Compaction of Metal Powders,” Hoeganaes Corp., Riverton, New Jersey (1967b)

15. G. Bockstiegel, H.Hausner, “Modern techniques for powder metallurgical fabricationo for low-alloy and tool steels,”Plenum Press, New York (1966); Vol. 1, pp. 155-187

16. S.F. Chukmasov, A.I. Zazimko, Porosh, “Calculation of radial pressures generated in the pressing of metal fiber materials,” Powder Metallurgy and Metal Ceramics, Volume 11, July, 1972,pp. 518-520

17. F. Tang, I.E. Anderson, S.B. Biner. “Solid state sintering and consolidation of Al powders and Al matrix composites,” Journal of Light Metals (2002) Vol 2; pp. 201–214.

18. W.D. Jones, “Fundamental Principles of Powder Metallurgy,” Edward Amold Ltd., London, 1960

19. Compilation of ASTM Standard Definitions,(1982) 5th ed., American Society for Testing and Materials, 1982

20. P.R. Soni, “Mechanical Alloying: Fundamentals and Applications, “Cambridge International Science Publishing, 1998.

21. El-Eskandarany, :Mechanical alloying: Fabrication of advanced materials at room temperature”.Dar Al Fekr Al Araby, 2000 1st edition,

22. Suryanarayana. “C: Mechanical alloying and milling,” Prog Mater Sci. 46, 1-184 (2001)

23. A. S. Edelstein, and R. C. Cammarata. “Nanomaterials: Synthesis, Properties and Applications.” London: The institute of physics publishing, 2007

24. Retsch PM400 manual, http://www.retsch.com/dltmp/www/11117895c56b5e0055/manual_pm400_20.535.xxxx_en.pdf, 12/4/2010

25. T.Kuzumaki. K Miyazawa. H. Ichinose, K. Ito: “Processing of Carbon Nanotube Reinforced aluminum Composite,” Journal of Materials Research (1998), Vol.13; pp. 2445-2449

26. R. Zhong, H.T. Cong, P.X. Hou: “Fabrication of nano-Al Based Composites Reinforced By Single-walled Carbon Nanotubes,” Carbon(2003), Vol 41, pp.848-851

27. R.George, K.T. Kashyap, R. Rahul, S.Yamdagni: “Strengthening in Carbon Nanotube/Aluminium (CNT/Al) Composites.” Scripta Materialia (2005); Vol 53, pp.1159–1163

28. L. Ci, Z. Ryu, N. Y. Jin-Phillipp, M. Rühle: "Investigation of the Interfacial Reaction Between Multi-Walled Carbon Nanotubes and Aluminum" Acta Materialia (2006); pp. 5367-5375

29. T. Noguchi, A. Magraio, S. Fukazawa, S. Shimizu, J. Beppu, M. Seki: "Carbon Nanotube/Aluminium Composites with Uniform Dispersion, Materials Transactions (2004), Vol. 45, pp. 602-604

30. C.L. Xu, B.Q Wei, R.Z. Ma, J. Liang, X.K. Ma, D.H Wu: "Fabrication of Aluminum-Carbon Nanotube Composites and Their Electrical Properties, "Carbon (1999); Vol 37; pp. 855-858

31. C.F Deng, D.Z.Wang, X.X. Zhang, A.B. Li: "Processing and Properties of Carbon Nanotubes Reinforced Aluminum Composites," Materials Science and Engineering A (2007); vol 444; pp. 138-145

32. C. Edtmaier, E. Wallnoefer, A. Koeck: " Aluminum Based Carbon Nanotube Composites by Mechanical Alloying," Euro PM (2004); Miniaturisation and Nanotechnology in PM.

33. L.M. Ang, T.S.A. Hor, G.Q. Xu, C.H. Tung, S.P. Zhao, J.L.S. Wang: "Decoration of Activated Carbon Nanotubes with Copper and Nickel," Carbon (2000); Vol 38; pp. 363-372

34. X.K Sun, H.T. Cong, M. Sun, M.C. Yang: "Properties and Mechanical Properties of Highly Densified Nanocrystalline Al, Metallurgical and Materials Transactions," Physical Metallurgy and Materials Science (2000), Vol 31, pp.1017-1024

35. C. Liu, H.T. Kong, F. Li: "Semi-Continuous Synthesis of Single-Walled Carbon Nanotubes by Hydrogen Arc Discharge Method," Carbon (1999), Vol 37(11), pp.1865-8

36. A. Esawi, K. Morsi: "Dispersion of Carbon Nanotubes (CNTs) in Aluminum Powder," Composites (2006), Part A 38, pp.646–650

37. A. Esawi, K. Morsi, "Effect of Mechanical Alloying time and Carbon Nanotubes (CNT) on the Evolution of Aluminum (Al)-CNT Composite Powder, "Journal of Material Science (2007), Vol. 42, pp.4954-4959

38. D. Poirier, R. Gauvin, R.A.L Drew: "Structural Characterization of a Mechanically Milled Carbon Nanotube/aluminum Mixture", Composites Part A (2009)

39. H.J. Choi, G.B. Kwon, G.Y. Lee, D.H. Bae: "Reinforcement with Carbon Nanotubes in Aluminum Matrix Composites," Scripta Materialia (2009); Vol 59; pp. 360-363

40. Y. Zhou, W. Yang, Y. Xia, P.K. Mallick, Material Science and Engineering (2003). Vol 361; pp.112

41. T. Tokunaga, K. Kaneko, Z. Horita: "Production of Aluminum – Matrix Carbon Nanotube Composite Using High Pressure Torsion," Materials Science and Engineering A(2008);Vol 490; pp. 300-304

42. L. Wang, H. Choi, J-M Myoung , W. Lee: "Mechanical Alloying of Multi-walled Carbon Nanotubes and Aluminum Powders for the Preparation of Carbon/Metal Composites," Carbon (2009)

43. K.Morsi, A.M.K. Esawi, P. Borah, S. Lanka, A. Sayed, "Characterization and Spark Plasma Sintering of Mechanically Milled Aluminum (Al) - Carbon Nanotube (CNT) composite powders," Journal of Composite Materials, In Press.

44. K. Morsi, A.M.K. Esawi, S. Lanka, A. Sayed, M.Taher, "Spark Plasma Extrusion (SPE) of Ball-milled Aluminum and Carbon Nanotube Reinforced Aluminum Composite Powders", Composites Part A: Applied Science and Manufacturing, doi:10.1016/j.compositesa.2009.09.028, 2009.

45. K. Morsi, A.M.K, Esawi, P.Borah, S.Lanka, A. Sayed "Spark Plasma Extrusion of single and dual matrix carbon nanotube-aluminum composites", Materials Science and Engineering A (accepted manuscript).

46. H. Kwon, M. Estili, K. Takagi, T. Miyazaki, A. Kawasaki: "Combination of Hot Extrusion and Spark Plasma Sintering for Producing Carbon Nanotube Reinforced Aluminum Matrix Composites," Carbon (2009); Vol 47; pp. 570-577

47. T. Noguchi, J. Beppu: "Latest Trends in Automobile Material: Iron and Steel, Metals and Ceramics. Development of Carbon Nanotube-Aluminum and Expectations as Lightening Members," Eng Mater (2004); Vol 8; pp. 36-39

48. D. Lahiri: "Dual Strengthening Mechanism Induced By CNT in Roll-bonded Aluminum Composite," Material Science and Engineering A (2009); Vol 523; pp.263-270

49. T. Laha, A. Agarwal, T. McKechnie, S. Seal, "Synthesis and Characterization of Plasma Spray Formed Carbon Nanotube Reinforced Aluminum Composite," Materials Science and Engineering A (2004), Vol 381, pp 249–258

50. A. Sayed, A.M.K. Esawi, K. Morsi. "Fabrication Of CNT-Aluminium Composites", ASME 2nd Multifunctional Nanocomposites and Nanomaterials International Conference and Exhibition, Sharm El-Sheikh, Jan. 11-13th (2008). Published in conference proceedings (CD)

51. ASTM, "E8 Standard Test Methods of Tension Testing of Metallic Materials" Annual Book or ASTM Standards, American Society for Testing and Materials, Vol. 3.01

52. A.M.K. Esawi, K. Morsi, A. Sayed, A. Abdel Gawad, P. Borah. "Fabrication And Properties of Dispersed Carbon Nanotube-Aluminium Composites" Materials Science and Engineering: A (2009), Vol 508, PP 167-173

53. E.J. Gonzalez, G.J. Piermarini: "Handbook of Nanostructured Materials and Nanotechnology," vol 1: Synthesis and Processing

54. B.D. Cullity & S.R. Stock: "Elements of X-Ray Diffraction" 3rd ed., Prentice-Hall Inc., 2001, pp. 167-171

55. Amal M.K. Esawi, Mostafa A.E. Borady, "Powder Rolling of Aluminium Carbon Nanotubes Composites" Composite Science andTechnology (2008); Vol 68; pp. 486-491

56. A.M.K. Esawi, K. Morsi, A. Sayed, M. Taher, S. Lanka, "Effect of Carbon Nanotube (CNT) Content on The Mechanical Properties of CNT-Reinforced Aluminium Composites", Composites Science and Technology (2010), doi: 10.1016/j.compscitech.2010.05.004

57. A.M.K. Esawi, K. Morsi, A. Sayed, M. Taher, and S. Lanka, "The Effect of Carbon Nanotube (CNT) Aspect Ratio on The Processing and Properties of CNT-Reinforced Aluminium Composites", submitted to Carbon, April 2010.